

**Systematically Developing the Chemistry of Bismuth and Other Heavy Metals With  
Biorelevant Ligands**

by

Melanie D. Eelman

Submitted in partial fulfillment of the requirements  
for the degree of Doctor of Philosophy

at

Dalhousie University

Halifax, Nova Scotia

December 2003

© Copyright by Melanie D. Eelman, 2003



National Library  
of Canada

Bibliothèque nationale  
du Canada

Acquisitions and  
Bibliographic Services

Acquisitions et  
services bibliographiques

395 Wellington Street  
Ottawa ON K1A 0N4  
Canada

395, rue Wellington  
Ottawa ON K1A 0N4  
Canada

*Your file    Votre référence*

*ISBN: 0-612-89802-4*

*Our file    Notre référence*

*ISBN: 0-612-89802-4*

The author has granted a non-exclusive licence allowing the National Library of Canada to reproduce, loan, distribute or sell copies of this thesis in microform, paper or electronic formats.

L'auteur a accordé une licence non exclusive permettant à la Bibliothèque nationale du Canada de reproduire, prêter, distribuer ou vendre des copies de cette thèse sous la forme de microfiche/film, de reproduction sur papier ou sur format électronique.

The author retains ownership of the copyright in this thesis. Neither the thesis nor substantial extracts from it may be printed or otherwise reproduced without the author's permission.

L'auteur conserve la propriété du droit d'auteur qui protège cette thèse. Ni la thèse ni des extraits substantiels de celle-ci ne doivent être imprimés ou autrement reproduits sans son autorisation.

---

In compliance with the Canadian Privacy Act some supporting forms may have been removed from this dissertation.

Conformément à la loi canadienne sur la protection de la vie privée, quelques formulaires secondaires ont été enlevés de ce manuscrit.

While these forms may be included in the document page count, their removal does not represent any loss of content from the dissertation.

Bien que ces formulaires aient inclus dans la pagination, il n'y aura aucun contenu manquant.

**Canada**

DALHOUSIE UNIVERSITY  
DEPARTMENT OF CHEMISTRY

The undersigned hereby certify that they have read and recommend to the Faculty of Graduate Studies for acceptance a thesis entitled "Systematically Developing the Chemistry of Bismuth and Other Heavy Metals with Biorelevant Ligands" by Melanie D. Eelman in partial fulfillment of the requirements for the degree of Doctor of Philosophy.

Dated: December 12, 2003

External Examiner:

Research Supervisor:

Examining Committee:

Departmental Representative:

DALHOUSIE UNIVERSITY

DATE: December 2003

AUTHOR: Melanie D. Eelman

TITLE: Systematically Developing the Chemistry of Bismuth and Other  
Heavy Metals With Biorelevant Ligands

DEPARTMENT OR SCHOOL: Department of Chemistry

DEGREE: Ph.D. CONVOCATION: May YEAR: 2004

Permission is herewith granted to Dalhousie University to circulate and to have copied for non-commercial purposes, at its discretion, the above title upon the request of individuals or institutions.

\_\_\_\_\_  
Signature of Author

The author reserves other publication rights, and neither the thesis nor extensive extracts from it may be printed or otherwise reproduced without the author's written permission.

The author attests that permission has been obtained for the use of any copyrighted material appearing in the thesis (other than the brief excerpts requiring only proper acknowledgement in scholarly writing), and that all such use is clearly acknowledged.

For Jake

## Table of Contents

<b>Table of Contents.....</b>	<b>v</b>
<b>List of Figures and Schemes.....</b>	<b>viii</b>
<b>List of Tables.....</b>	<b>x</b>
<b>Abstract.....</b>	<b>xi</b>
<b>List of Abbreviations and Symbols.....</b>	<b>xii</b>
<b>Acknowledgments.....</b>	<b>xiv</b>
<b>Chapter 1: Introduction.....</b>	<b>1</b>
<b>1.1 General Introduction to Heavy Metals.....</b>	<b>1</b>
<b>1.2 The Biorelevance of Heavy Metals.....</b>	<b>1</b>
<b>1.3 Medicinal Relevance of Bismuth Chemistry.....</b>	<b>4</b>
<b>1.4 Scope of the Thesis.....</b>	<b>6</b>
<b>1.5 General Comments.....</b>	<b>7</b>
<b>1.6 The Importance of Electrospray Ionisation Mass Spectrometry.....</b>	<b>8</b>
<b>Chapter 2: Qualitative Bonding Models for Coordination Complexes of Heavy Metals.....</b>	<b>10</b>
<b>2.1 Introduction.....</b>	<b>10</b>
<b>2.2 Secondary Bonding Models for Heavy Metal Complexes.....</b>	<b>10</b>
<b>2.3 Conclusions.....</b>	<b>19</b>
<b>Chapter 3: Synthesis and Structures of the First Bismuth-Ester Complexes Using Hetero-Bifunctional Thiolate Anchored Ligands.....</b>	<b>20</b>
<b>3.1 Introduction.....</b>	<b>20</b>
<b>3.2 Results and Discussion.....</b>	<b>23</b>

3.3 Conclusions.....	39
<b>Chapter 4: Mass Spectrometric Identification of Bismuth Complexes Involving Carboxylate Derivatives.....</b>	<b>40</b>
4.1 Introduction.....	40
4.2 Results and Discussion.....	40
4.3 Conclusions and Future Directions.....	49
<b>Chapter 5: A Generally Applicable Synthetic Approach for Heteroleptic Thiolate Complexes of Bismuth.....</b>	<b>50</b>
5.1 Introduction.....	50
5.2 Results and Discussion.....	52
5.3 Conclusions.....	58
<b>Chapter 6: Electrospray Mass Spectrometric Identification of Amido- Thiolato Bismuth Complexes.....</b>	<b>59</b>
6.1 Introduction.....	59
6.2 Results and Discussion.....	59
6.3 Conclusions and Future Directions.....	62
<b>Chapter 7: Definitive Identification of Bismuth Complexes Involving Small Biomolecules.....</b>	<b>63</b>
7.1 Introduction.....	63
7.2 Interactions of Bismuth with Amino Acids, Peptides and Proteins.....	64
7.2.1 Amino Acids.....	64
7.2.2 Peptides and Proteins.....	64
7.3 Results and Discussion.....	66
7.3.1 Identification of Bismuth Complexes Involving Amino Acids by ESI-MS.....	66
7.3.2 Identification of Bismuth Complexes Involving Glutathione by ESI-MS.....	77

7.3.3 <i>Synthesis and Structure of the First Bismuth-Amino Acid Conjugate Base Complex</i> .....	79
7.4 <b>Conclusions and Future Directions</b> .....	85
<b>Chapter 8: Identification of Lead-Amino Acid Adducts by Electrospray Ionisation Mass Spectrometry and Crystallographic Characterisation of the First Lead-Amino Acid Complex</b> .....	88
8.1 <b>Introduction</b> .....	88
8.2 <b>Results and Discussion</b> .....	89
8.3 <b>Conclusions and Future Directions</b> .....	95
<b>Chapter 9: Application of Electrospray Ionisation Mass Spectrometry to Identify Heavy Metal Complexes Involving Amino Acids</b> .....	96
9.1 <b>Introduction</b> .....	96
9.2 <b>Results and Discussion</b> .....	96
9.3 <b>Conclusions and Future Directions</b> .....	100
<b>Chapter 10: Experimental</b> .....	102
10.1 <b>General Procedures</b> .....	102
10.2 <b>Synthetic Procedures</b> .....	102
<b>Appendix: List and Structure of Ligands</b> .....	110
<b>References</b> .....	112



## List of Figures and Schemes

<b>Figure 1.1:</b> A section from the periodic table of elements highlighting the heavy metals discussed in this thesis.....	3
<b>Figure 2.1:</b> Qualitative molecular orbital energy level diagrams for the series $\text{TiX}$ , $\text{PbX}^+$ , or $\text{PnX}^{2+}$ , $\text{TiX}_2^-$ , $\text{PbX}_2$ , or $\text{PnX}_2^-$ , and $\text{TiX}_3^{2-}$ , $\text{PbX}_3^-$ , or $\text{PnX}_3$ .....	12
<b>Scheme 2.1</b> .....	13
<b>Figure 2.2:</b> An orbital interaction diagram illustrating how the symmetry of each molecular orbital changes upon coordination to L for the isoelectronic series $\text{TiX}_3^{2-}$ , $\text{PbX}_3^-$ , or $\text{PnX}_3$ .....	15
<b>Figure 2.3:</b> A Walsh diagram illustrating how the symmetry of the molecular orbitals changes with a molecular structure adjustment of $\text{TiX}_6^{5-}$ , $\text{PbX}_6^{4-}$ , or $\text{PnX}_6^{3-}$ ..	18
<b>Figure 3.1:</b> A qualitative orbital energy diagram depicting the frontier orbital separation between hard acid-base pairs and soft acid-base pairs.....	21
<b>Figure 3.2:</b> ESI-MS of a reaction mixture containing $\text{BiCl}_3$ and MTG in absolute ethanol.....	25
<b>Figure 3.3:</b> ESI-MS of a reaction mixture containing $\text{BiCl}_3$ and 2 equivalents of MTG in 95% ethanol.....	27
<b>Figure 3.4:</b> ESI-MS of a reaction mixture containing $\text{BiCl}_3$ and 3 equivalents of MTG and KOH in 95% ethanol.....	29
<b>Figure 3.5:</b> Representative ESI-MS of an equimolar reaction mixture containing $\text{BiCl}_3$ and KMTS in ethanol.....	31
<b>Figure 3.6:</b> Crystallographic views of (i) <u>3.1c</u> $\text{Cl}_2$ , (ii) <u>3.2c</u> $\text{Cl}$ and (ii) [ <u>3.3c</u> ] $_2$ .....	35
<b>Figure 3.7:</b> Crystallographic view [ <u>3.4</u> ] $_2$ .....	37
<b>Figure 4.1:</b> An ESI-MS of an equimolar aqueous reaction mixture containing $\text{BiCl}_3$ and Msuc.....	42
<b>Figure 4.2:</b> An ESI-MS of an equimolar reaction mixture containing $\text{BiCl}_3$ and Tsai in ethanol.....	45
<b>Figure 4.3:</b> An ESI-MS of an equimolar reaction mixture containing $\text{Bi}(\text{NO}_3)_3$ and Mal in 50% ethanol.....	47

<b>Figure 4.4:</b> An ESI-MS of an equimolar reaction mixture containing $\text{Bi}(\text{NO}_3)_3$ and Suc in 50% ethanol.....	48
<b>Figure 5.1:</b> Crystallographic views of (i) <u>5.3a</u> , (ii) <u>5.3b</u> and (ii) <u>5.6a</u> .....	56
<b>Figure 5.2:</b> Crystallographic views of (i) <u>5.4a</u> , and (ii) <u>5.5</u> .....	57
<b>Figure 6.1:</b> ESI-MS of an equimolar reaction mixture containing $\text{BiCl}_3$ and ACA in MeOH.....	61
<b>Figure 7.1:</b> An ESI-MS ( $m/z$ 200-550) of an equimolar reaction mixture containing $\text{Bi}(\text{NO}_3)_3$ and L-cysteine in 50% ethanol.....	69
<b>Figure 7.2:</b> An ESI-MS of an equimolar reaction mixture containing $\text{Bi}(\text{NO}_3)_3$ and DL-homocysteine in 50% ethanol.....	70
<b>Figure 7.3:</b> ESI-MS of a solution mixture containing $\text{Bi}(\text{NO}_3)_3$ and L-methionine in 50% ethanol.....	71
<b>Figure 7.4:</b> ESI-MS of a solution containing $\text{Bi}(\text{NO}_3)_3$ , L-cysteine, and L-asparagine in 50% ethanol.....	75
<b>Figure 7.5:</b> ESI-MS of a solution containing $\text{Bi}(\text{NO}_3)_3$ , L-cysteine, and L-lysine in 50% ethanol.....	76
<b>Figure 7.6:</b> ESI-MS of a solution containing bismuth nitrate and glutathione in 50% ethanol.....	78
<b>Figure 7.7:</b> Crystallographic view of $\text{Bi}(\text{Cys})(\text{Phen})(\text{NO}_3)_2\text{H}_2\text{O}$ ( <u>7.2</u> ).....	81
<b>Figure 7.8:</b> Proposed polyprotic equilibria of L-cysteine leading to a variety of coordination modes towards metals.....	84
<b>Figure 8.1:</b> ESI-MS of a solution mixture containing lead nitrate and L-threonine in 50% ethanol.....	92
<b>Figure 8.2:</b> (i) Crystallographic view of the empirical formula unit of $\text{Pb}(\text{Val})_2(\text{H}_2\text{O})_2(\text{NO}_3)_2$ ( <u>8.1</u> ).....	94
<b>Figure 9.1:</b> An ESI-MS of the reaction mixture containing $\text{Hg}(\text{NO}_3)_2\cdot\text{H}_2\text{O}$ and L-cysteine in 50% ethanol.....	99

## List of Tables

<b>Table 3.1:</b> Comparison of selected internuclear distances (Å) for the ester-thiolate complexes <b>3.1cCl<sub>2</sub></b> , <b>3.2cCl</b> , <b>[3.3c]<sub>2</sub></b> and <b>[3.4]<sub>2</sub></b> .....	34
<b>Table 4.1:</b> ESI-MS data of reaction mixtures containing BiCl <sub>3</sub> with Msuc or Tsal, and Bi(NO <sub>3</sub> ) <sub>3</sub> with mal or suc.....	43
<b>Table 5.1:</b> Selected internuclear distances (Å) listed in order of increasing bond length for the compounds represented by <b>3.1 - 3.4</b> and <b>5.1 - 5.7</b> .....	55
<b>Table 7.1:</b> ESI-MS data of reaction mixtures containing bismuth nitrate and an amino acid in 50% ethanol.....	68
<b>Table 7.2:</b> ESI-MS data of reaction mixtures containing bismuth nitrate, cysteine and another amino acid in 50% ethanol.....	74
<b>Table 8.1:</b> ESI-MS data of reaction mixtures containing lead nitrate and an amino acid in 50% ethanol.....	91
<b>Table 9.1:</b> Monocation assignments from ESI-MS data of reaction mixtures containing a heavy metal reagent and an amino acid in 50% ethanol.....	98
<b>Table 10.1:</b> Crystal data for <b>3.1cCl<sub>2</sub></b> , <b>3.4</b> , <b>5.5</b> , <b>5.6a</b> , <b>7.2</b> , and <b>8.1</b> .....	109

## Abstract

In contrast to the toxicity displayed by many heavy metals, especially those in the *p*-block (e.g. lead, arsenic), bismuth compounds are well known for their therapeutic application in the treatment of gastrointestinal disorders and have a long history of medicinal use. Although the mechanisms of bioactivity are not understood, the thiophilicity of bismuth has prompted speculation that sulfur-containing biomolecules represent the primary target for pharmaceuticals such as ‘colloidal bismuth subcitrate’ and ‘bismuth subsalicylate’, the active ingredients of De-Nol<sup>®</sup> and Pepto-Bismol<sup>®</sup>, respectively. However, definitive characterisation of bismuth and other heavy metal complexes involving biomolecules has been elusive.

This work establishes the utility of electrospray ionisation mass spectrometry (ESI-MS) as a characterisation method to identify interactions of heavy metals with small biomolecules and other biorelevant ligands. In addition, the first examples of a bismuth and a lead complex involving amino acids have been isolated and structurally characterised. These observations provide important insight into how heavy metals, bioactive or otherwise, may become incorporated into biological systems.

### List of Abbreviations and Symbols

Å	angstrom	ESI	electrospray ionisation
ACA	<i>N</i> -acetylcysteamine	Et	ethyl
Aet	2-aminoethanethiol	FT	Fourier transform
Ala	alanine	Fw	formula weight
Am	monoanionic conjugate base of the amino acid	Gln	glutamine
Arg	arginine	Glu	glutamic acid
Asn	asparagine	Gly	glycine
Asp	aspartic acid	Hcys	homocysteine
AO	atomic orbital	His	histidine
bipy	2,2'-bipyridine	HM	heavy metal
BSS	bismuth subsalicylate	HOMO	highest occupied molecular orbital
°C	degrees Celsius	<i>Hp</i>	<i>Helicobacter pylori</i>
CBS	colloidal bismuth subcitrate	HSAB	hard-soft acid-base
CI	chemical ionisation	H <sub>2</sub> sal	salicylic acid
Cys	cysteine	Ile	isoleucine
DMF	<i>N,N</i> -dimethylformamide	Int	intensity
DNA	deoxyribonucleic acid	IR	infrared
dp	decomposition point	K	Kelvin
EA	elemental analysis	KMTS	potassium methyl thiosalicylate
EDTA	ethylenediaminetetraacetic acid	Leu	leucine
EI	electron impact		

LUMO	lowest unoccupied molecular orbital	$m/z$	mass-to-charge ratio
Lys	lysine	NMR	nuclear magnetic resonance
Mal	malic acid	Phe	phenylalanine
Me	methyl	phen	1,10-phenanthroline
Met	methionine	Rel	relative
MetI	2-mercaptoethanol	RNA	ribonucleic acid
MeOH	methanol	Ser	serine
mL	millilitres	sh	shoulder
mmol	millimoles	Suc	succinic acid
MO	molecular orbital	Thr	threonine
mp	melting point	Trp	tryptophan
MS	mass spectrometry or mass spectra	Tsal	thiosalicylic acid
MS/MS	tandem mass spectrometry	Tyr	tyrosine
Msuc	mercaptosuccinic acid	V	volts
MT	metallothionein	Val	valine
MTG	methyl thioglycolate	VSEPR	valence shell electron pair repulsion
MTS	methyl thiosalicylate		

## Acknowledgments

First of all, I thank my husband Jake for his support, patience, understanding and helpful comments during my academic career. During this time, both of our families have been extremely supportive and a huge thank you goes out to them as well.

I would like to express my gratitude to my supervisor, Dr. Neil Burford, for his enthusiasm, inspiration, encouragement and discussions during my time at Dalhousie University and for teaching me about the “continuum” and “chromatogram of life”.

I also offer my appreciation to Drs. T. S. Cameron and K.N. Robertson for their crystallographic expertise and assistance; Drs. J.S. Grossert and D. Pinto for their mass spectrometry support and taking the time to instruct and aid me when needed; Dr. W. Davidson for allowing me the opportunity to spend valuable research time at MDS Sciex using their instrumentation (a whole mass spectrometer for myself!); Paul Ragogna for his camaraderie and discussions; Wes Leblanc and Deanna MacKay for their experimental contributions; Dr. M. Stradiotto for his assistance; and members of the Burford group (past and present) for their support and conversation.

I would like to acknowledge the Maritime Mass Spectrometry Laboratory, NRC-IMB and MDS Sciex for use of facilities; Dr. K. Grundy for sitting on my committee; and Dr. D. Mahony, Dr. S.J.O.V. van Zanten, and M. Morash, our collaborators to the “Bismuth Project” in microbiology and gastroenterology,.

Finally, I would like to thank Dalhousie University, NSERC, MDS Sciex, the Killam Trusts, and the Walter C. Sumner foundation for funding my research.

## Chapter 1: Introduction

### 1.1 General Introduction to Heavy Metals

The term “heavy metal” is ambiguous and is used to describe a number of elements in the periodic table, especially those that are associated with toxicity. A metal is typically characterised by lustre, ductility, malleability, and high electric and thermal conductivity.<sup>1</sup> In this context, a heavy metal can be viewed as a metal of high specific gravity or molecular weight. As such, this term can be applied across the table to encompass many of the transition metals, and a number of metals located amongst the *s*-, *p*- and *f*- block elements. However, the discrimination between metals and non-metals can sometimes be trivial, especially when considering those elements classified as “metalloids”, such as arsenic and tellurium, which exhibit some of the characteristics attributed to metals. For the purposes of this thesis, “heavy metal” is used to describe metals and metalloids in the *p*-block located in the 3<sup>rd</sup> row and below, as well as 5<sup>th</sup> and 6<sup>th</sup> row transition metals.

### 1.2 The Biorelevance of Heavy Metals

Many heavy metals are notorious for their toxic effects. However, toxicity is a relative term and everything is potentially toxic if the quantity of that substance exceeds the accepted levels. In this context, metal ions in general have the ability to promote responses in biological systems that range from deficiency to toxicity.<sup>2</sup> The toxicity for heavy metals varies from very low (i.e. bismuth) to high (e.g. mercury and lead) and complexes incorporating heavy metals such as bismuth have demonstrated therapeutic



bioactive properties and have been used to treat a variety of medicinal disorders.<sup>3</sup>

Therefore, the chemistry of heavy metals is biologically relevant whether the metal in question is highly toxic or bioactive. Indeed, it has been widely suggested that toxicity and/or bioactivity is manifested through the interaction of heavy metals with large biomolecules such as enzymes, proteins, and peptides,<sup>4-8</sup> although there have been few definitive studies concerning the chemistry of many heavy metals involving such biomolecules as ligands. The heavy metals discussed in this thesis are bismuth, arsenic, antimony, lead, thallium, mercury and cadmium. Figure 1.1 shows a section of the periodic table in which these metals are located. Those elements that have a biological role are also indicated.

	13	14	15	16	17
	<b>B</b> 4 g	<b>C</b>	<b>N</b>	<b>O</b>	<b>F</b> 20 mg (F <sup>-</sup> )
12	<b>Al</b> 5 g	<b>Si</b>	<b>P</b>	<b>S</b>	<b>Cl</b>
	<b>Zn</b> 150-600 mg	<b>Ga</b>	<b>Ge</b>	<b>As</b> 5-50 mg	<b>Se</b> 5 mg
	<b>Cd</b> 3-330 mg	<b>In</b> 30 mg	<b>Sn</b> 2 g	<b>Sb</b> 100 mg	<b>Te</b> 0.25 mg
	<b>Hg</b> 0.4 mg	<b>Tl</b> *600 mg	<b>Pb</b> 1 mg	<b>Bi</b> **	<b>Po</b> n/a
					<b>At</b> n/a

\* Lethal Dose  
\*\* Lethal Dose: 221 mg/kg

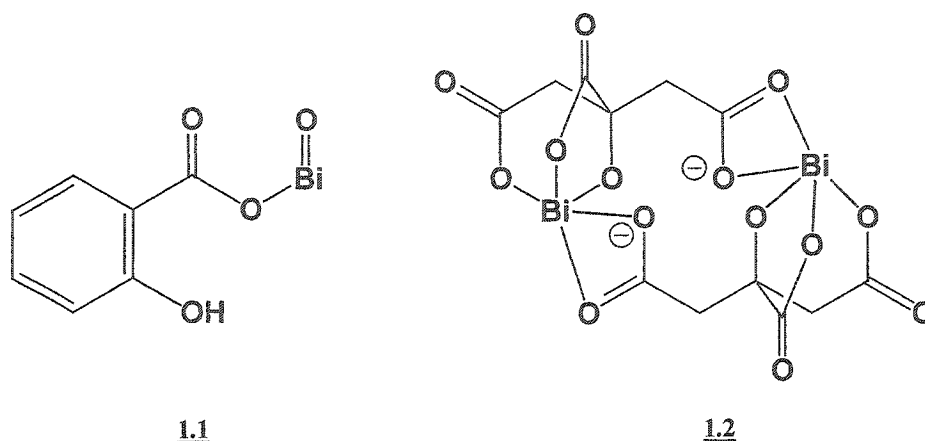
metals ← → non-metals

**Figure 1.1:** A section from the periodic table of elements highlighting the heavy metals discussed in this thesis (circles) and elements that have a biological role (squares). The toxic intake levels for elements (except those considered to be non-toxic) in humans are also indicated.<sup>9;10</sup>

### 1.3 Medicinal Relevance of Bismuth Chemistry

Bismuth has an extensive medicinal history that dates back approximately 250 years.<sup>3,11-15</sup> Afflictions that have been treated using bismuth preparations (e.g.  $\text{Bi}(\text{NO}_3)_3$ ,  $\text{BiOCl}$ , or bismuth subnitrate) include syphilis,<sup>15</sup> tumors,<sup>16,17</sup> and gastrointestinal disorders such as travellers' diarrhea,<sup>18,19</sup> nonulcer dyspepsia,<sup>20</sup> and gastroduodenal ulcers.<sup>20,21</sup> A decline in the medicinal use of bismuth compounds occurred in the latter half of the twentieth century as a result of outbreaks in France and Austria of bismuth encephalopathy, a disorder associated with the rapid onset of dementia that is reversible with treatment. It was also around this time that other heavy metals (e.g. lead, mercury) were receiving a lot of attention for their highly toxic effects. However, it has since been determined that bismuth compounds exhibit relatively low toxicity in comparison to other heavy metals, although dosages need to be monitored as this metal has been shown to accumulate over time in the kidneys.<sup>22</sup>

Bismuth(III) compounds remain to be used to a great extent in the treatment of many gastric disorders. Most obvious is the extensive use of the commercially available preparations Pepto-Bismol<sup>®</sup> and De-Nol<sup>®</sup> that contain the active ingredients 'bismuth subsalicylate' (BSS 1.1) and 'colloidal bismuth subcitrate' (CBS, 1.2), respectively. The modes of bioactivity are not understood for these compounds, nor for any bioactive bismuth compound, and little is known about the chemistry of BSS or CBS. The number of characterisation methods available to analyse BSS is limited by the fact that this compound is inherently insoluble in most solvents. The structure provided for BSS (1.1) represents only the empirical formula as determined by elemental analysis.



In contrast to BSS, CBS is soluble in aqueous solvents and has been characterised extensively by a variety of techniques, including X-ray crystallography.<sup>23-27</sup> Many solid state structural arrangements involving various cations ( $K^+$ ,  $NH_4^+$  and/or  $Na^+$ ) have been reported with many of them exhibiting a dimeric structure, such as that provided for CBS (1.2), indicating a sensitivity to experimental conditions. Although the chemistry of CBS is complex, it is clear that this compound does not contain the bismuthyl unit implied in the “sub” designation. Understanding the chemistry of CBS in solution may be important in understanding the bioactivity of ‘colloidal bismuth subcitrate’.  $^1H$  and  $^{13}C$  NMR spectroscopic studies have indicated that citrate fragments in CBS may be rapidly exchanging bismuth sites in solution at low concentration. At higher concentrations, it appears that CBS arranges into oligomeric or polymeric units.<sup>23-25;28</sup>

BSS and CBS have proven effective in the treatment of ulcers associated with stomach flora, such as *Helicobacter pylori* (*Hp*).<sup>29;30</sup> Infection of *Hp* in certain individuals has also been linked to gastric cancer.<sup>31</sup> In order to cure gastroduodenal ulcers, *Hp* needs to be eradicated and a successful treatment is a triple therapy regimen

that includes BSS or CBS. In North America, BSS is used in tandem with metronidazole and either amoxicillin or tetracycline.

The considerable array of medicinal or antimicrobial uses for bismuth compounds is indicative of the diverse biorelevance of this element. A wide selection of compounds has been explored for potential bioactivity simply on the basis of the fact that they contain bismuth. However, systematic and comprehensive investigations of series of related compounds are rare. The structural complexity of many bismuth compounds and the relatively superficial understanding of their chemistry inhibit experimental studies. Nevertheless, the medicinal properties of many bismuth salts highlight the need for the continued development of bismuth chemistry and discovery of potential pharmaceutical agents.

#### **1.4 Scope of the Thesis**

This thesis examines the chemistry of heavy metals [Bi(III), As(III), Sb(III), Pb(II), Tl(I), Hg(I), Hg(II) and Cd(II)] involving ligands of biological relevance, with the majority of this work focusing on the chemistry of bismuth. In the context of the use of hetero-bifunctional thiolate ligands to develop the coordination chemistry of bismuth, the significance of the ester- (Chapter 3), medically relevant carboxylato- (Chapter 4), amino- and hydroxy-/alkoxy- (Chapter 5) and amido- (Chapter 6) functionalities are discussed. These chapters emphasise the chelating ability of the hetero-bifunctional thiolate ligands and control of the thiolation and Lewis acidity of the bismuth centre. Chapter 5 also discusses in detail general synthetic approaches to the preparation of complexes of bismuth involving hetero-bifunctional ligands. Chapters 7, 8 and 9 discuss

the chemistry of bismuth and lead involving small biomolecules, with an emphasis on twenty-one common amino acids as ligands. Throughout this thesis, the usefulness of ESI-MS for investigating the coordination chemistry of metal systems is highlighted.

In essence, the research involved in this thesis has been a systematic approach to understanding complex metal systems, especially those involving biological systems. The exploitation of hetero-bifunctional thiolate ligands to develop the coordination chemistry of bismuth(III) provides simple models of how bismuth interacts with biologically relevant functional groups. It also provides the necessary background to branch into the chemistry of bismuth, as well as other heavy metals, with biomolecules as ligands. Although the significance of conclusions based on accurate empirical observations without over-interpretation of the results is stressed, heavy metal-biomolecule complexes lend important insight into how heavy metals, bioactive or otherwise, may become incorporated into biological systems.

## 1.5 General Comments

Molecular drawings are intended to illustrate connectivity of the heavy metal only; in some instances, dashed lines (-----) are used to represent long or intermolecular contacts. Drawings of these compounds aimed at describing bonding features, such as Lewis structures, are not meaningful or are misleading for the heavy metal complexes discussed, although they are employed for the description of some ligands. Crystallographic figures are drawn with 50% probability thermal ellipsoids.

Molecular drawings are numbered in a sequential manner according to the chapter in which they are discussed (e.g. **3.3** signifies Chapter 3, compound 3). Some of the

compounds considered in this work have similar compositional features and, in these cases, a letter is provided after the number to relate and differentiate the compounds according to their ligands (e.g. **3.1a**, **3.1b** or **3.1c**). Many of the complexes identified from ESI-MS performed on reaction mixtures are designated by a heavy metal:ligand ratio (i.e. **1:1** or **2:3**).

## **1.6 The Importance of Electrospray Ionisation Mass Spectrometry**

As ESI-MS is highlighted in this thesis as a key characterisation technique for investigating heavy metal coordination complexes, a brief discussion of this method is required. The use of mass spectrometric methods to study metal systems has not been common practice until recently.<sup>32</sup> In the past, mass spectrometric analysis was limited to those compounds that are highly volatile. As such, synthesis and understanding of specific complexes has previously driven the understanding of the reaction and structural chemistry of many inorganic elements. Now, there is a range of mass spectrometric methods available such that large, complex and fragile molecules can be analysed effectively and definitive relationships between observations made for gas phase samples and those in the solid state can be made. Today, many cluster and transition metal chemists use mass spectrometric methods routinely<sup>33</sup> to elucidate the stoichiometry of metal compounds as many metals often possess a characteristic isotopic pattern, which may be used to decipher the number of metals in an ion.

Heavy metal compounds are typically thermally unstable and are of low volatility. As a result, mass spectrometric techniques that involve high energy volatilisation of the

sample, such as electron impact (EI) or chemical ionisation (CI), are ineffective. ESI-MS introduces the sample in a solution without heating. Moreover, due to the high sensitivity of the mass spectrometry, low sample concentrations can be used (i.e.  $10^{-6} - 10^{-2}$  M).<sup>34</sup>

The process of ESI involves spraying a solution of a substance (often in a polar solvent) through a capillary into a chamber, with a stream of dry gas passing in the opposite direction of the spray.<sup>35-37</sup> A potential of several kilovolts is applied between the capillary and the chamber wall and charged droplets are produced that become smaller as the solvent is evaporated. The bare ions formed from this desolvation process, pass through a glass capillary into the pre-analyser region, where the remaining bath gas and residual solvent is pumped away. The ions are then focused through the lensing system into the analyser of the mass spectrometer. In essence, ESI allows for ions to be transferred from solution to the gas phase with little fragmentation such that metal-ligand complexes remain intact, although there is evidence for the formation of ions from neutrals.<sup>38</sup>

ESI is a soft ionisation technique, with little fragmentation occurring and the spectra generally consist of a single isotopomer envelope due to the parent ion. This property makes ESI-MS an advantageous method for studying mixtures as each component can appear in the spectrum as a single peak. As such, the majority of the compounds discussed in this thesis have been identified by positive ion ESI-MS performed on reaction mixtures.



## Chapter 2: Qualitative Bonding Models for Coordination Complexes of Heavy Metals

### 2.1 Introduction

Complexes of heavy metals, especially those in the *p*-block, often demonstrate a vast structural diversity in the solid state with metal centres accommodating a wide range of coordination numbers. Bismuth in particular typically has coordination numbers from three to ten and as such more variable geometries are observed for compounds of this element than those of transition metals. The high coordination numbers of heavy metal centres are often the result of extensive intermolecular bonding and the ability of these complexes to behave as Lewis acids. The structural features of heavy metal compounds, such as those described in this thesis, can be explained in terms of covalent and secondary bonding. This chapter discusses bonding models employed to rationalise Lewis acid-base bonding in complexes of this type.

### 2.2 Secondary Bonding Models for Heavy Metal Complexes

The ability of many heavy main group metal complexes to partake in secondary bonding has often been explained by the substantial involvement of low energy, vacant *d*-orbitals on the central atom in Lewis acid-base interactions. However, theoretical calculations have indicated that the *d*-orbitals of heavier *p*-block atoms, are too high in energy and too diffuse to enable significant contribution in this type of bonding.<sup>39</sup>

A more accepted model invokes the use of  $\sigma^*$ -orbitals that are lower in energy than the *d*-orbitals<sup>40,41</sup> for compounds of the type  $EX_n$  (where E is a heavier main group

atom, X is any ligand with an electronegativity greater than that of E and  $n = 1 - 3$ ). For E equal to  $Tl^+$ ,  $Pb^{2+}$ , or  $Pn^{3+}$  (where Pn is a heavier element in Group 15) a series of compounds  $TlX$ ,  $PbX^+$ , or  $PnX^{2+}$ ,  $TlX_2^-$ ,  $PbX_2$ , or  $PnX_2^+$  and  $TlX_3^{2-}$ ,  $PbX_3^-$ , or  $PnX_3$  can be envisaged with each series having  $C_{\infty v}$ ,  $C_{2v}$  and  $C_{3v}$  symmetry, respectively.

Qualitative molecular orbital energy level diagrams for  $EX$ ,  $EX_2$ , and  $EX_3$  (where  $X = H$ ) are presented in Figure 2.1. The acceptor MOs are designated along with their respective symmetry labels. These  $\sigma^*$ -orbitals are regarded as having a significant contribution from the  $p$ -orbitals of the heavy main group atom. The lower electronegativity of E results in higher atomic orbital energies and relatively poor orbital overlap with the ligand, producing low energy  $\sigma^*$ -orbitals. As a result, a Lewis base (L) will interact with the E centre. Moreover, the nature of the  $\sigma^*$ -orbitals requires a nearly linear L-E-X geometry, and lengthening in the E-X bond. This lengthening is a result of the increasing occupation of the  $\sigma^*$ -orbital as the L-E interaction increases.

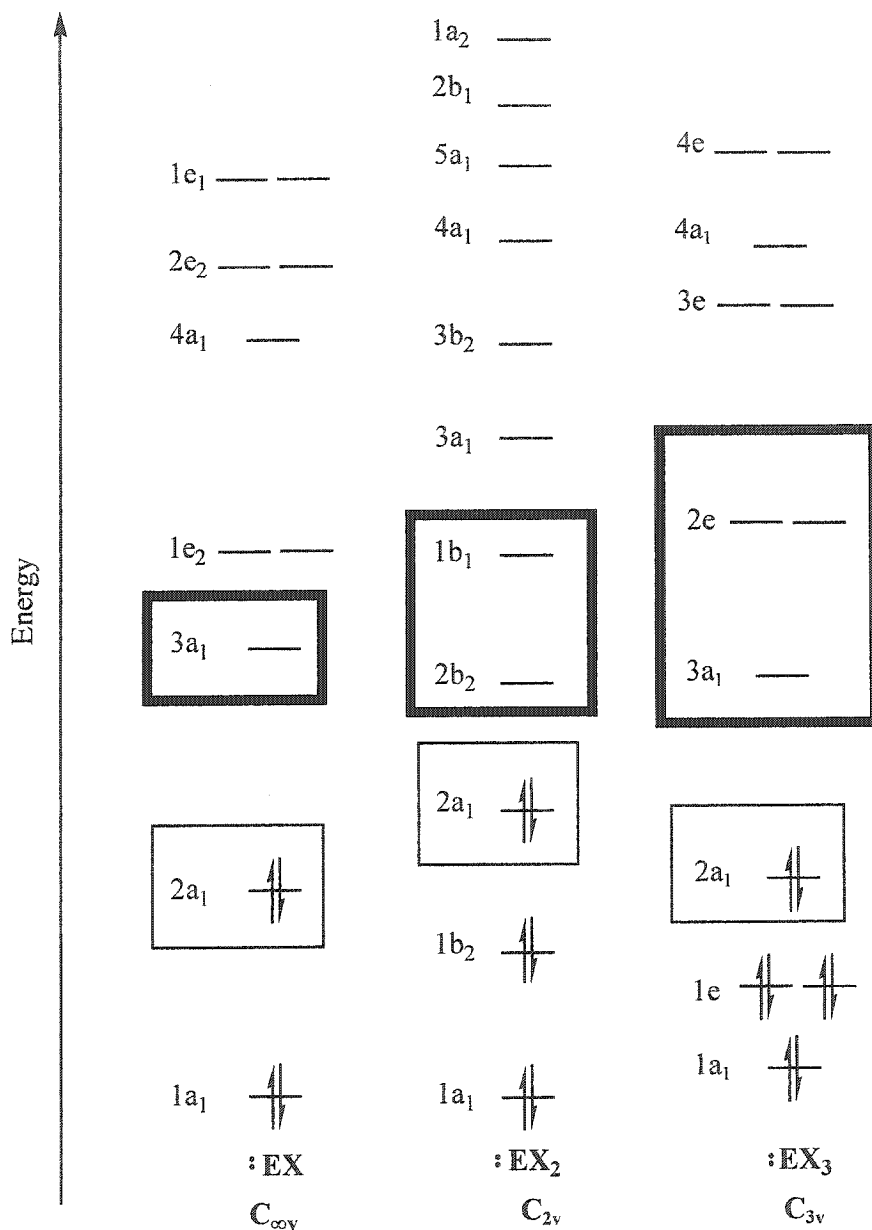
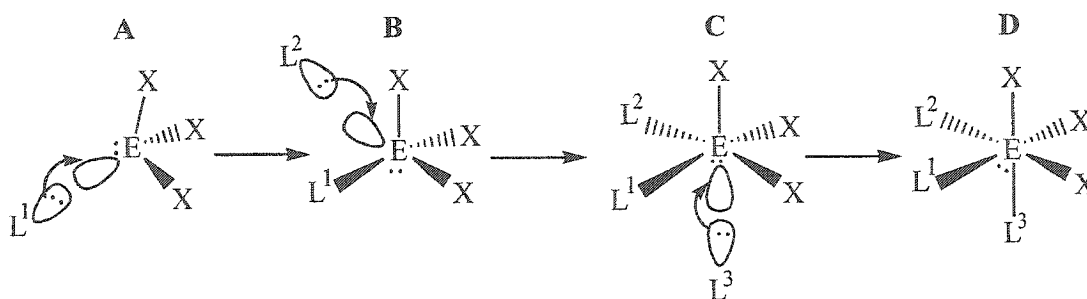


**Figure 2.1:** Qualitative molecular orbital energy level diagrams for the series  $TlX$ ,  $PbX^+$ , or  $PnX^{2+}$ ,  $TlX_2^-$ ,  $PbX_2$ , or  $PnX_2^+$  and  $TlX_3^{2-}$ ,  $PbX_3^-$ , or  $PnX_3$  represented by  $EX$ ,  $EX_2$ ,  $EX_3$  where  $X = H$  and  $Pn = As, Sb$  and  $Bi$ . The  $\sigma^*$ -orbitals are highlighted in the bolded box. The other box indicates the non-bonding electrons (lone pair) of the central E atom.



Scheme 2.1

A change in geometry at the heavy metal centre is required for the atom to accommodate the increase in coordination number upon interaction with a Lewis base (L). This is illustrated above in Scheme 2.1 for  $\text{TiX}_3^{2-}$ ,  $\text{PbX}_3^-$ , or  $\text{PnX}_3$  as represented by  $\text{EX}_3$  where the coordination number changes from three (A) to four (B), to five (C) or to six (D) giving disphenoidal, square pyramidal, and octahedral molecular geometries, respectively. Three  $\text{E-X } \sigma^*$ -orbitals interact sequentially in a Lewis acid-base fashion with three Lewis base  $\sigma$ -orbitals from the ligands  $\text{L}^1$ ,  $\text{L}^2$ , and  $\text{L}^3$ . In the case of a six-coordinate heavy metal centre, an octahedral molecular geometry (D) is not in accordance with VSEPR theory as seven electron pairs around the metal centre are expected to give a pentagonal pyramidal geometry. However, non-VSEPR, octahedral molecular structures have been reported in the literature with explanations invoking a stereochemically inactive lone pair on the central atom.<sup>40,42</sup> In these cases, the lone pair is believed to reside in an  $s$ -orbital that does not exert stereochemical influence.

The changes in the symmetry of the heavy main group atom complexes are dependent upon the nature of the Lewis base. However, if a complex of the type  $\text{EX}_3$  is considered then the simplest scenario in this case is when  $\text{L}^1 = \text{L}^2 = \text{L}^3 \neq \text{X}$ . Upon

addition of the Lewis base (L), the point group of the four- and five- coordinate complex would be  $C_s$  and the six-coordinate complex is expected to have  $C_{3v}$  symmetry. An illustration of how the symmetries of the MOs change upon coordination of three Lewis bases (L) to  $EH_3$  is given in Figure 2.2.

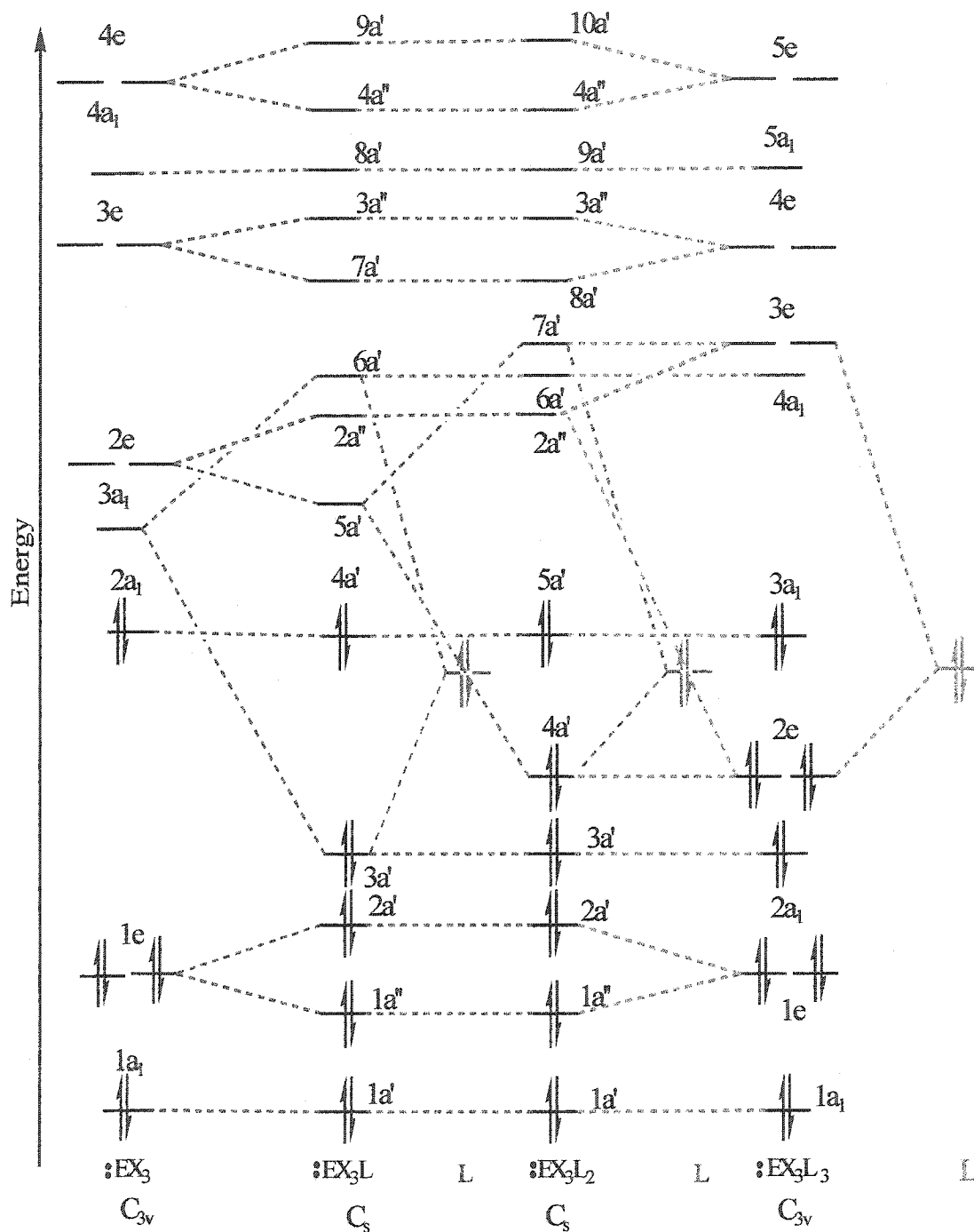


**Figure 2.2:** An orbital interaction diagram illustrating how the symmetry of each molecular orbital changes upon coordination to L for the isoelectronic series  $\text{TlX}_3^{2-}$ ,  $\text{PbX}_3^-$ , and  $\text{PnX}_3$  ( $\text{Pn} = \text{As}, \text{Sb}, \text{or Bi}$ ) represented by  $\text{EX}_3$  ( $\text{X} = \text{H}$ ).

In Figure 2.2, three acceptor  $\sigma^*$ -orbitals of  $\text{EX}_3$ , representing  $\text{TiX}_3^{2-}$ ,  $\text{PbX}_3^-$ , or  $\text{PnX}_3$  ( $\text{X} = \text{H}$ ;  $\text{Pn} = \text{As}, \text{Sb}, \text{or Bi}$ ), are shown interacting sequentially in a Lewis acid-base fashion with three donating ligands  $\text{L}$ . The first interaction involves  $\text{EX}_3$  and  $\text{L}$  (indicated in red) and results in the stabilisation of the two electrons from the HOMO of  $\text{L}$  and formal destabilisation of the  $\sigma^*$ -orbital of  $a_1$  symmetry. The resulting bonding molecular orbital,  $3a'$ , is of lower energy than the non-bonding  $4a'$  MO. In accordance to the change in point group from  $\text{C}_{3v}$  to  $\text{C}_s$ , the MOs carrying the  $a_1$  symmetry label become  $a'$  and the degenerate molecular orbitals of  $e$  symmetry will separate in energy and become of  $a'$  and  $a''$  symmetry.

The second ligand addition (designated in blue) involves the interaction of the LUMO of  $\text{EX}_3\text{L}$  with the HOMO of  $\text{L}$  to generate the complex  $\text{EX}_3\text{L}_2$ , also having  $\text{C}_s$  symmetry. The LUMO, previously one of the  $2e$  MOs in  $\text{EX}_3$ , is either of  $a'$  or  $a''$  symmetry depending on how the degenerate orbital separates. In the diagram given, however, the LUMO was arbitrarily chosen to have  $a'$  symmetry. As the point group of the new complex is the same as the starting complex, the MOs not directly involved in the Lewis acid-base reaction of  $\text{EX}_3\text{L}$  and  $\text{L}$  essentially remain at the same relative energies and retain the same symmetry labels.

The addition of the third ligand (shown in green) results in the generation of the complex  $\text{EX}_3\text{L}_3$ , having  $\text{C}_{3v}$  symmetry and an octahedral geometry. The LUMO of  $\text{EX}_3\text{L}_2$  has  $a''$  symmetry and upon interaction with the HOMO of  $\text{L}$ , the new MOs will be of  $e$  symmetry and degenerate with the  $a'$  molecular orbital produced in the formation of

$\text{EX}_3\text{L}_2$ . Hence, the overall effect of adding three equivalent ligands (L) to  $\text{EX}_3$  will be to add three new occupied MOs of e and  $a_1$  symmetry.

Upon addition of three Lewis bases (L) to  $\text{EX}_3$ , it is important to note that if  $\text{L} = \text{X}$ , and the resulting molecular geometry is octahedral, the expected point group symmetry for the complex would be  $\text{O}_h$ . A Walsh diagram for such a consideration is shown in Figure 2.3 and demonstrates how the energies of the MOs would alter, if the point group symmetry of  $\text{EX}_6^{3-}$  changes from  $\text{C}_{3v}$  to  $\text{O}_h$ . The MOs having the greatest contribution from the *d*-orbitals of bismuth will become the  $2e_g$  ( $d_z^2$  and  $d_{x^2-y^2}$  AOs) and  $1t_{2g}$  ( $d_{xy}$ ,  $d_{xz}$ , and  $d_{yz}$  AOs) molecular orbitals for  $\text{EX}_6^{3-}$  with  $\text{O}_h$  symmetry. As such, the bonding model considering the use of low energy  $\sigma^*$ -orbitals as the major contributors in Lewis acid-base bonding predicts that the effect of adding Lewis bases to  $\text{EX}_3$  should not change the relative energies of the *d*-orbitals associated with heavier main group atoms.



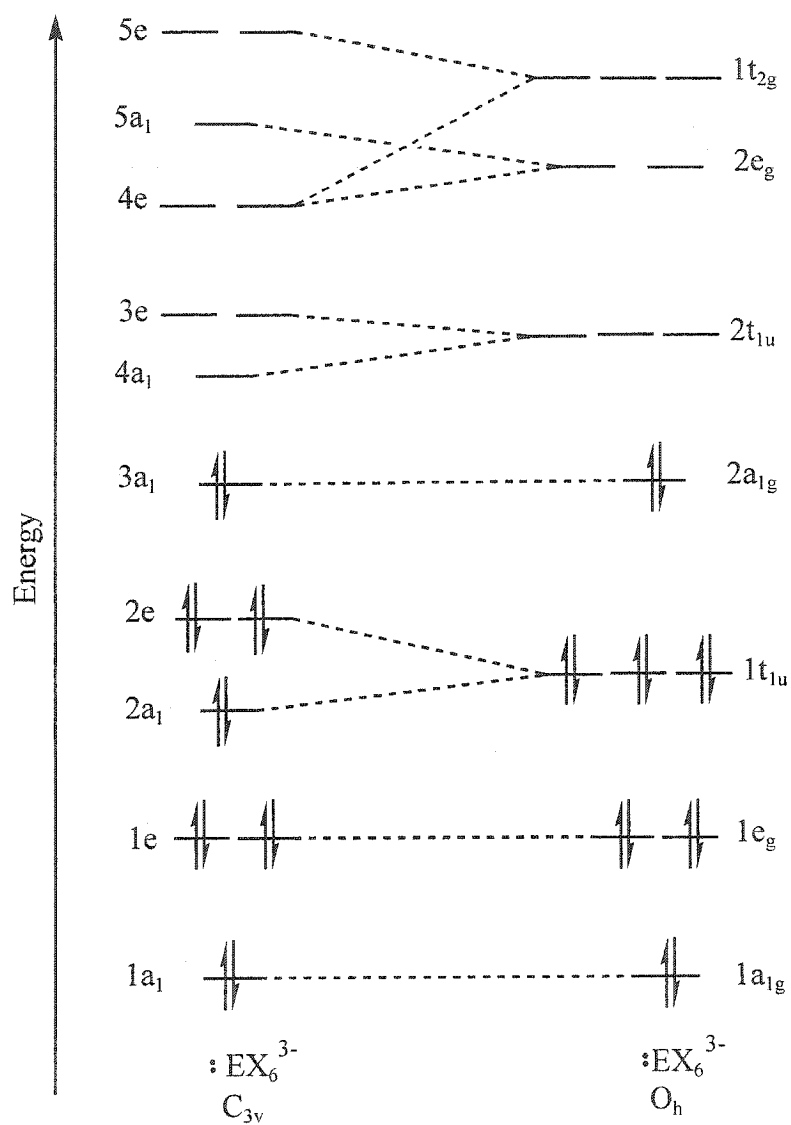


**Figure 2.3:** A Walsh diagram illustrating how the symmetry of the molecular orbitals changes with a molecular structure adjustment of  $TlX_6^{5-}$ ,  $PbX_6^{4-}$ , or  $PnX_6^{3-}$  (Pn = As, Sb, Bi) as represented by  $EX_6^{3-}$  (X = H) between  $C_{3v}$  and  $O_h$ .

Although invoking the use of  $\sigma^*$ -orbitals is a useful bonding model for understanding Lewis acid-base interactions with heavier main group elements such as arsenic, antimony, bismuth, lead and thallium, the bonding considerations are different for compounds involving mercury and cadmium. Unlike for heavy *p*-block atoms, mercury(II) and cadmium(II) have accessible *d*-orbitals that are full and their *s*-orbitals (6*s* for Hg(II) and 5*s* for Cd(II)) are considered empty. As such, the *d*-orbitals would not have much involvement in Lewis acid-base interactions for Hg(II) or Cd(II) complexes. However, it is conceivable that the empty *s*-orbitals are involved considerably in addition to low energy  $\sigma^*$ -orbitals for compounds of this type.

### 2.3 Conclusions

There are many bonding models that have been used to explain the “secondary” or Lewis acid-base bonding observed with heavy metal complexes.<sup>39-41</sup> The model most appropriate for this work involves the  $\sigma^*$ -orbitals at the metal centre as it offers a qualitatively useful rationale for the structures of a number of Lewis base adducts of heavy main group atom complexes.<sup>40;43-46</sup>

## Chapter 3: Synthesis and Structures of the First Bismuth-Ester Complexes Using Hetero-Bifunctional Thiolate Anchored Ligands

### 3.1 Introduction

Compounds involving thiolates represent the most extensive series of bismuth complexes for which there is a reliable set of data, as a result of the high thermal and hydrolytic stability of the Bi-S bond.<sup>47</sup> As such, bismuth is considered to be very thiophilic. This term refers to the preference for certain atoms, especially heavy metals, to form strong bonds with sulfur as demonstrated by the observation of many sulfur-containing compounds or complexes.

Hard-soft acid-base theory (HSAB) has been used to explain thiophilicity,<sup>48</sup> although this theory provides only a rough guideline. Nevertheless, HSAB is a useful starting point and interprets the observation that hard acids favour bonds to hard bases over soft bases and vice versa. Soft acids and bases are regarded as more covalent and polarisable than hard acids and bases and hard atoms are considered to be those with high ionisation energies.<sup>49</sup> Molecular and atomic hardness and softness are often described in terms of frontier orbitals as hard acid-base pairs and soft acid-base pairs have different HOMO/LUMO separations as depicted in Figure 3.1. This separation is large for a hard acid-base complex such that the energetics of the interaction is primarily electrostatic. Conversely, the frontier orbital separation is small for a soft acid-base pair, giving a substantially covalent bond in the resulting complex. Using the example of the thiophilicity of bismuth, sulfur is considered to be a soft Lewis base and bismuth is a soft Lewis acid, hence, the thiophilicity of bismuth primarily involves a covalent interaction.

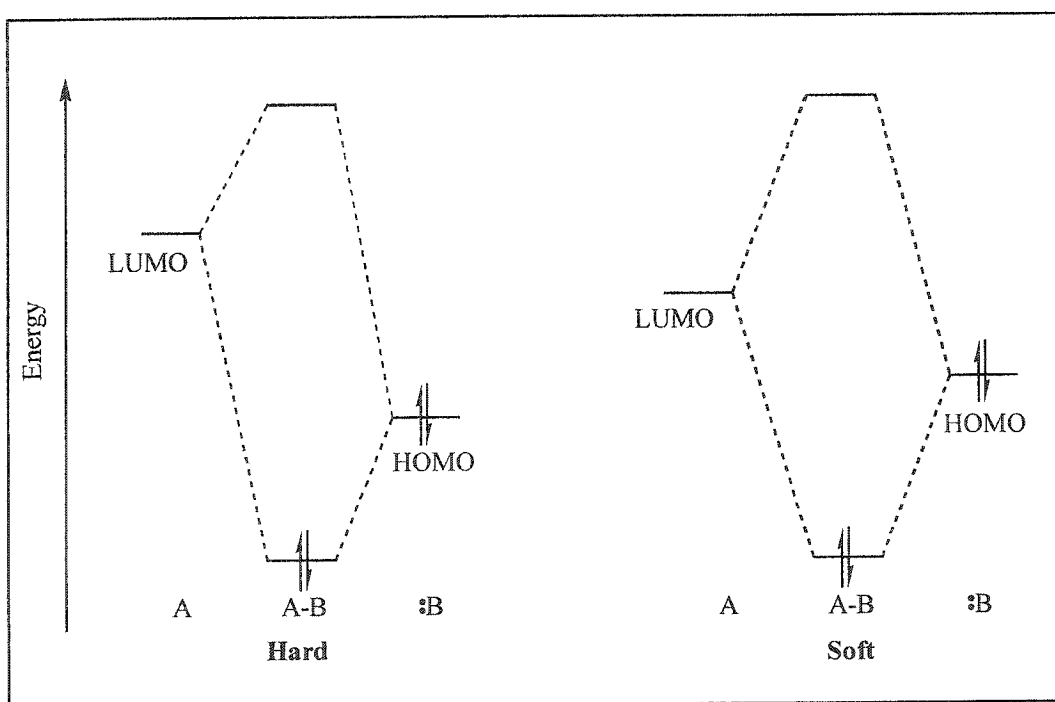
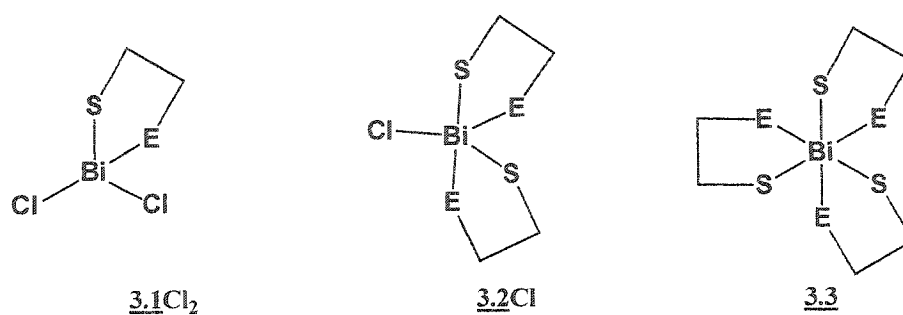


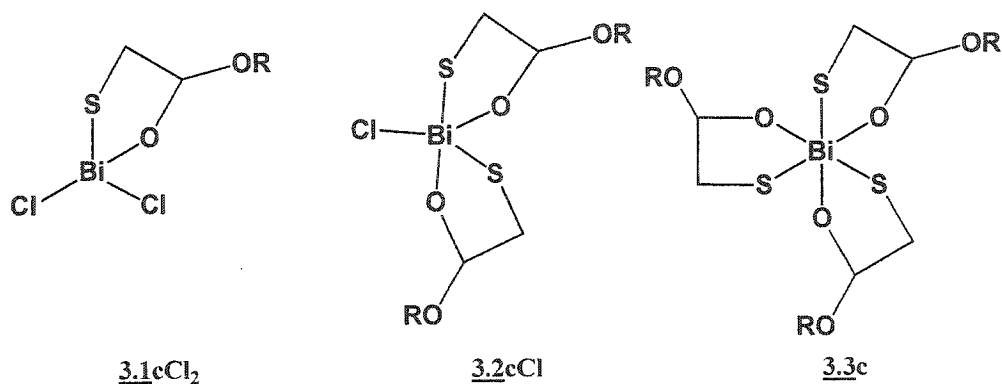
**Figure 3.1:** A qualitative orbital energy diagram depicting the frontier orbital separation between hard acid-base pairs and soft acid-base pairs.

Although there are many examples of bismuth-thiolate complexes, development of the coordination chemistry of bismuth has been hindered by the facile hydrolysis of many bismuth-element bonds. Complexes containing weakly donating functionalities can often be isolated only in the absence of moisture and many conventional types of ligands have yet to be observed coordinated with bismuth. In this context, the use of hetero-bifunctional ligands containing a thiolate group has been investigated.<sup>50-52</sup> The thiolate fragment serves to stabilise bismuth complexes with respect to hydrolysis and promotes or assists interaction of weaker tethered donors with bismuth. The utilisation of such ligands has enabled control of the reaction stoichiometry providing access to series of complexes bearing one, two, and three thiolate ligands, of which the chloride derivatives will be designated as **3.1Cl<sub>2</sub>**, **3.2Cl**, and **3.3**, respectively.

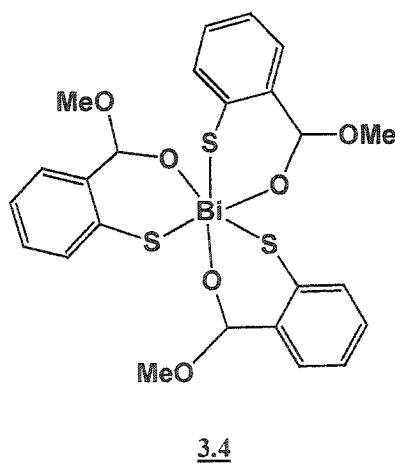
Complexes of bismuth involving hetero-bifunctional thiolate ligands exhibit substantially higher solubility as the auxiliary donor in these ligands mimics the role of donor solvents. Therefore, these compounds can be routinely recrystallised and are amenable to studies of solutions by ESI-MS. Extending this approach to ligands containing functional groups that are prevalent in biosystems, the first bismuth-ester complexes, **3.1cCl<sub>2</sub>**, **3.2cCl**, **3.3c** and **3.4**,<sup>53-55</sup> have been characterised comprehensively. ESI-MS and X-ray crystallographic data consistently shows chelate and ligand-bridged associated complexes, allowing for important comparisons with the chemistry of the pharmaceutical agents ‘bismuth subsalicylate’ (BSS; **1.1**) and ‘colloidal bismuth subcitrate’ (CBS; **1.2**)<sup>24,25,27,56-58</sup>



a: E = NR<sub>2</sub>  
b: E = OH



R = Me or Et

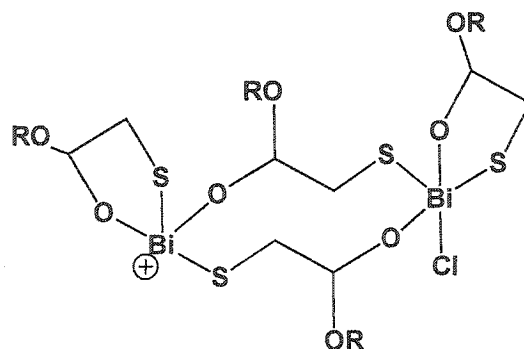


### 3.2 Results and Discussion

ESI-MS of reactions between methyl thioglycolate (MTG) and bismuth(III) chloride in absolute ethanol, 95% ethanol or methanol reveal the presence of mono-, bis- and tris-ester complexes of the type [3.1c]<sup>+</sup>, [3.2c]<sup>+</sup> and [3.3c]<sup>+</sup> as well as 'ligand-

bridged' dibismuth monocations  $[\underline{3.2c}\cdot\underline{3.2cCl}]^+$  and  $[\underline{3.3c}\cdot\underline{3.2c}]^+$ . The observations made from mass spectral data are consistent with the isolation and solid state characterisation data described for  $\underline{3.1cCl}_2$ ,  $\underline{3.2cCl}$  and  $\underline{3.3c}$ .

Figure 3.2 shows the ESI-MS of an equimolar reaction mixture of  $\text{BiCl}_3$  and MTG in absolute ethanol. The prominent mass peaks that contain bismuth all possess ethoxide functionalities (rather than the methoxide) indicating that quantitative transesterification of the ligand has occurred.<sup>59</sup> HCl resulting from the metathetical thiolation of bismuth is responsible for acidic conditions that facilitate exchange of methoxide for ethoxide from the solvent. With an equilibrium constant typically near unity, the transesterification reaction is driven to completion by the excess of ethanol. Consistently,  $\underline{3.2cCl}$  ( $R = \text{Me}$ ) is the only product isolated from the analogous reaction performed in methanol. Tandem ESI-MS data confirm the identification of  $[\underline{3.1c}]^+$ ,  $[\underline{3.2c}]^+$  and the sodiated complexes  $[\text{Na}\underline{3.2cCl}]^+$  and  $[\text{Na}\underline{3.3c}]^+$ . The presence of sodium in these complexes is an artifact of sodium ions being leached from the glassware by the solvent. An adduct  $[\underline{3.2c}\cdot\underline{3.2cCl}]^+$  is assigned to a peak at  $m/z$  929, for which we propose the topological ligand-bridged structure based on the solid state structures described later in this section.



$\underline{3.2c}\cdot\underline{3.2cCl}$

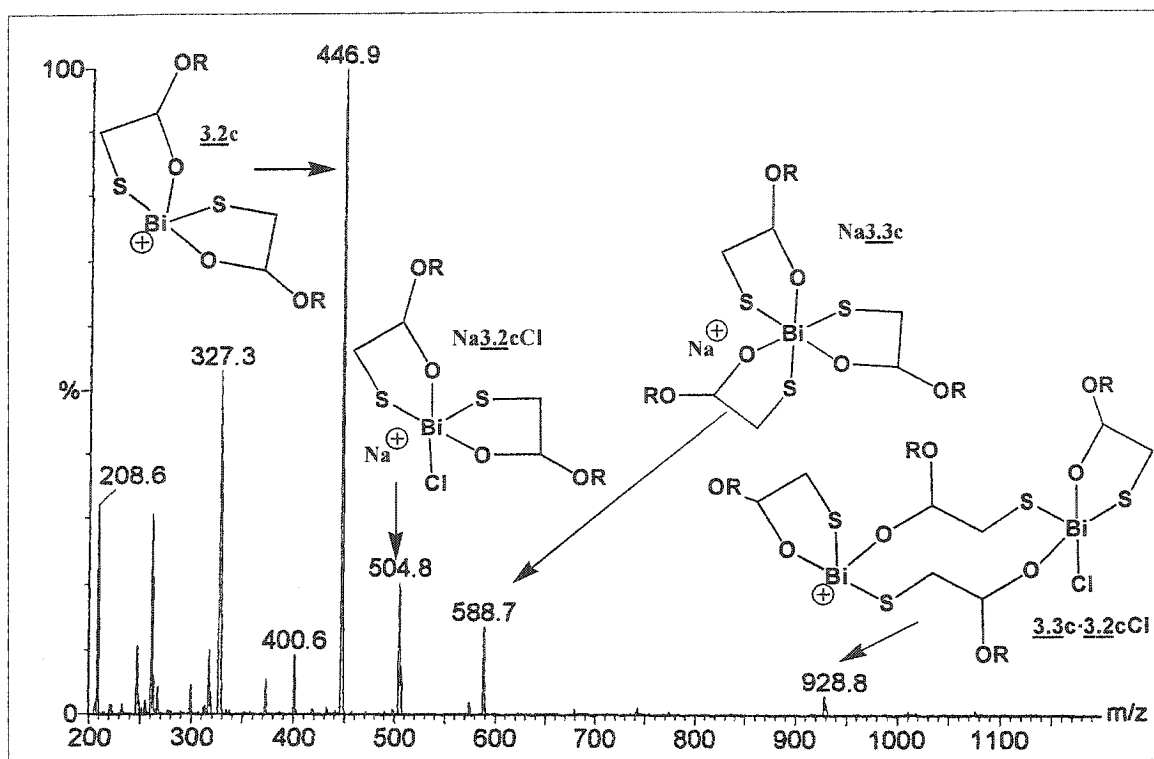


**Figure 3.2:** ESI-MS of a reaction mixture containing  $\text{BiCl}_3$  and MTG in absolute ethanol.

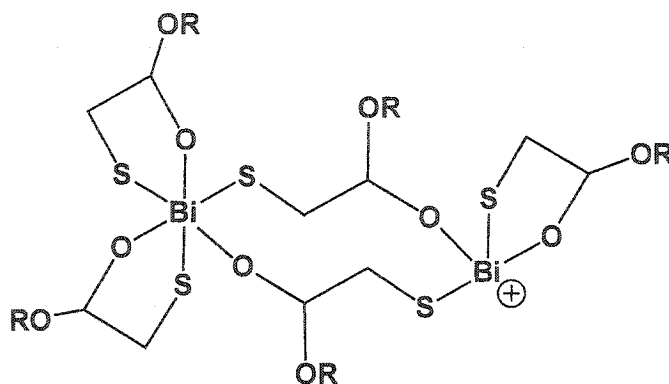
Assignments for prominent peaks are based on ESI-MS/MS data and represent

monocations:  $m/z$  327 3.1c ( $\text{R} = \text{Et}$ );  $m/z$  447 3.2c ( $\text{R} = \text{Et}$ );  $m/z$  505  $\text{Na}\underline{3.2c}\text{Cl}$  ( $\text{R} = \text{Et}$ );

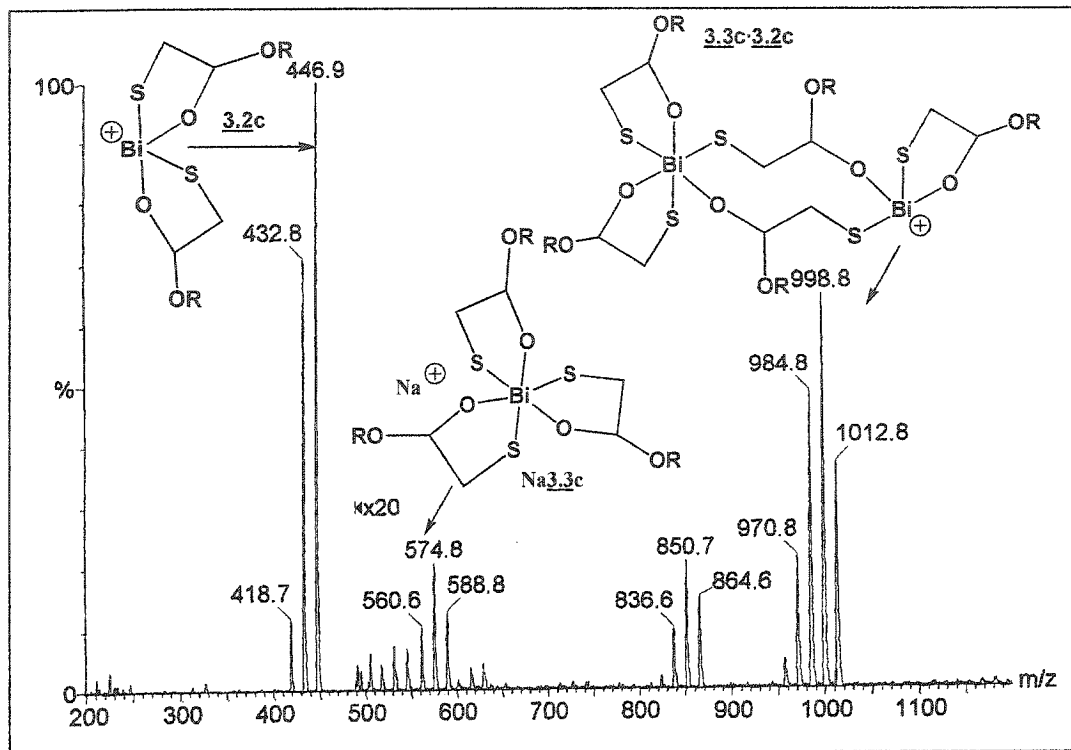
$m/z$  589  $\text{Na}\underline{3.3c}$  ( $\text{R} = \text{Et}$ );  $m/z$  929  $\underline{3.2c}\text{-}\underline{3.2c}\text{Cl}$  ( $\text{R} = \text{Et}$ ).



Transesterification of the ligand is mediated in 95% ethanol, as illustrated in Figure 3.3, which shows an ESI-MS of a reaction mixture involving excess MTG ( $\text{BiCl}_3 + 2\text{MTG}$ ). All combinations of ethyl ( $\text{R} = \text{Et}$ ) and methyl ( $\text{R} = \text{Me}$ ) derivatives of  $[\underline{3.2c}]^+$  and  $[\text{Na}\underline{3.3c}]^+$  are observed, as well as the ligand-bridged adduct  $[\underline{3.3c}\cdot\underline{3.2c}]^+$ .

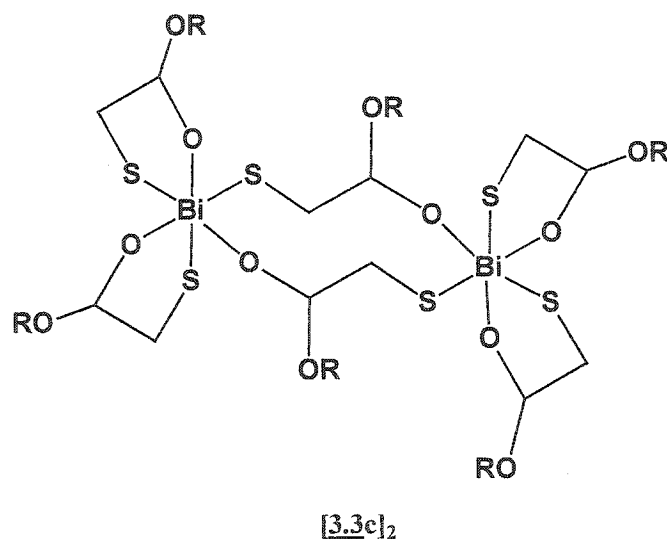


$\underline{3.3c}\cdot\underline{3.2c}$



**Figure 3.3:** ESI-MS of a reaction mixture containing  $\text{BiCl}_3$  and 2 equivalents of MTG in 95% ethanol. The peak intensity is x20 from  $m/z$  475-1000. Assignments for prominent peaks are based on ESI-MS/MS data and represent monocations:  $m/z$  419 3.2c ( $R = \text{Me}$ );  $m/z$  433 3.2c ( $R = \text{Me, Et}$ );  $m/z$  447 3.2c ( $R = \text{Et}$ );  $m/z$  547 Na3.3c ( $R = \text{Me}$ );  $m/z$  561 Na3.3c ( $R = 2\text{Me, Et}$ );  $m/z$  575 Na3.3c ( $R = \text{Me, 2Et}$ );  $m/z$  589 Na3.3c ( $R = \text{Et}$ );  $m/z$  943 3.3c·3.2c ( $R = \text{Me}$ );  $m/z$  957 3.3c·3.2c ( $R = 4\text{Me, Et}$ );  $m/z$  971 3.3c·3.2c ( $R = 3\text{Me, 2Et}$ );  $m/z$  985 3.3c·3.2c ( $R = \text{Me, 3Et}$ );  $m/z$  999 3.3c·3.2c ( $R = \text{Me, 4Et}$ );  $m/z$  1013 3.3c·3.2c ( $R = \text{Et}$ ).

Figure 3.4 shows the ESI-MS of the reaction mixture involving an excess of KMTG ( $\text{BiCl}_3 + 3\text{MTG} + 3\text{KOH}$ ) in 95% ethanol, in which thiolation of bismuth is facilitated by KCl metathesis. In this spectrum potassiated complexes are more prevalent than sodiated complexes. Most interesting is the potassiated ligand-bridged dimer  $[\text{K}[\mathbf{3.3}]_2]^+$ , which is consistent with the solid state structure of  $[\mathbf{3.3c}]_2$ . The absence of ethyl ester derivatives is a result of the presence of KOH in the reaction mixture, which serves to maintain a reasonably high pH and precludes transesterification of the ligand.



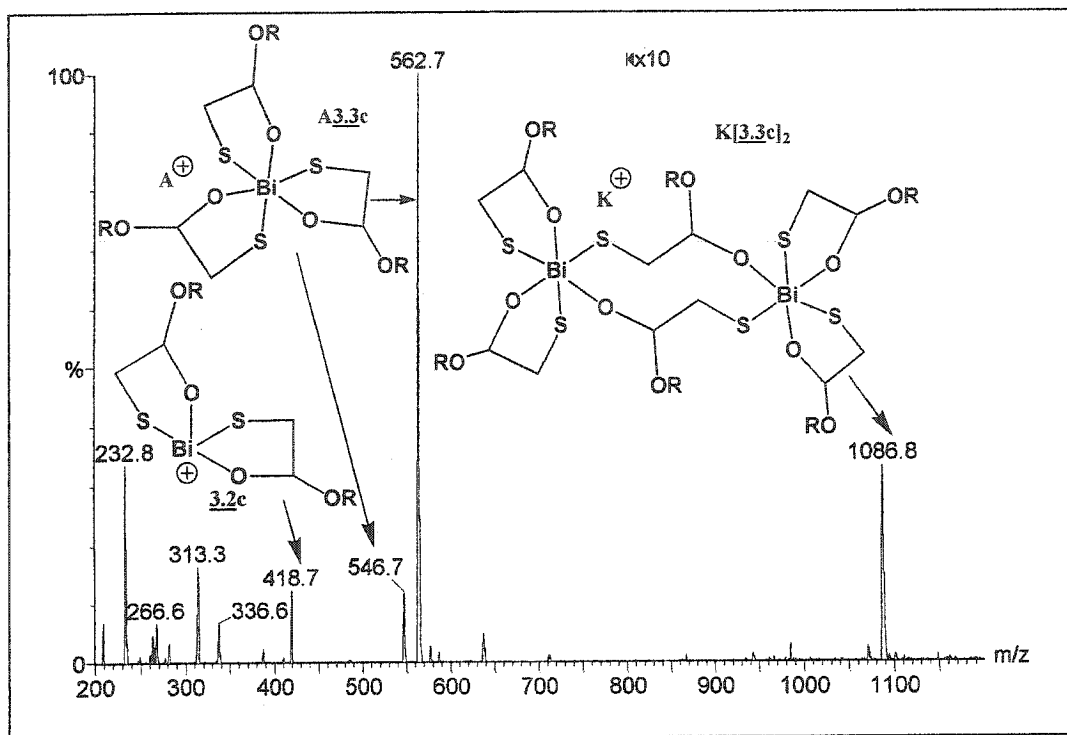


**Figure 3.4:** ESI-MS of a reaction mixture containing  $\text{BiCl}_3$  and 3 equivalents of MTG and KOH in 95% ethanol. The peak intensity is  $\times 10$  from  $m/z$  800 to 1000. Assignments for prominent peaks are based on ESI-MS/MS data and represent monocations:  $m/z$  419 3.2c ( $R = \text{Me}$ );  $m/z$  547  $\text{Na}\underline{3.3c}$  ( $R = \text{Me}$ ,  $A = \text{Na}$ );  $m/z$  563  $\text{K}\underline{3.3c}$  ( $R = \text{Me}$ ,  $A = \text{K}$ );  $m/z$  1087  $\text{K}[\underline{3.3c}]_2$  ( $R = \text{Me}$ ).

Reaction mixtures containing  $\text{BiCl}_3$  with methylthiosalicylate (MTS), or potassium methylthiosalicylate (KMTS) in ethanol at various stoichiometric combinations (1:1, 1:2; Bi:Ligand) were examined by ESI-MS. Irrespective of stoichiometry, prominent peaks are present in these spectra corresponding to the monocations  $[\text{K } \underline{\text{3.4}}]^+$ ,  $[\text{Na } \underline{\text{3.4}}]^+$  and  $[\underline{\text{3.5}}]^+$ , respectively. A representative spectrum of the equimolar reaction mixture containing  $\text{BiCl}_3$  and KMTS is provided in Figure 3.5. The tris-  $[\underline{\text{3.4}}]^+$  and bithiolate  $[\underline{\text{3.5}}]^+$  complexes are consistent with the ester-thiolate derivatives, and the solid state structures reported for the amino-thiolate complexes.<sup>52</sup> Peaks are also present in these spectra consistent with sodiated and potassiated disulfide dimers of the MTS ligand ( $[\underline{\text{3.6}}]^+$ ). It is interesting to note that in contrast to the reaction mixtures containing the ester-thiolates of bismuth,<sup>54</sup> the acidic mixtures containing  $\text{BiCl}_3$  and MTS do not demonstrate the occurrence of transesterification.

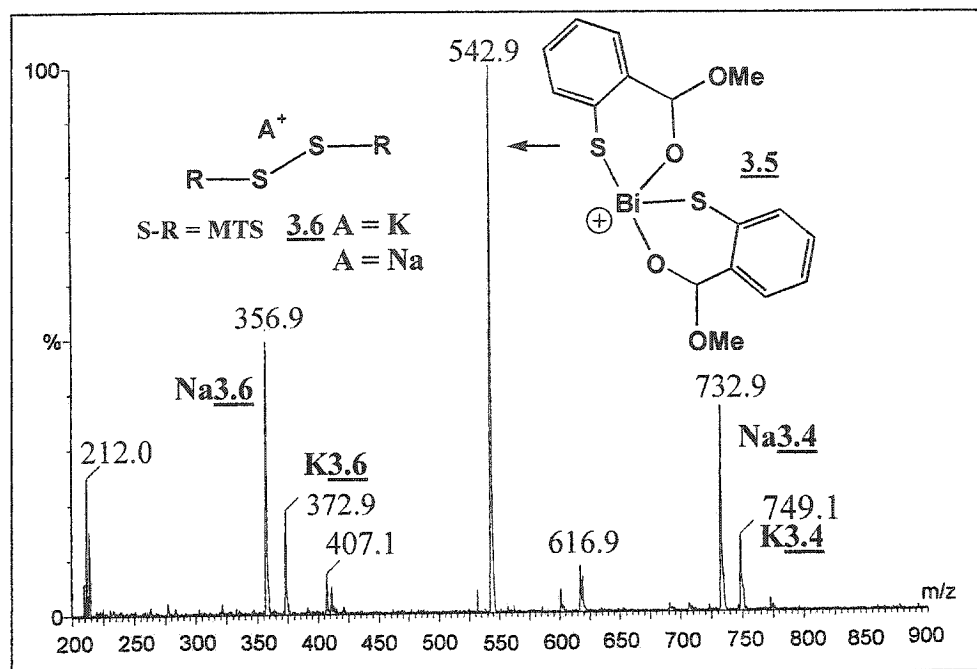


**Figure 3.5:** Representative ESI-MS of an equimolar reaction mixture containing  $\text{BiCl}_3$  and KMTS in ethanol. Structural assignments for prominent peaks are based on ESI-MS/MS data and represent monocations.

The three thiolation products [(ethylester)methane-thiolato]dichlorobismuth **3.1cCl<sub>2</sub>**, bis[(methylester)methanethiolato]chlorobismuth **3.2cCl** and tris[(methylester)methanethiolato]-bismuth **3.3c** are nominally obtained from the reaction mixtures containing bismuth chloride with MTG used in the ESI-MS experiments described previously.

The solid state structures of **3.1cCl<sub>2</sub>** (R = Et), **3.2cCl** (R = Me) and [**3.3c**]<sub>2</sub> (R = Me) have been confirmed by X-ray crystallography and Figure 3.6 shows the crystallographic views. Table 3.1 provides a comparison of selected bond lengths for each of the compounds. The interaction of the carbonyl donor is promoted by the chelate arrangement in most cases, but a non-chelate arrangement is evident for **3.3c**. There are few reported examples of bismuth complexes involving O<sub>carbonyl</sub> donors. Most also rely on hetero-bifunctional ligands and Bi-O<sub>carbonyl</sub> bond lengths range from 2.31-2.46 Å,<sup>60-64</sup> which compares with the range (2.4-2.6 Å) reported for structures of CBS.<sup>23,25-27,57</sup> These thiolate anchored complexes exhibit considerably longer Bi-O<sub>carbonyl</sub> bonds (2.56-2.86 Å) perhaps as a result of the preference for Bi-S bonds.

Compounds **3.1cCl<sub>2</sub>** and **3.3c** are dimeric in the solid state, while **3.2cCl** is polymeric. Compound **3.1cCl<sub>2</sub>** (R = Et) associates *via* μ-thiolate interactions (Figure 3.6(i)), and the chelated carbonyl oxygen imposes a distorted square pyramidal environment for bismuth. Compound **3.2cCl** (R = Me) forms a one-dimensional polymeric array (representative section shown in Figure 3.6(ii)) with hepta-coordination for bismuth imposed by four equatorially disposed sulfur centres, two oxygen centres (carbonyl) and a chloride. The four essentially equivalent Bi-S distances can be understood in terms of the strong trans influence<sup>65</sup> resulting from intermolecular Bi-S

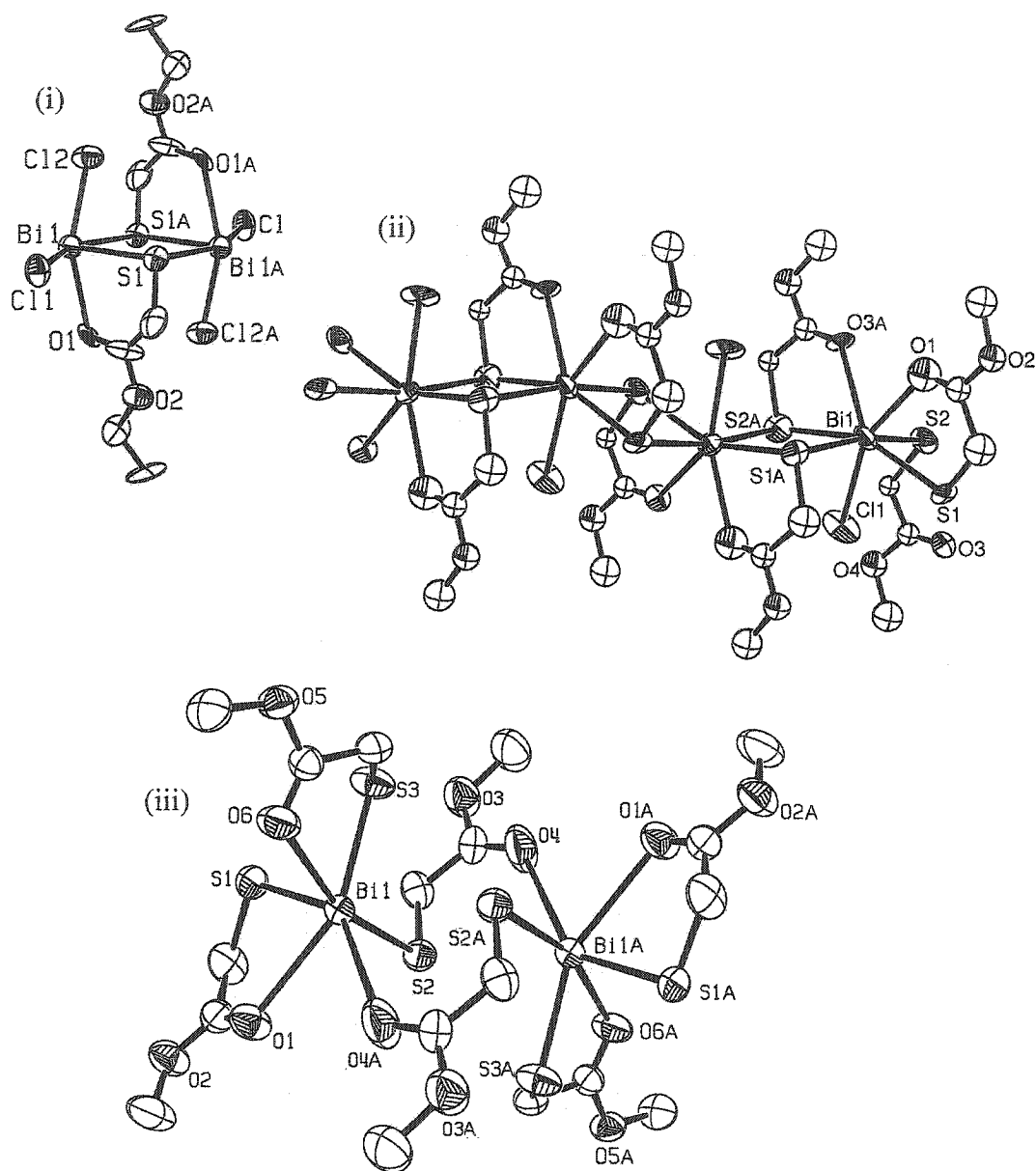
contacts. Consequently, the shorter Bi-S distances in 3.2cCl are longer than those observed in 3.3c, while the longer intermolecular contacts in 3.2cCl are shorter than those observed in both 3.1cCl<sub>2</sub> and 3.3c. Although a molecular unit represented by drawing 3.2Cl is not discernable in the polymeric solid state structure of 3.2cCl, there is a clear analogy with the bis(hydroxyethanethiolate) 3.2aCl<sup>50</sup> and bis(aminoethanethiolate) 3.2bCl<sup>52</sup> complexes. The structure of 3.3c may be viewed as a dimer [3.3c]<sub>2</sub> (Figure 3.6(iii)) involving two bridging and four terminal chelate ligands. The bridging ligands exhibit chelation with a longer  $\mu$ -thiolate Bi—S—Bi distance [Bi—S(2A), 3.331(2) Å] than that responsible for the bridging ligand interaction [Bi-S(2), 2.608(2) Å]. Interestingly, the Bi-S distance trend for the series 3.1cCl<sub>2</sub> > 3.2cCl > 3.3c is counter that of the Bi-O distance trend (3.1cCl<sub>2</sub> < 3.2cCl < 3.3c).

In comparison with the polymeric structure of 3.2cCl, substitution of the chloride for a third thiolate in 3.3c is manifested in a disruption of the equatorial (square plane, trans) arrangement of the sulfur interactions around bismuth resulting in a distorted facial arrangement of thiolate interactions and consequential relative shortening of Bi-S. The dimeric structure for [3.3c]<sub>2</sub>, imposed by the pendant ester ligand, is analogous to that observed for CBS (1.2),<sup>56;58</sup> but is relatively simple due to the presence of methyl groups that preclude the interdimer interactions observed in the latter.



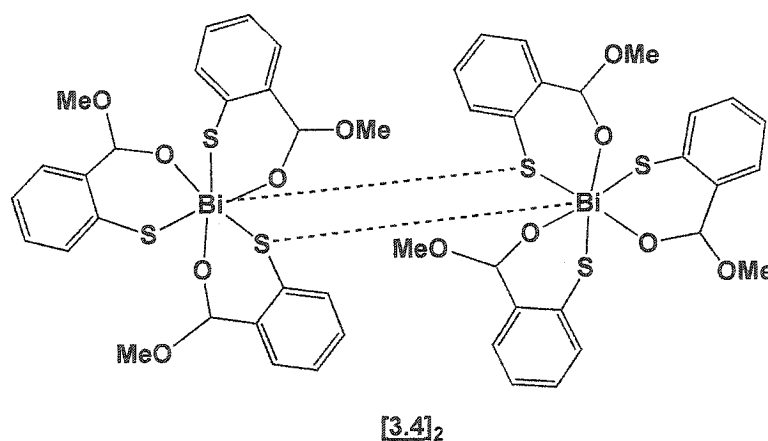
**Table 3.1:** Comparison of selected internuclear distances (Å) for the ester-thiolate complexes **3.1cCl<sub>2</sub>** (R = Et), **3.2cCl** (R = Me), **[3.3c]<sub>2</sub>** (R = Me) and **[3.4]<sub>2</sub>**.

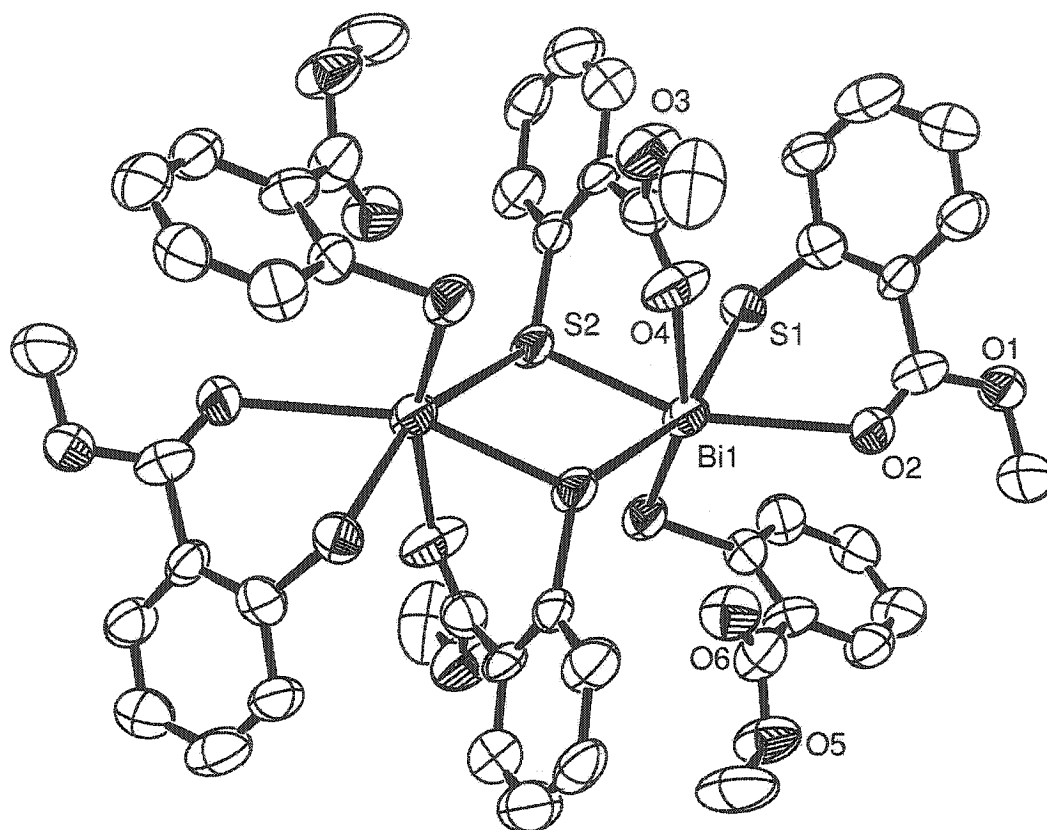
<b>3.1cCl<sub>2</sub></b> (R = Et)		<b>3.2cCl</b> (R = Me)		<b>[3.3c]<sub>2</sub></b> (R = Me)		<b>[3.4]<sub>2</sub></b>	
Bi-O1	2.562(6)	Bi-O1	2.68(2)	Bi-O1	2.807(5)	Bi-O2	2.84(1)
		Bi-O3A	2.77(2)	Bi-O6	2.861(5)	Bi-O4	2.72(1)
				Bi--O4A	3.071(7)	Bi-O6	3.08(2)
Bi-S1	3.021(2)	Bi-S1	2.849(7)	Bi-S1	2.568(2)	Bi-S1	2.606(5)
		Bi-S2	2.884(6)	Bi-S2	2.608(2)	Bi-S2	2.597(5)
				Bi-S3	2.574(2)	Bi-S3	2.602(6)
Bi--S1A	3.250(2)	Bi--S1A	2.963(7)	Bi--S2A	3.331(2)	Bi--S2A	3.277(5)
		Bi--S2A	2.861(9)				
Bi-Cl1	2.593(2)	Bi-Cl1	2.535(6)				
Bi-Cl2	2.552(2)						
Bi-Cl1A	3.371(3)						
Bi-Cl2A	3.565(3)						



**Figure 3.6:** Crystallographic views of (i) 3.1cCl<sub>2</sub>, (ii) 3.2cCl and (iii) [3.3c]<sub>2</sub>. Hydrogen atoms have been omitted for clarity.

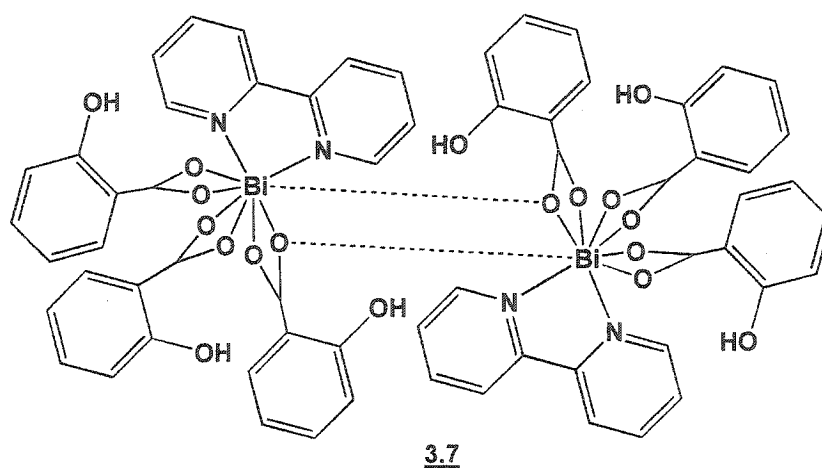
Tris(methylthiosalicylato)bismuth(III) **3.4** has been isolated and structurally characterised in the solid state and the crystallographic view is provided in Figure 3.7. As with the tris[(methylester)methane thiolato]bismuth(III) complex **[3.3c]<sub>2</sub>** (R = Me), compound **3.4** adopts a dimeric arrangement **[3.4]<sub>2</sub>** in contrast to the complicated hexanuclear structure of a thiosalicylate derivative reported by Asato and coworkers in 1994.<sup>66</sup> However, the ligand-bridged dimeric structures of **[3.3c]<sub>2</sub>**<sup>53;54</sup> and **1.2**,<sup>25-27;56;57</sup> involve pendant ligand linkages, while **[3.4]<sub>2</sub>** associates through  $\mu$ -thiolate bridges similar to that observed for **3.1c** and **3.2c**. The bond lengths of **[3.4]<sub>2</sub>** are listed in Table 3.1 and are comparable to those of **[3.3c]<sub>2</sub>**. Coordinate interaction of the carbonyl donor with bismuth is also apparent in **[3.4]<sub>2</sub>**, analogous to that observed for **3.1c** – **3.3c**, such that two of the methylthiosalicylate ligands chelates through six-membered chelate rings bringing the coordination number of bismuth to six.

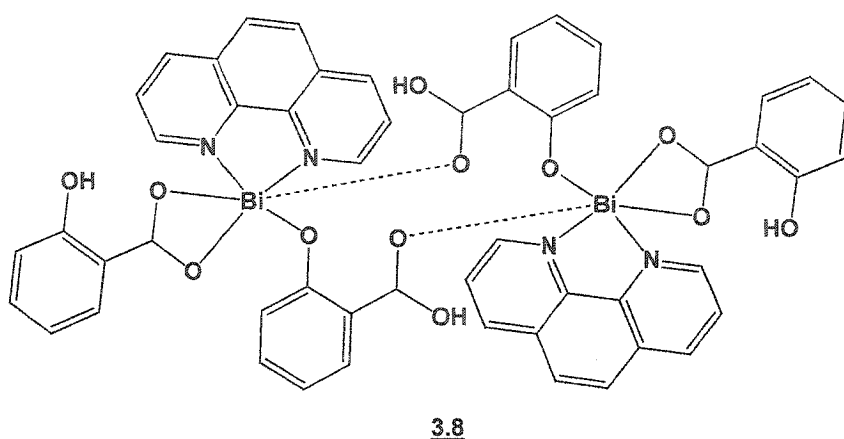




**Figure 3.7:** Crystallographic view of  $[3.4]_2$ . Hydrogen atoms have been omitted for clarity.

In 2002, Whitmire and coworkers<sup>67</sup> reported the structures of two bismuth-salicylate complexes,  $[\text{Bi}(\text{Hsal})_3(\text{bipy}) \cdot \text{C}_7\text{H}_8]_2$  (**3.7**) and  $[\text{Bi}(\text{Hsal})(\text{sal})(\text{phen}) \cdot \text{C}_7\text{H}_8]_2$  (**3.8**) that can be compared with that of **3.4**. In contrast to the conditions from which **3.4** was isolated, the isolation and crystallisation of **3.7** and **3.8** were facilitated by either 2,2'-bipyridine or 1,10-phenanthroline. Although both **3.7** and **3.8** are dimeric in the solid state, these complexes associate through  $\mu\text{-O}_{\text{carbonyl}}$  bridges. Compound **3.7** consists of a nona-coordinate bismuth centre, with the remaining coordination sites occupied by three monoanionic salicylate ligands chelating through the carboxylate groups to form four-membered chelate rings and  $N,N'$ -chelation from the bipyridyl group. Compound **3.8** has a seven coordinate bismuth centre involving both a dianionic and monoanionic salicylate ligand. The monoanionic ligand coordinates *via* the carboxylate group analogous to that of **3.7**, while the dianionic salicylate is coordinated through both the phenolic and carboxylate groups to form a six-membered chelate ring. The 1,10-phenanthroline occupies the two other coordination sites.





### 3.3 Conclusions

A series of the first (ester-thiolato)bismuth complexes has been identified using a variety of characterisation techniques. Most useful is ESI-MS to characterise reaction mixtures such that a broader appreciation of the chemistry of ester-thiolates with bismuth is obtained and definitive relationships between gas phase and solid state samples have been identified.

Compounds **3.1cCl<sub>2</sub>**, **3.2cCl**, **3.3c**, and **3.4** have been isolated from these reaction mixtures and crystallographically characterised. These structures represent simple models of medically relevant bismuth-carboxylates and emerge as potential platforms for the study of bismuth pharmaceutical agents such as BSS (**1.1**) and CBS (**1.2**). In addition, the results illustrate the coordinative flexibility of bismuth(III) and confirm the general synthetic applicability of hetero-bifunctional thiolate ligands to facilitate and stabilise interactions between bismuth and weak donors.

## Chapter 4: Mass Spectrometric Identification of Bismuth Complexes Involving Carboxylate Derivatives

### 4.1 Introduction

This chapter discusses the identification of bismuth complexes involving carboxylate derivatives (mercaptosuccinate, thiosalicylate,<sup>55</sup> malate and succinate) using ESI-MS. Given the biorelevance of bismuth chemistry and the medicinal use of bismuth preparations involving carboxylate ligands, such as salicylate and citrate, much emphasis has been placed on investigating the chemistry of bismuth with carboxylates and carboxylate derivatives. Indeed, citrate salts of bismuth represent the most extensively investigated series of bismuth compounds and there are a variety of formulae based on solid state structures and other characterisation methods reported for “colloidal bismuth subcitrate” (CBS)<sup>25-27;56;57;68-77</sup> In addition to the studies of bismuth-citrate salts, there have been many investigations involving simple hydroxy-carboxylic acid ligands including lactic<sup>78</sup>, malic,<sup>79</sup> and tartaric acid,<sup>79;80</sup> which have been crystallographically characterised. A number of bismuth complexes involving thioglycolic acid have also been isolated<sup>81-83</sup> and assessed for pharmacological and antimicrobial activity.<sup>82</sup>

### 4.2 Results and Discussion

ESI-MS was performed on aqueous reaction mixtures containing bismuth(III) chloride and mercaptosuccinic acid (Msuc) at various stoichiometric combinations (1:1, 1:2, 1:3; Bi:ligand). These spectra demonstrate prominent peaks for monocations of mono – ([ $(1:1)\text{-H}^+$ ], 1:1:Cl) and bisthiolates (1:2) where assignments are given as

Bi:Msuc<sup>-</sup> ratios ( and Msuc<sup>-</sup> is the monoanionic conjugate base of Msuc) . Peaks are also observed for ligand-bridged dibismuth monocations of [(2:3:Cl)-H<sup>+</sup>]-, 2:3:2Cl and [(2:4)-H<sup>+</sup>] Bi:Msuc<sup>-</sup> ratios. These peaks are consistent with monocations observed from ESI-MS of reaction mixtures involving ester-thiolates of bismuth.<sup>54</sup> A representative mass spectrum of an equimolar reaction mixture of BiCl<sub>3</sub> and Msuc is provided in Figure 4.1 and a summary of prominent peaks at *m/z* values assigned to cations is listed in Table 4.1 together with their relative intensity and MS/MS assignments. Attempts to isolate crystalline material from the reaction mixtures to confirm the structures of bismuth-mercaptosuccinates were unsuccessful.



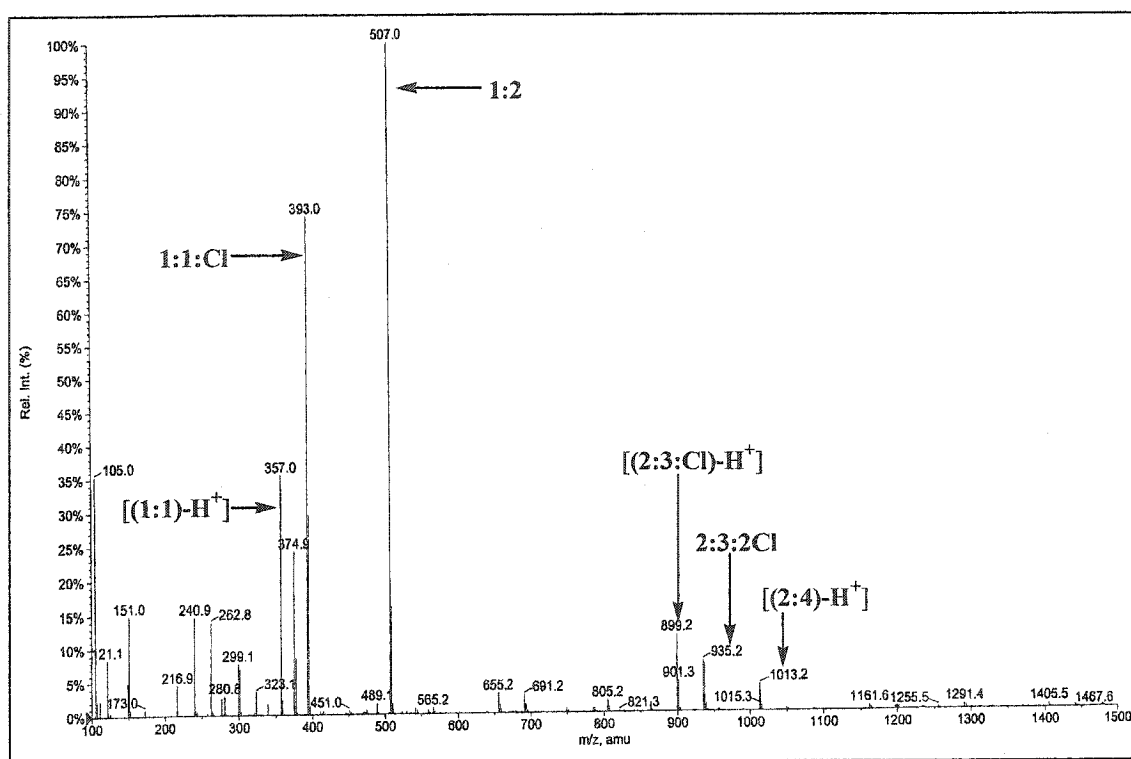
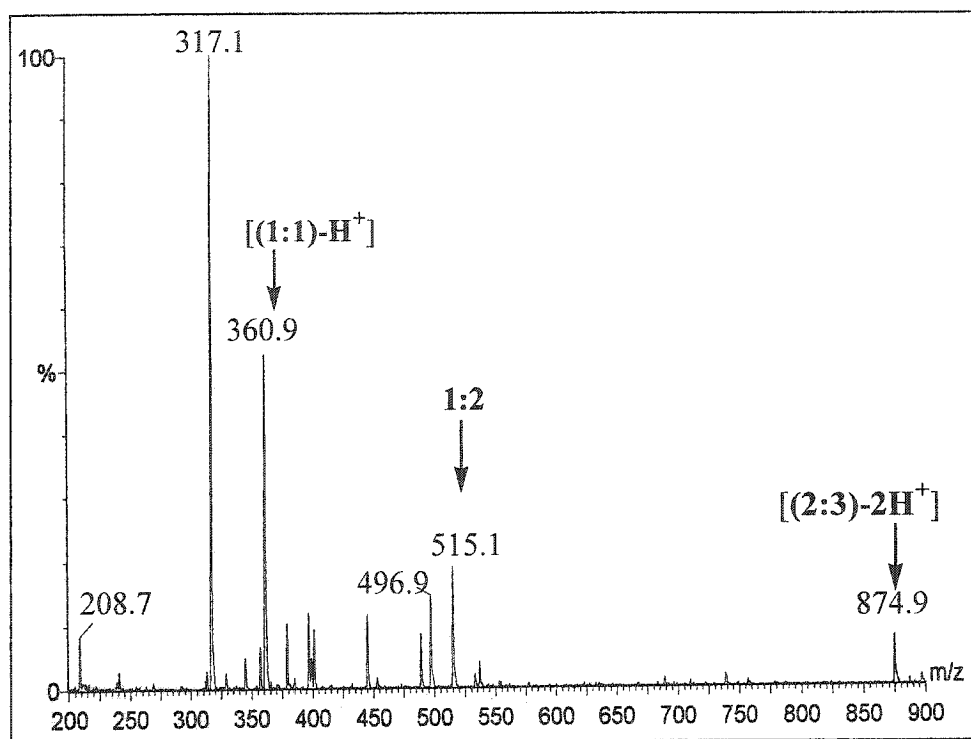


Figure 4.1: An ESI-MS of an equimolar aqueous reaction mixture of  $BiCl_3$  and Msuc.

**Table 4.1:** ESI-MS data of reaction mixtures containing  $\text{BiCl}_3$  with Msuc or Tsal, and  $\text{Bi}(\text{NO}_3)_3$  with Mal or Suc. Assignments are given as  $\text{Bi:Ligand}^+$  ratios (where  $\text{Ligand}^+$  is the monoanionic conjugate base of the ligand) or empirical formulae and are supported by MS/MS.

$m/z$	Assignment	Relative Intensity (%)	MS/MS ( $m/z$ )	Assignment
<b><math>\text{BiCl}_3 + \text{Msuc}</math></b>				
357.0	$[(1:1)\text{-H}^+]$	35	240.8 208.8	$\text{BiS}^+$ $\text{Bi}^+$
374.9	$\text{C}_4\text{H}_4\text{BiO}_3\text{S}^+$	25	240.8 208.8	$\text{BiS}^+$ $\text{Bi}^+$
393.0	1:1:Cl	75	357.0 240.8 208.8	$[(1:1)\text{-H}^+]$ $\text{BiS}^+$ $\text{Bi}^+$
507.1	1:2	100	357.0 240.8 208.8	$[(1:1)\text{-H}^+]$ $\text{BiS}^+$ $\text{Bi}^+$
655.1	$\text{C}_{12}\text{H}_{15}\text{BiO}_{11}\text{S}_3^+$	5	506.9 357.0 240.8 208.8	1:2 $[(1:1)\text{-H}^+]$ $\text{BiS}^+$ $\text{Bi}^+$
691.2	$\text{C}_{12}\text{H}_{16}\text{ClBiO}_{11}\text{S}_3^+$	4	654.9 506.9 357.0 240.8 208.8	$\text{C}_{12}\text{H}_{15}\text{BiO}_{11}\text{S}_3^+$ 1:2 $[(1:1)\text{-H}^+]$ $\text{BiS}^+$ $\text{Bi}^+$
899.1	$[(2:3)\text{-Cl})\text{-H}^+]$	10	863.0 506.9 356.8 209.0	$[(2:3)\text{-2H}^+]$ 1:2 $[(1:1)\text{-H}^+]$ $\text{Bi}^+$
935.2	2:3:2Cl	8	898.8 506.9 356.8 240.8 208.8	$[(2:3)\text{-Cl})\text{-H}^+]$ 1:2 $[(1:1)\text{-H}^+]$ $\text{BiS}^+$ $\text{Bi}^+$
1013.2	$[(2:4)\text{-H}^+]$	6	862.8 506.9 240.8	$[(2:3)\text{-2H}^+]$ 1:2 $\text{BiS}^+$
<b><math>\text{BiCl}_3 + \text{Tsal}</math></b>				
317.1	$\text{C}_6\text{H}_4\text{BiS}^+$	100	208.8	$\text{Bi}^+$
360.9	$[(1:1)\text{-H}^+]$	50	317.1 208.7	$\text{C}_6\text{H}_4\text{BiS}^+$ $\text{Bi}^+$
515.1	1:2	25	360.9 317.0 208.8	$[(1:1)\text{-H}^+]$ $\text{C}_6\text{H}_4\text{BiS}^+$ $\text{Bi}^+$
874.9	$[(2:3)\text{-2H}^+]$	10	515.0 361.0	1:2 $[(1:1)\text{-H}^+]$
<b><math>\text{Bi}(\text{NO}_3)_3 + \text{Mal}</math></b>				
340.9	$[(1:1)\text{-H}^+]$	30	209.0	$\text{Bi}^+$
474.9	1:2	15	340.9	$[(1:1)\text{-H}^+]$
<b><math>\text{Bi}(\text{NO}_3)_3 + \text{Suc}</math></b>				
324.9	$[(1:1)\text{-H}^+]$	5	209.0	$\text{Bi}^+$
342.9	1:1: $\text{H}_2\text{O}$	25	324.9	$[(1:1)\text{-H}^+]$
442.9	1:2	100	324.9 209.0	$[(1:1)\text{-H}^+]$ $\text{Bi}^+$
560.9	$[(1:3)\text{-H}^+]$	35	442.9	1:2
766.7	$[(2:3)\text{-2H}^+]$	15	442.9	1:2

ESI-MS was performed on reaction mixtures containing  $\text{BiCl}_3$  and thiosalicylic acid (Tsal) in ethanol of varying stoichiometric combinations (1:1, 1:2; Bi:Ligand). Irrespective of reaction stoichiometry, prominent peaks are observed in these spectra at  $m/z$  360.9 and 515.1 and are assigned to mono- ( $[(1:1)\text{-H}^+]$ ; Bi:Tsal<sup>-</sup> ratio where Tsal<sup>-</sup> is the monoanionic conjugate base of Tsal) and bithiolate (1:2) monocations, respectively. A peak is also present at  $m/z$  874.9 and is assigned to a  $[(2:3)\text{-2H}^+]$  Bi:Tsal<sup>-</sup> ratio and is speculated to represent a ligand-bridged dibismuth monocation. Unlike for the reaction mixtures of Msuc, the mixtures involving Tsal do not demonstrate peaks corresponding to cations containing chlorides. A representative spectrum of an equimolar reaction mixture of  $\text{BiCl}_3$  and Tsal is shown in Figure 4.2 and a summary of the ESI-MS data is presented in Table 4.1.



**Figure 4.2:** An ESI-MS of an equimolar reaction mixture containing  $BiCl_3$  and Tsal in ethanol.

ESI-MS of reaction mixtures containing bismuth(III) nitrate with either malic acid (Mal) or succinic acid (Suc) in 50 % ethanol/water demonstrate peaks corresponding to monocations of bismuth-carboxylates species. In the mass spectra of the bismuth-malate reaction mixture, peaks corresponding to the monocations of [(1:1)-H<sup>+</sup>] and 1:2 Bi:Mal<sup>-</sup> ratios (where Mal<sup>-</sup> is a monoanion conjugate base of Mal) are evident at  $m/z$  340.9 and  $m/z$  474.9. In the reaction mixture of Bi(NO<sub>3</sub>)<sub>3</sub> and Suc in 50 % ethanol/water, prominent peaks are observed corresponding to monocationic complexes of [(1:1)-H<sup>+</sup>], 1:2, [(1:3)+H<sup>+</sup>] and [(2:3)-2H<sup>+</sup>] Bi:Suc<sup>-</sup> ratios (Suc<sup>-</sup> is the monoanionic conjugate base of Suc). A monocation of bismuth with Sal<sup>-</sup> is also observed involving a water molecule [(1:1:H<sub>2</sub>O)-H<sup>+</sup>]. Representative mass spectra are provided in Figures 4.3 and 4.4 for reaction mixtures containing Bi(NO<sub>3</sub>)<sub>3</sub> and malic or succinic acids, respectively, and the summary of the ESI-MS data is presented in Table 4.2. ESI-MS of similar reaction mixtures containing lactic, tartaric, fumaric and pyruvic acids did not demonstrate peaks of ions involving bismuth, although in the case of lactate and tartrate, complexes of bismuth containing these ligands have been structurally characterised.<sup>78-80</sup> These observations may be indicative of the kinetic instability of such complexes under mass spectrometric conditions.

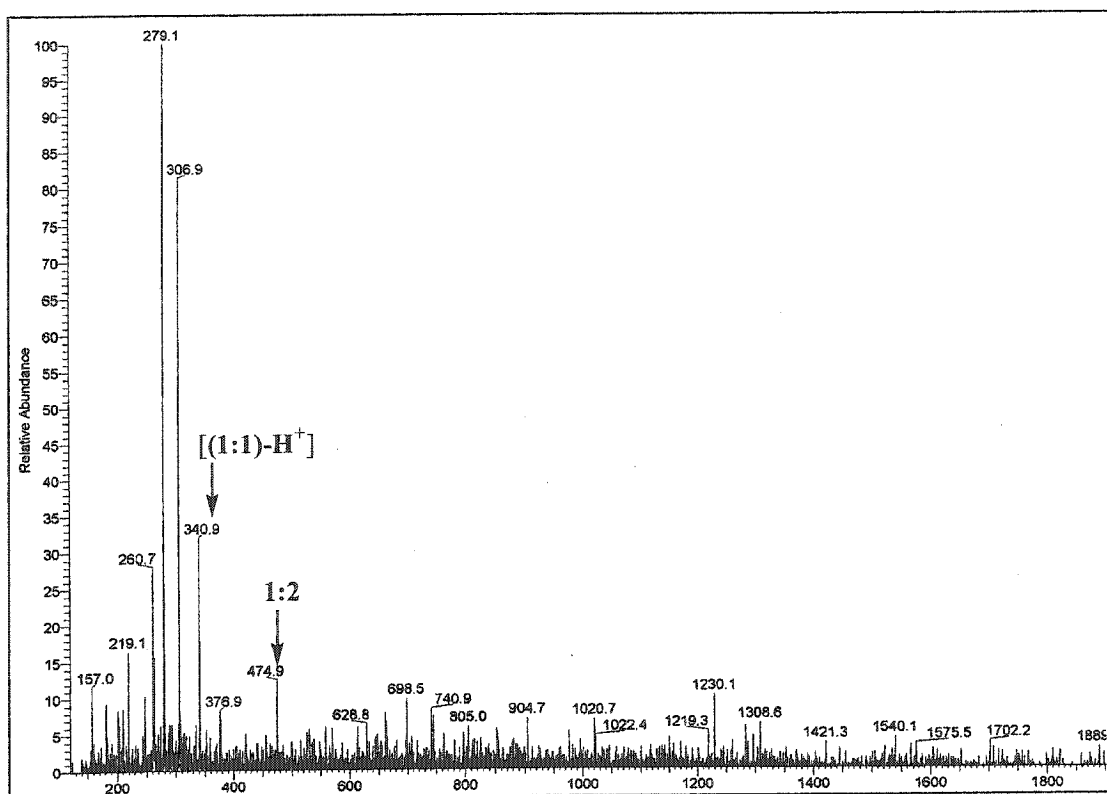


**Figure 4.3:** An ESI-MS of an equimolar reaction mixture of  $\text{Bi}(\text{NO}_3)_3$  and Mal in 50 % ethanol/water.

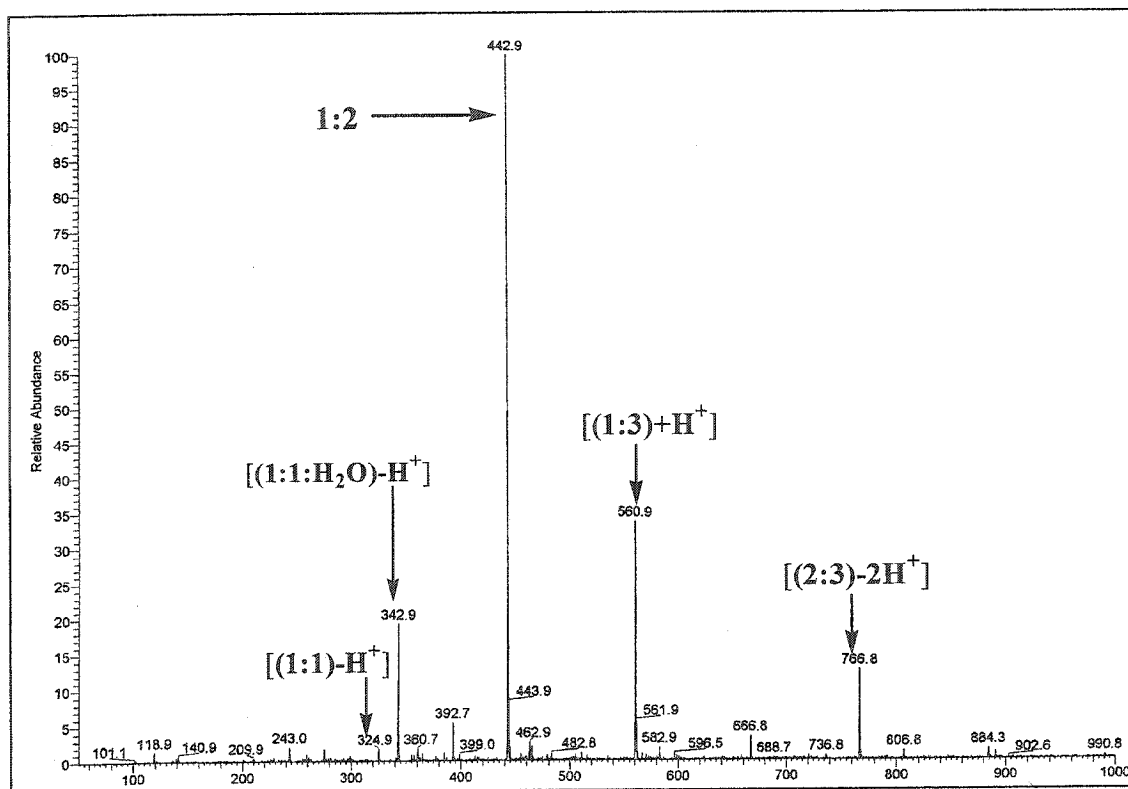


**Figure 4.4:** An ESI-MS of an equimolar reaction mixture of  $\text{Bi}(\text{NO}_3)_3$  and Suc in 50 % ethanol/water.

### 4.3 Conclusions and Future Directions

Complexes of bismuth involving thiolato- (Msuc and Tsal), hydroxy-(Mal) and dicarboxylates (Suc) have been identified by ESI-MS revealing a variety of stoichiometric combinations (eg. 1:1 – 2:4) for complexes of this type as a result of the polyprotic nature of carboxylate ligands. The observation of dibismuth cations of [(2:3)-2H<sup>+</sup>] Bi:Ligand ratios most likely represent ligand-bridged complexes analogous to those observed in mass spectra and in the solid state for the ester-thiolate complexes of bismuth. As such, the results re-emphasise the consideration of bismuth-ester complexes as simple models for the medically relevant bismuth-carboxylates.

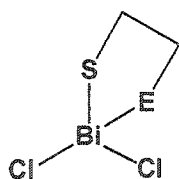
The value of thiolate anchors in hetero-bifunctional ligands to stabilise interactions between bismuth with biorelevant functional groups has also been confirmed in this chapter from the work concerning mercaptosuccinic acid and thiosalicylic acid. In addition, the importance of ESI-MS for assessing the chemistry of reaction mixtures has been demonstrated and this technique now arises as a potentially powerful and viable method for studying the chemistry of bismuth with carboxylate ligands of any type and especially those that are prevalent in bismuth pharmaceutical agents such as citrate.



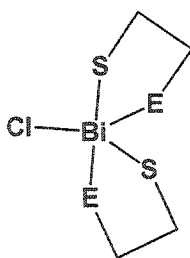
## Chapter 5: A Generally Applicable Synthetic Approach for Heteroleptic Thiolate Complexes of Bismuth

### 5.1 Introduction

The chemical database for bismuth is superficially developed as a result of the relative instability of many bismuth-elements bonds, especially towards hydrolysis. The high thermal and hydrolytic stability of the sulfur-bismuth bond are responsible for the fact that sulfur compounds represent the most extensive series of bismuth complexes for which there is a reliable set of data.<sup>47</sup> As such, it is now necessary to devise universally applicable synthetic procedures that enable rational development of the thiolate coordination chemistry for bismuth in the presence of other donors. To this end, complexes have been examined with hetero-bifunctional ligands bearing a thiolate functionality that serves as an anchor to promote or assist interaction of weaker tethered donors with bismuth. This has enabled control of the reaction stoichiometry, providing access to series of complexes bearing one (3.1Cl<sub>2</sub>), two (3.2Cl) and three (3.3) thiolate ligands.<sup>50;52;53</sup>

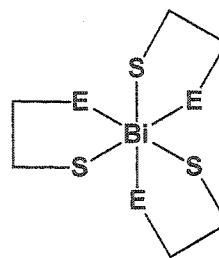


3.1Cl<sub>2</sub>

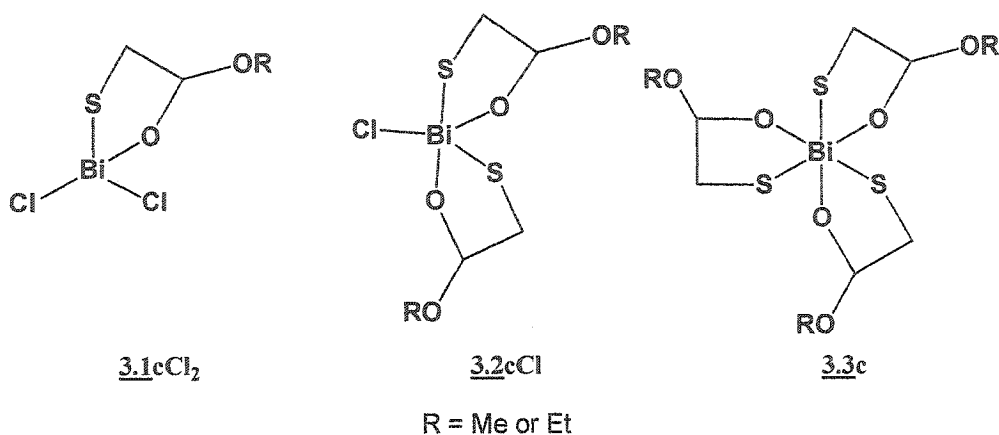


3.2Cl

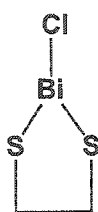
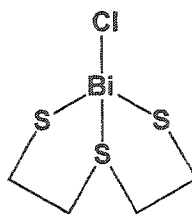
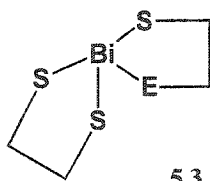
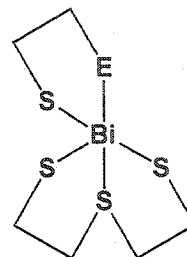
a: E = NR<sub>2</sub>  
b: E = OH



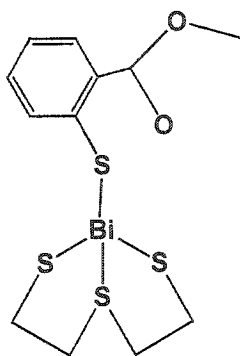
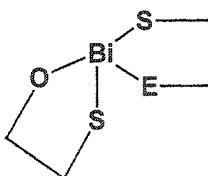
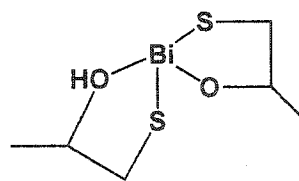
3.3



The first systematic preparation and comprehensive characterisation of heteroleptic complexes of bismuth involving bifunctional thiolate ligands is described in this chapter.<sup>84</sup> The facile synthesis and isolation of the chlorodithiolate compounds **5.1** and **5.2**<sup>85</sup> highlights their suitability as precursors for the synthesis of dithiolate/aminothiolates **5.3a** (R = Me) and **5.4a** (R = H), the dithiolate/hydroxy-thiolate **5.3b**, and the dithiolate/ester-thiolate **5.5**. Compound **3.1bCl<sub>2</sub>**, generated *in situ*, is similarly versatile and enables the isolation of the first oxothiolate-aminothiolate **5.6a** (R = H). These compounds are rare, resilient examples of amino-, hydroxy-, alkoxo- and ester-complexes of bismuth.

5.15.25.35.4a: E = NR<sub>2</sub>

b: E = OH

5.55.65.7

## 5.2 Results and Discussion

The utilisation of hetero-bifunctional thiolate ligands has been exploited to develop general synthetic procedures for heteroleptic bismuth complexes. The starting materials 5.1<sup>86</sup> and 5.2,<sup>85</sup> react slowly at room temperature with potassium thiolate solutions to produce a slurry with little or no change in the visual appearance of the reaction mixture. Nevertheless, the precipitates are characterised as analytically pure metathesis products formed in reasonable yield, although some yields are relatively low and conditions to optimise them have not yet been assessed.

Compounds 5.3 - 5.6a have been crystallographically and spectroscopically characterised. The molecular structures of each are provided in Figures 5.1 and 5.2 and selected bond lengths are compared with those of related compounds (5.1, 5.2, 3.1 – 3.4 and 5.7) in Table 5.1. The spirocyclic environments observed for bismuth in 5.3a, 5.3b, 5.4a and 5.6a confirm auxiliary coordination of the hydroxyl (5.3b), amino (5.3a, 5.4a) and alkoxide (5.6a) functional groups to the bismuth centre in each respective example. The structures are consistent with the homoleptic thiolate series 3.1-3.3,<sup>50;52;54</sup> except for compound 5.5 in that the ester functionality is terminal [Bi-O, 3.55(2) Å; c.f Bi-O 2.56-2.86 Å, showing no evidence of a chelating interaction with bismuth. This is an unexpected structural feature, when compared to the structure of the trithiolate compound of bismuth involving methyl thiosalicylate (3.4), which exhibits a definitively hexa-coordinate site for bismuth and typical Bi-O coordinate bond distances [Bi-O 2.72(2)-3.08(2)Å].<sup>54;55;84</sup> Although the cross-ring Bi-S2 distance is relatively long [3.0688(4) Å] in 5.5, this may lower the Lewis acidity of the bismuth centre to render the carbonyl donation ineffective.

Many of the complexes listed in Table 5.1 are observed to have Bi-S bond lengths within a narrow range (2.5-2.6 Å), such that the thiolate interaction is essentially independent of the number of thiolate ligands, the presence of auxiliary intramolecular coordination to bismuth or the number of intermolecular interactions at bismuth. The unusually long Bi-S bonds in 3.1cCl<sub>2</sub>, 3.2bCl and 3.2cCl are likely the result of the strong intermolecular interactions in the solid state that provide for a dimeric arrangement for 3.1cCl<sub>2</sub> and a polymeric (ribbon-like) structure for 3.2bCl and 3.2cCl.<sup>50;54</sup> The fourth Bi-S contact in 5.4a and 5.5 represent the intramolecular cross-ring thioether donation,

which is predictably weaker than those of the thiolates. The relatively weak interactions of the amines are presumably made possible by the thiolate anchor to the bismuth centre enabling a chelate arrangement. The Bi-N distances are comparable with those of the thiolates despite the smaller size of nitrogen and are comparable to those found in complexes involving pyridine derivatives,<sup>47</sup> which are in the range of the Bi-N distances listed in Table 5.1. The Bi-O distances are in agreement with the relative Lewis basicity of the oxygen donor in that interactions of hydroxyl (3.2bCl, 5.3b, 5.6b, 5.7) and carbonyl (3.1cCl<sub>2</sub>, 3.2cCl, 3.3c, 5.5, 4.3) ligands are longer than interactions with alkoxide (5.6a, 5.6b, 5.7) functionalities.

**Table 5.1:** Selected internuclear distances (Å) listed in order of increasing bond length (i.e.  $A < B < C < D$ ) for compounds represented by 3.1 - 3.4, and 5.1 - 5.7.

	Ref	Bi-S <sub>A</sub>	Bi-S <sub>B</sub>	Bi-S <sub>C</sub>	Bi-S <sub>D</sub>	Bi-N <sub>A</sub>	Bi-N <sub>B</sub>	Bi-N <sub>C</sub>	Bi-O <sub>A</sub>	Bi-O <sub>B</sub>	Bi-O <sub>C</sub>
<u>3.1a</u> Cl <sub>2</sub>	52	2.530(7)				2.52(2)					
<u>3.1c</u> Cl <sub>2</sub>	54	3.021(2)							2.562(6)		
<u>3.2a</u> Cl	52	2.569(3)	2.608(3)			2.398(8)	2.528(9)		2.86(1)		
<u>3.2b</u> Cl	50	2.558(4)	2.595(3)						2.80(1)	2.86(1)	
<u>3.2b</u> NO <sub>3</sub>	51	2.663(6)	2.853(6)						2.58(2)	2.64(2)	
<u>3.2c</u> Cl	54	2.849(7)	2.884(6)						2.68(2)	2.77(2)	
<u>3.3a</u>	52	2.567(5)	2.654(5)	2.748(7)		2.64(2)	2.81(2)	2.83(2)			
<u>3.3c</u>	54	2.568(2)	2.574(2)	2.608(2)					2.807(5)	2.861(5)	3.071(7)
<u>5.1-2py</u>	85	2.542(6)	2.545(4)								
<u>5.3a</u>	84	2.542(4)	2.572(4)	2.589(5)		2.72(1)					
		Bi-S3	Bi-S2	Bi-S1		Bi-N1					
<u>5.3b</u>	84	2.532(5)	2.558(5)	2.639(6)					2.77(2)	Bi-O1	
		Bi-S1	Bi-S2	Bi-S3							
<u>5.2</u>	85	2.541(6)	2.849(5)	3.534(7)							
<u>5.4a</u>	84	2.574(2)	2.592(3)	2.621(3)	3.248(3)	2.723(9)					
		Bi-S1	Bi-S4	Bi-S3	Bi-S2	Bi-N1					
<u>5.5</u>	84	2.543(5)	2.550(5)	2.602(5)	3.068(4)				3.55(2)		
		Bi-S3	Bi-S1	Bi-S4	Bi-S2				Bi-O1		
<u>3.4</u>	55	2.597(5)	2.602(6)	2.606(5)					2.72(2)	2.84(1)	3.08(2)
<u>5.6a</u>	84	2.57(2)	2.58(2)			2.41(7)			2.22(4)		
		Bi-S1	Bi-S2			Bi-N1			Bi-O1		
<u>5.6b</u>	51	2.527(3)	2.564(3)						2.195(9)	2.577(9)	
<u>5.7</u>	87	2.582(1)	2.560(1)						2.197(4)	2.589(4)	

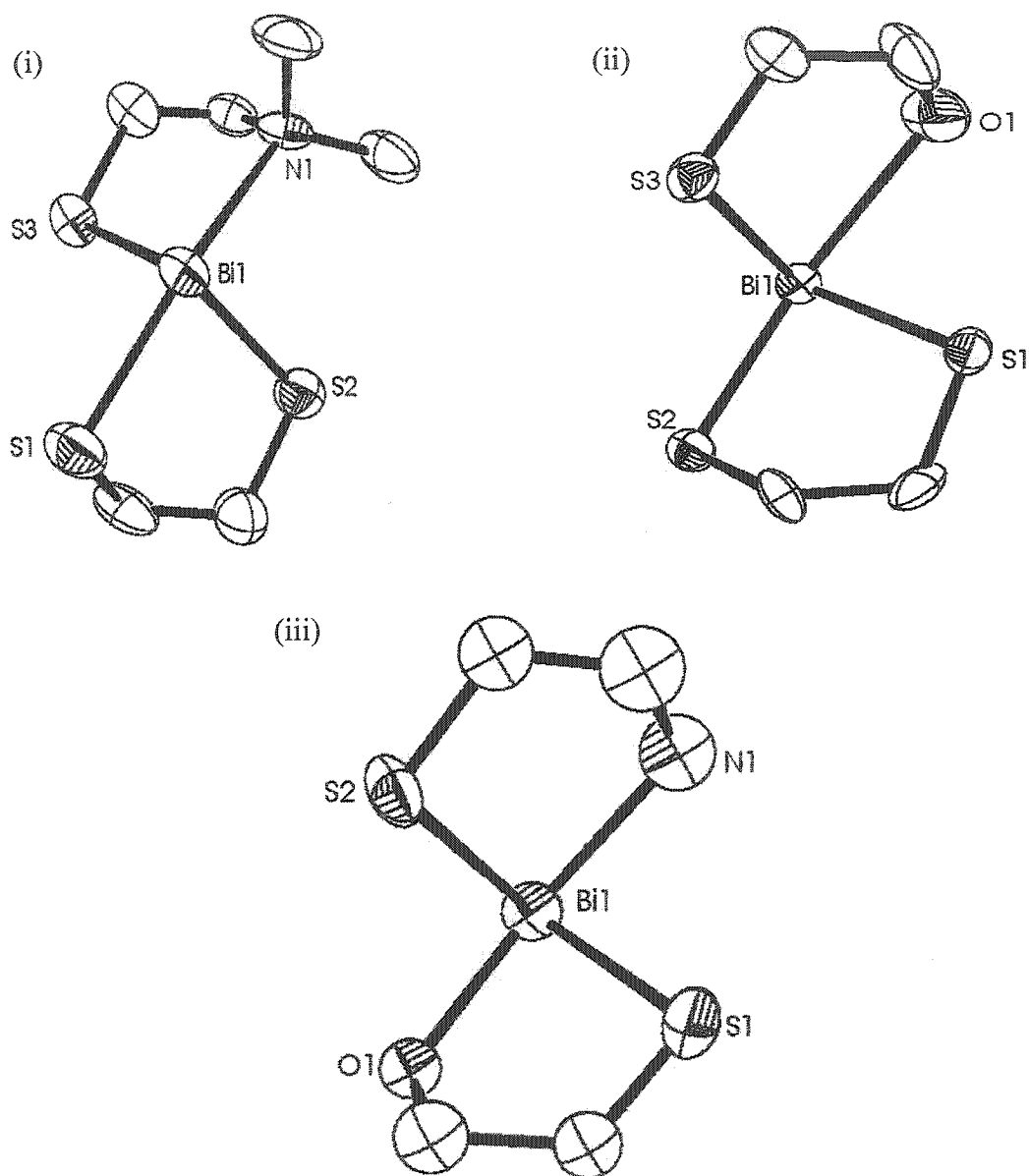


**Figure 5.1:** Crystallographic views of (i) **5.3a** ( $R = \text{Me}$ ), (ii) **5.3b**, and (iii) **5.6a** ( $R = \text{H}$ ).

Hydrogen atoms have been omitted for clarity.

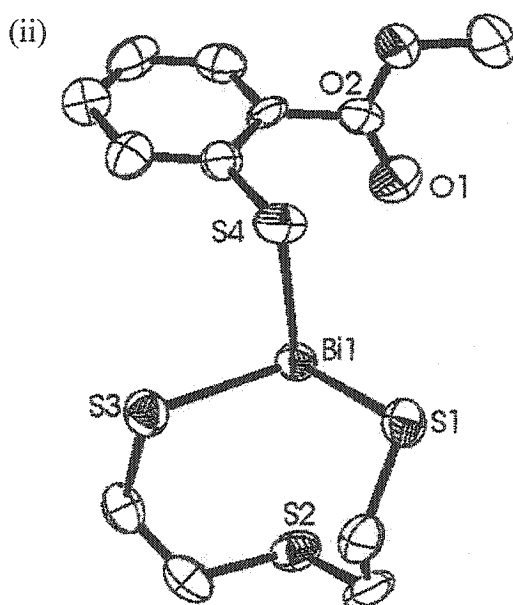
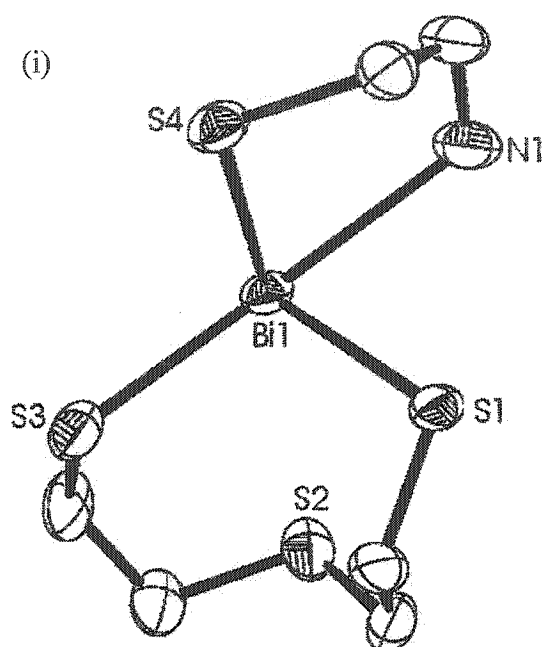


**Figure 5.2:** Crystallographic views of (i) **5.4a** (R = H) and (ii) **5.5**. Hydrogen atoms have been omitted for clarity.



### 5.3 Conclusions

Although the database for the thiolate chemistry of bismuth is extensive, many examples only represent unique complexes for a particular ligand. The series of compounds 5.3a, 5.3b, 5.4a, 5.5 and 5.6a described above represent a useful contribution to the developing database for the chelate-thiolate coordination chemistry of bismuth. The structures of these compounds, in addition to other bismuth complexes involving hetero-bifunctional ligands,<sup>50;52;54</sup> demonstrate that the geometry at bismuth varies considerably throughout the series of complexes and includes a variety of coordination numbers. The synthesis and characterisation of 5.3 - 5.6a validate the use of thiolates in bifunctional ligands as a synthetically versatile approach to study bismuth complexes involving weak Lewis donors and provides a general systematic and comprehensive development of bismuth chemistry.

## Chapter 6: Electrospray Mass Spectrometric Identification of Amido-Thiolato Bismuth Complexes

### 6.1 Introduction

The amido-  $[\text{C}(\text{O})\text{NR}_2]$  functionality is prevalent in biological systems as amino acid residues in peptides and proteins are held together through amide or ‘peptide’ bonds. However, there are no reports to date of bismuth compounds containing amido- groups. Exploitation of thiolate functionalities in hetero-bifunctional ligands and ESI-MS have made possible the first definitive identification of bismuth complexes involving amido-functionalities.

### 6.2 Results and Discussion

ESI-MS was performed on reaction mixtures containing  $\text{BiCl}_3$  and *N*-acetylcysteamine (ACA) with stoichiometric ratios of 1:1, 1:2 or 1:3 (Bi:Ligand) in methanol. Attempts to isolate crystalline material from these reaction mixtures were unsuccessful. In the ESI mass spectra, peaks are observed at  $m/z$  325.9, 444.9 and 585.9 and are assigned to monocations of  $[(1:1)\text{-H}^+]$ , 1:2, and 1:3Na Bi:ACA<sup>-</sup> ratios (ACA<sup>-</sup> is a monoanionic conjugate base of ACA), respectively. Figure 6.1 shows the ESI-MS of an equimolar reaction mixture of  $\text{BiCl}_3$  and ACA in methanol. Although not all peaks in the spectrum have been assigned, there are prominent peaks also present at  $m/z$  236.8 and 258.9 consistent with the protonated ( $[\text{H}3.6]^+$ ) and sodiated disulfide dimers ( $[\text{Na}3.6]^+$ ) of the free ligand, respectively. Tandem mass spectrometry was performed to support the peak assignments. The parent ion  $[(1:1)\text{-H}^+]$  ( $m/z$  325.9) gives fragments at  $m/z$  240.9

( $\text{BiS}^+$ ) and 208.8 ( $\text{Bi}^+$ ),  $m/z$  444.9 (1:2) gives  $m/z$  325.9 ( $[(1:1)\text{-H}^+]$ ), and  $m/z$  585.9 (1:3Na) gives  $m/z$  325.9 ( $[(1:1)\text{-H}^+]$ ) and 258.9 (Na3.6).

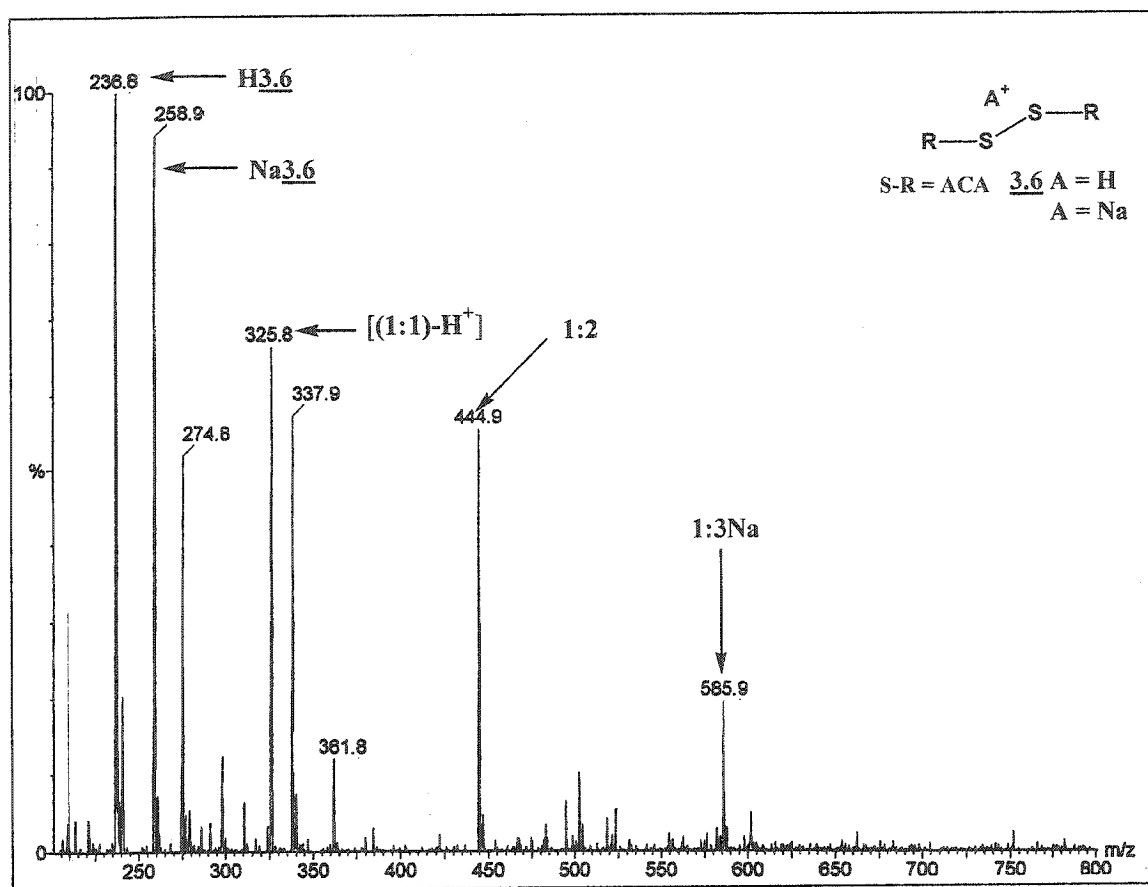


**Figure 6.1:** ESI-MS of the equimolar reaction mixture containing  $BiCl_3$  and ACA in MeOH.

### 6.3 Conclusions and Future Directions

The use of hetero-bifunctional ligands offers a synthetic versatility to explore the interaction of biorelevant functional groups with bismuth, as well as other heavy metals. Using this approach, the first amido-thiolate complexes of bismuth assigned to [(1:1)-H<sup>+</sup>], 1:2, 1:3Na Bi:ACA ratios have been identified using ESI-MS.

In addition to exploring the interaction of bismuth with biorelevant “organic” functional groups, “inorganic” functionalities can also be considered. The employment of the established hetero-bifunctional ligand approach can be broadened to include nitrate, phosphate, phosphonate, sulfate, and sulfonate functionalities. The utility of such ligand systems has been demonstrated by the reaction of bismuth nitrate and a phosphonato-carboxylate ligand in water or acetone to generate [Bi(O<sub>3</sub>PC<sub>2</sub>H<sub>4</sub>CO<sub>2</sub>)(H<sub>2</sub>O)] or [Bi(O<sub>3</sub>PC<sub>2</sub>H<sub>4</sub>CO<sub>2</sub>H)(H<sub>2</sub>O)]<sup>+</sup>, respectively.<sup>88</sup>

## Chapter 7: Definitive Identification of Bismuth Complexes Involving Small Biomolecules

### 7.1 Introduction

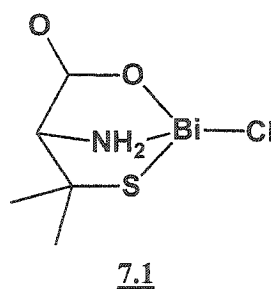
The interaction of bismuth with proteins of exposed ulcer tissue and the formation of a protective coating is proposed as a mode of action for the antiulcer behaviour exhibited by some bismuth compounds.<sup>4</sup> It has been speculated that sulfur-based biomolecules represent the primary target for pharmaceuticals such as BSS and CBS. As such, the chemistry of bismuth complexes involving biomolecules, especially amino acids, peptides and proteins as ligands, represents an important component in understanding aspects of the bioactivity of this element, providing a basis for conclusions of pharmacological and pharmacokinetic studies. Complexes of amino acids and proteins are rare and their formation is predictably pH dependent.<sup>89,90</sup> As well, characterisation of these compounds is generally incomplete resulting in structural assignments and formulations that are speculative.

This chapter provides the first assessment of the chemistry of bismuth with the naturally occurring amino acids and one peptide, glutathione, using ESI-MS.<sup>91</sup> In addition, a bismuth complex containing L-cysteine has been isolated and structurally characterised to confirm the nature of this Bi-amino acid interaction.

## 7.2 Interactions of Bismuth with Amino Acids, Peptides and Proteins

### 7.2.1 Amino Acids

The amino acids containing sulfur in the side chain are expected to achieve trisubstitution in  $\text{Bi}(\text{methionine})_3$  (mp, EA, IR, and solubility)<sup>92</sup> and  $\text{Bi}(\text{cysteine})_3 \cdot \text{H}_2\text{O}$  (IR and spectrophotometric),<sup>93,94</sup> while D-penicillamine, a dimethyl derivative of cysteine, is shown by X-ray crystallography to behave as a dianionic ligand coordinated to bismuth (**7.1**),<sup>95</sup> the structure of which will be discussed further in this chapter. This complex and other dialkylcysteines, have been suggested for medicinal use.<sup>96,97</sup> In addition to these reports, there have been less definitive amperometric studies of glycine complexes,<sup>98</sup> pH-metric studies of L-lysine complexes,<sup>99</sup> and polarographic studies of serine complexes.<sup>100</sup>



### 7.2.2 Peptides and Proteins

More extensive data are available for glutathione (a tripeptide containing glutamic acid, cysteine and glycine residues) complexing with bismuth, and such preparations have been suggested for the treatment of syphilis and other diseases.<sup>101</sup> From NMR spectroscopic studies in aqueous media and in red blood cells<sup>102</sup> it is speculated that the

ligand is sulfur-bound to bismuth.<sup>103</sup> Stability constant determinations reveal that this binding is competitive with EDTA and is pH dependent. The binding of the  $\text{Bi}^{3+}$  cation to human serum transferrin, an iron transport glycoprotein, has been examined by UV-vis and NMR spectroscopies.<sup>104;105</sup> The effect of the concentration of bismuth on plasma protein and red blood cell binding, as well as bismuth binding to human serum albumin, bovine serum albumin and human serum, have also been studied.<sup>106</sup> Other studies have examined the interaction of bismuth compounds with alkaline protein solutions under biuretic reaction conditions,<sup>107</sup> and the behaviour of elemental bismuth with various proteins under anaerobic conditions.<sup>108;109</sup> Bismuth compounds have also been found to inhibit the action of certain enzymes.<sup>110</sup>

Bismuth(III) has been found to form a saturated 7:1 (Bi:ligand) complex with rat liver metallothionein (MT), a protein containing many thiol functionalities from cysteine residues.<sup>111</sup> However, similar results have been obtained for other metal ions, suggesting little binding preference for bismuth. There has been debate over whether proteins binding with bismuth are related to MT or belong to another family of proteins such as “renal metal binding proteins” (RMBP). Nevertheless, it has been shown that the bismuth binding proteins are different from MT<sup>112</sup> from isolation, separation and amino acid analysis. These bismuth induced RMBPs in rats have been divided into two major components that have been studied spectroscopically.<sup>113</sup> The hepatic protein spectra demonstrate predominantly zinc-thiolate transitions, while the renal protein transitions can be accounted for by both bismuth and copper thiolate binding sites.



### 7.3 Results and Discussion

#### 7.3.1 *Identification of Bismuth Complexes Involving Amino Acids by ESI-MS*

As ligands, many biomolecules (e.g. peptides, proteins) are multifunctional bases that most likely engage metals as chelating ligands. Although the chelate chemistry for bismuth is extensive relative to that for many heavy metals, identification and characterisation of bismuth complexes involving biomolecules is difficult due to ineffectual NMR spectroscopic features and low success in obtaining suitable samples for X-ray crystallographic studies. Therefore, ESI-MS has been exploited as a data rich approach to evaluate interactions between bismuth and amino acids. Values of  $m/z$  assigned to bismuth species observed in the gas phase from the introduction of solution samples into the mass spectrometer can in some instances be correlated with complexes that have been isolated and comprehensively characterised.<sup>54</sup>

Mass spectra of 1:1 stoichiometric reaction mixtures containing bismuth nitrate and each of the twenty common L-amino acids (as well as DL-homocysteine) in some cases exhibit peaks corresponding to monocations involving bismuth. Prominent peaks at  $m/z$  values assigned to these cations are listed in Table 7.1 together with their relative intensity, assignment as Bi:Am ratios (Am = monoanionic conjugate base of amino acid) and MS/MS peaks with assignments. Cations corresponding to complexes of bismuth with each of seven amino acids are observed. For mixtures containing L-histidine, L-threonine, L-asparagine or L-glutamine relatively minor peaks are observed for 1:2 Bi:Am ratios. Prominent peaks are observed for cations with [(1:1)-H<sup>+</sup>], 1:2, [(2:2)-3H<sup>+</sup>] and [(2:3)-2H<sup>+</sup>] Bi:Am ratios for mixtures involving L-methionine, L-cysteine, or DL-homocysteine, indicating that the presence of sulfur lends a greater kinetic stability to the

gas phase bismuth-containing ions. Sodiated complexes of the type [(1:2Na)-H<sup>+</sup>] and [(2:3Na)-3H<sup>+</sup>] Bi:Am ratios are also present in the mass spectra of mixtures containing L-methionine. Peaks are also present in the spectra obtained from reaction mixtures containing BiCl<sub>3</sub> or BSS with either cysteine or homocysteine consistent with the [(1:1)-H<sup>+</sup>], 1:2, [(2:2)-3H<sup>+</sup>] and [(2:3)-2H<sup>+</sup>] assignments, irrespective of reaction stoichiometry (1:1, 1:2, 1:3; Bi:Ligand). Representative mass spectra for the reactions of L-cysteine, DL-homocysteine, and L-methionine are provided in Figure 7.1 – 7.3.

**Table 7.1:** ESI-MS data for reaction mixtures containing bismuth nitrate and an amino acid in 50% ethanol for spectra that show prominent cation peaks ( $m/z$ ) containing bismuth. Relative peak intensities (%) are given with respect to the 100% peak for protonated amino acid, except for Cys and Hcys. MS assignments are supported by MS/MS.

Amino Acid	$m/z$	Rel. Int. (%)	Bi:Am	MS/MS ( $m/z$ )	Bi:Am
His	516.9	5	1:2	361.9	[(1:1)-H <sup>+</sup> ]
Thr	444.9	10	1:2	208.9	Bi <sup>+</sup>
Met	881.7	20	[(2:3Na)-3H <sup>+</sup> ]	526.9	1:2Na
	859.7	40	[(2:3)-2H <sup>+</sup> ]	504.9	1:2
	710.7	10	[(2:2)-3H <sup>+</sup> ]	355.9	[(1:1)-H <sup>+</sup> ]
	526.9	30	[(1:2Na)-H <sup>+</sup> ]	355.9	[(1:1)-H <sup>+</sup> ]
	504.9	65	1:2	355.9	[(1:1)-H <sup>+</sup> ]
	355.9	35	[(1:1)-H <sup>+</sup> ]	209.0	Bi <sup>+</sup>
Cys	775.9	5	[(2:3)-2H <sup>+</sup> ]	328.0	[(1:1)-H <sup>+</sup> ]
	654.9	20	[(2:2)-3H <sup>+</sup> ]	328.0	[(1:1)-H <sup>+</sup> ]
	448.8	45	1:2	328.0	[(1:1)-H <sup>+</sup> ]
	327.7	100	[(1:1)-H <sup>+</sup> ]	241.0	BiS <sup>+</sup>
	240.7	40	BiS <sup>+</sup>	209.0	Bi <sup>+</sup>
	208.7	10	Bi <sup>+</sup>	209.0	Bi <sup>+</sup>
Hcys	818.0	5	[(2:3)-2H <sup>+</sup> ]	477.2	1:2
				342.0	[(1:1)-H <sup>+</sup> ]
				209.0	Bi
	682.8	10	[(2:2)-3H <sup>+</sup> ]	341.9	[(1:1)-H <sup>+</sup> ]
	477.0	100	1:2	342.0	[(1:1)-H <sup>+</sup> ]
				209.0	Bi <sup>+</sup>
	342.0	55	[(1:1)-H <sup>+</sup> ]	241.0	BiS <sup>+</sup>
	208.9	35	Bi <sup>+</sup>	209.0	Bi <sup>+</sup>
Asn	471.1	5	1:2	338.9	[(1:1)-H <sup>+</sup> ]
				209.1	Bi <sup>+</sup>
Gln	498.9	10	1:2	352.9	[(1:1)-H <sup>+</sup> ]

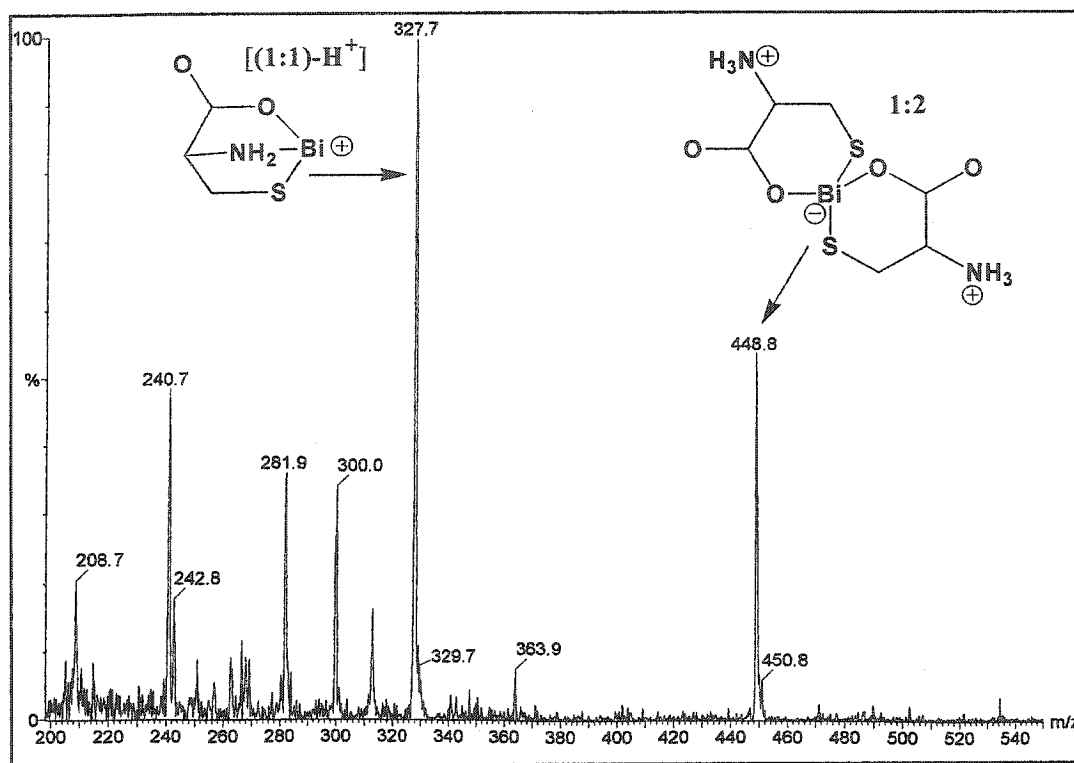


**Figure 7.1:** An ESI-MS ( $m/z$  200 – 550) of an equimolar reaction mixture containing  $\text{Bi}(\text{NO}_3)_3$  and L-cysteine in 50% ethanol/water. Peak assignments of bismuth containing monocations are given as Bi:Am ratios present in the corresponding complexes.

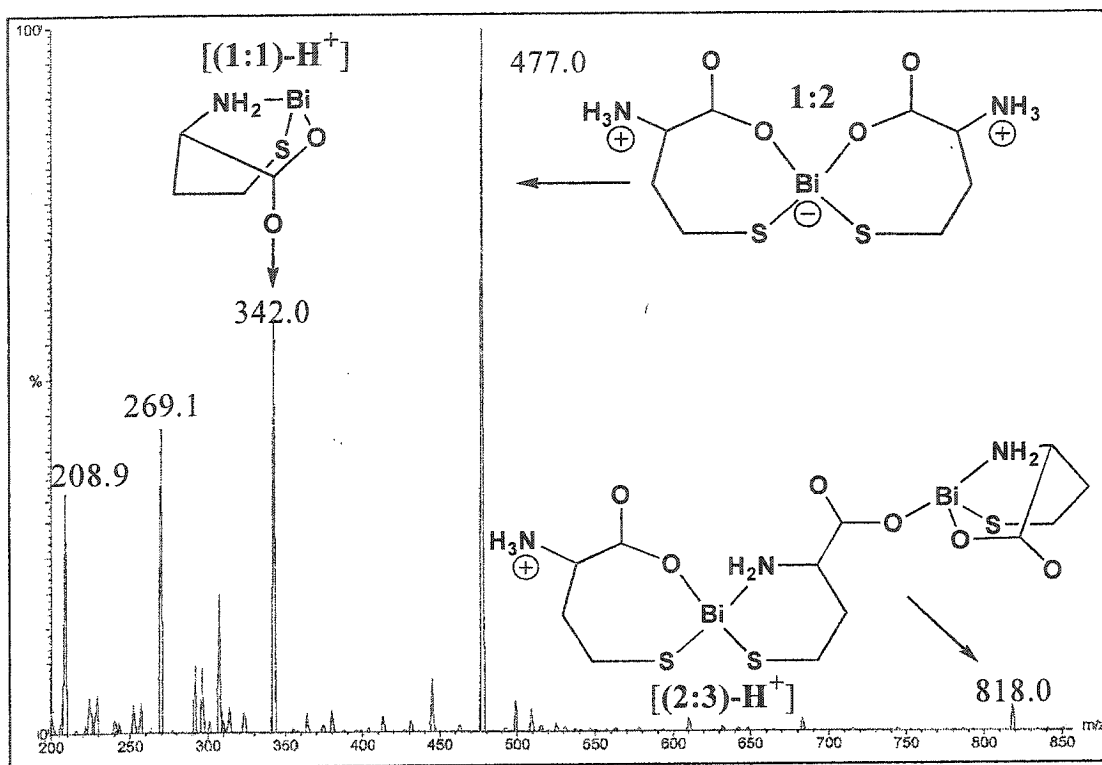


**Figure 7.2:** An ESI-MS of an equimolar reaction mixture containing Bi(NO<sub>3</sub>)<sub>3</sub> and DL-homocysteine in 50% ethanol/water. Peak assignments of bismuth containing monocations are given as Bi:Am ratios present in the corresponding complexes.

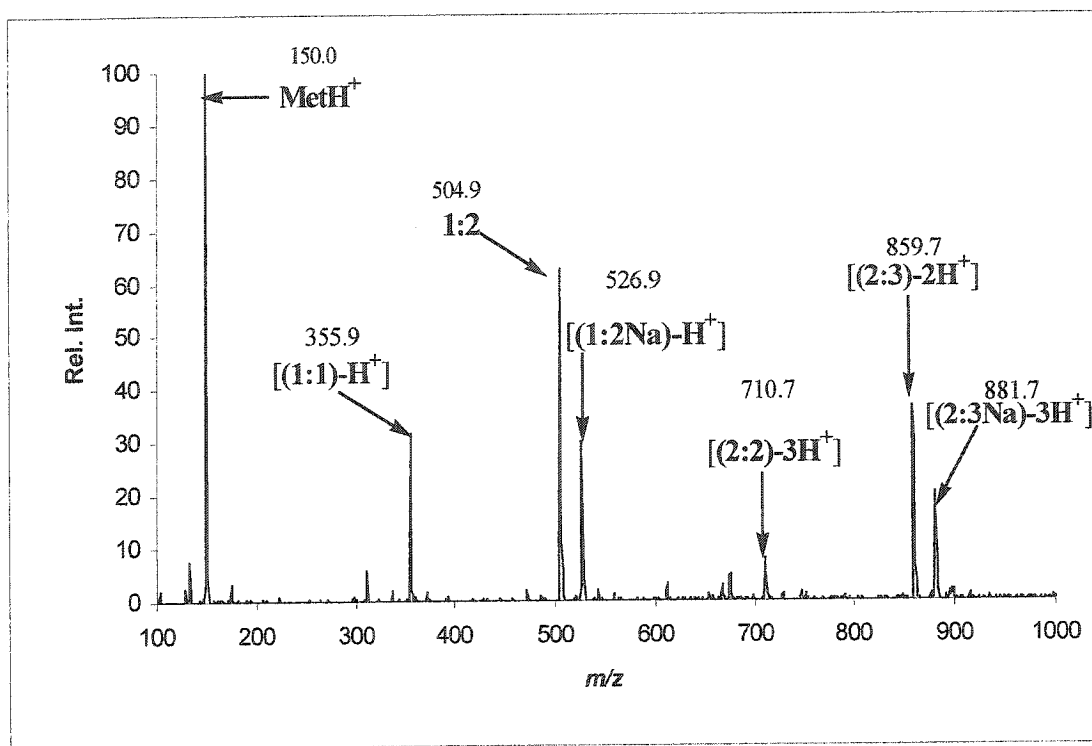


**Figure 7.3:** ESI-MS of a solution containing bismuth nitrate and L-methionine in 50% ethanol. Peak assignments of bismuth containing monocations are given as Bi:Am ratios present in the corresponding complexes.

Table 7.2 summarises the ESI-MS data for 1:1:1 stoichiometric reaction mixtures containing bismuth nitrate, cysteine and each of the other L-amino acids (as well as DL-homocysteine). Representative mass spectra for the reactions containing L-asparagine and L-lysine are shown in Figures 7.4 and 7.5, respectively. Peaks corresponding to monocations composed of bismuth, one or more cysteinate moieties (Cys) and the conjugate base(s) of the amino acid (Am) are observed for 12 amino acids and are assigned according to Bi:Cys:Am ratio. In addition, peaks corresponding to cations containing only bismuth and cysteinate(s) are observed, as listed in Table 7.1, but are not listed in Table 7.2. As well, the assignments of [(1:1)-H<sup>+</sup>] and 1:2 Bi:Am ratios are consistent with those listed in Table 7.2.

With the exception of the mixture containing homocysteine, many of the prominent peaks are assigned to 1:1:1 Bi:Cys:Am cations that contain at least one cysteinate moiety. Although those peaks corresponding to 1:1:1 Bi:Cys:Am ratios are of relatively low intensity, their identity is unequivocal and they confirm the formation of complexes of bismuth with tryptophan, serine, lysine, arginine and proline, that were not observed in the absence of cysteine. It is tempting to speculate that cysteine facilitates the coordination of these amino acid conjugates with bismuth. Indeed, most of the prominent peaks correspond to cations of 1:1:1, [(2:2:1)-2H<sup>+</sup>] or [(2:1:2)-2H<sup>+</sup>] Bi:Cys:Am ratios.

Under the conditions examined, none of the amino acids containing alkyl side chains interact with bismuth to form a kinetically stable complex in the gas phase. This is likely a result of the fact that the ability of these amino acids to form chelate complexes is greatly reduced as the amine functionality is presumably protonated in acidic solutions.

In contrast to reports of bismuth-carboxylate complexes<sup>78-80</sup> and evidence of such ions from ESI-MS (as discussed in Chapter 4) aspartic acid and glutamic acid, the two amino acids containing the carboxylic acid side chains, also do not form complexes with bismuth under the conditions these ESI-MS experiments were performed. This may be due to the fact that the reactions are performed under acidic conditions, thus protonating both the amino and one of the carboxylate functional groups.



**Table 7.2:** ESI-MS data for reaction mixtures containing bismuth nitrate, cysteine and another amino acid in 50% ethanol showing prominent cation peaks ( $m/z$ ) containing bismuth. Relative peak intensities (%) are given with respect to the 100% peak for protonated amino acid. MS assignments are supported by MS/MS. Peaks corresponding to bismuth-cysteinate complexes (as listed in Table 7.1) are observed at different relative intensities for each amino acid combination, but are not listed in this table.

Amino Acid	$m/z$	Rel Int (%)	Bi:Cys:Am	MS/MS ( $m/z$ )	Bi:Cys:Am
His	516.9	25	1:0:2	361.9	[(1:0:1)-H <sup>+</sup> ]
	482.9	10	1:1:1	327.9	[(1:1:0)-H <sup>+</sup> ]
				156.1	HisH <sup>+</sup>
	362.0	5	[(1:0:1)-H <sup>+</sup> ]	209.0	Bi <sup>+</sup>
Trp	859.1	5	[(2:2:1)-2H <sup>+</sup> ]	532.0	1:1:1
				327.9	[(1:1:0)-H <sup>+</sup> ]
	532.2	15	1:1:1	327.9	[(1:1:0)-H <sup>+</sup> ]
				204.9	TrpH <sup>+</sup>
Tyr	508.9	10	1:1:1	328.0	[(1:1:0)-H <sup>+</sup> ]
				181.8	TyrH <sup>+</sup>
Ser	760.2	5	[(2:2:1)-2H <sup>+</sup> ]	433.0	1:1:1
				208.9	Bi <sup>+</sup>
Thr	433.1	25	1:1:1	328.0	[(1:1:0)-H <sup>+</sup> ]
	773.7	35	[(2:2:1)-2H <sup>+</sup> ]	327.8	[(1:1:0)-H <sup>+</sup> ]
	446.9	30	1:1:1	327.8	[(1:1:0)-H <sup>+</sup> ]
Met	803.8	97	[(2:2:1)-2H <sup>+</sup> ]	449.1	1:2:0
				328.1	[(1:1:0)-H <sup>+</sup> ]
	504.9	5	1:0:2	355.9	[(1:0:1)-H <sup>+</sup> ]
	476.9	15	1:1:1	327.9	1:1:0
				149.9	MetH <sup>+</sup>
Hcys	356	3	1:0:1	209.0	Bi <sup>+</sup>
	817.8	10	[(2:0:3)-2H <sup>+</sup> ]	477.2	1:0:2
				341.8	[(1:0:1)-H <sup>+</sup> ]
	803.8	25	[(2:1:2)-2H <sup>+</sup> ]	341.8	[(1:0:1)-H <sup>+</sup> ]
				462.9	1:1:1
	790.1	30	[(2:2:1)-2H <sup>+</sup> ]	327.9	[(1:1:0)-H <sup>+</sup> ]
	476.9	100	1:0:2	342.0	[(1:0:1)-H <sup>+</sup> ]
				240.8	BiS <sup>+</sup>
				208.8	Bi <sup>+</sup>
	462.9	95	1:1:1	240.8	BiS <sup>+</sup>
Asn				209.0	Bi <sup>+</sup>
	342.0	45	1:0:1	240.8	BiS <sup>+</sup>
				208.8	Bi <sup>+</sup>
	786.7	20	[(2:2:1)-2H <sup>+</sup> ]	448.9	1:2:1
				338.8	[(1:0:1)-H <sup>+</sup> ]
Gln	470.9	60	1:0:2	339.0	[(1:0:1)-H <sup>+</sup> ]
	459.9	15	1:1:1	327.9	[(1:1:0)-H <sup>+</sup> ]
	339.0	17	[(1:0:1)-H <sup>+</sup> ]	209.0	Bi <sup>+</sup>
Lys	800.8	45	[(2:2:1)-2H <sup>+</sup> ]	327.9	[(1:1:0)-H <sup>+</sup> ]
	498.9	20	1:0:2	352.9	[(1:0:1)-H <sup>+</sup> ]
	473.9	50	1:1:1	327.8	[(1:1:0)-H <sup>+</sup> ]
				147.0	GlnH <sup>+</sup>
Arg	800.7	10	[(2:2:1)-2H <sup>+</sup> ]	353.3	[(1:0:1)-H <sup>+</sup> ]
	498.9	5	1:0:2	352.7	[(1:0:1)-H <sup>+</sup> ]
	473.9	25	1:1:1	147.0	LysH <sup>+</sup>
Pro	502.0	5	1:1:1	174.9	ArgH <sup>+</sup>
Pro	443.2	10	1:1:1	327.9	[(1:1:0)-H <sup>+</sup> ]
				115.7	ProH <sup>+</sup>

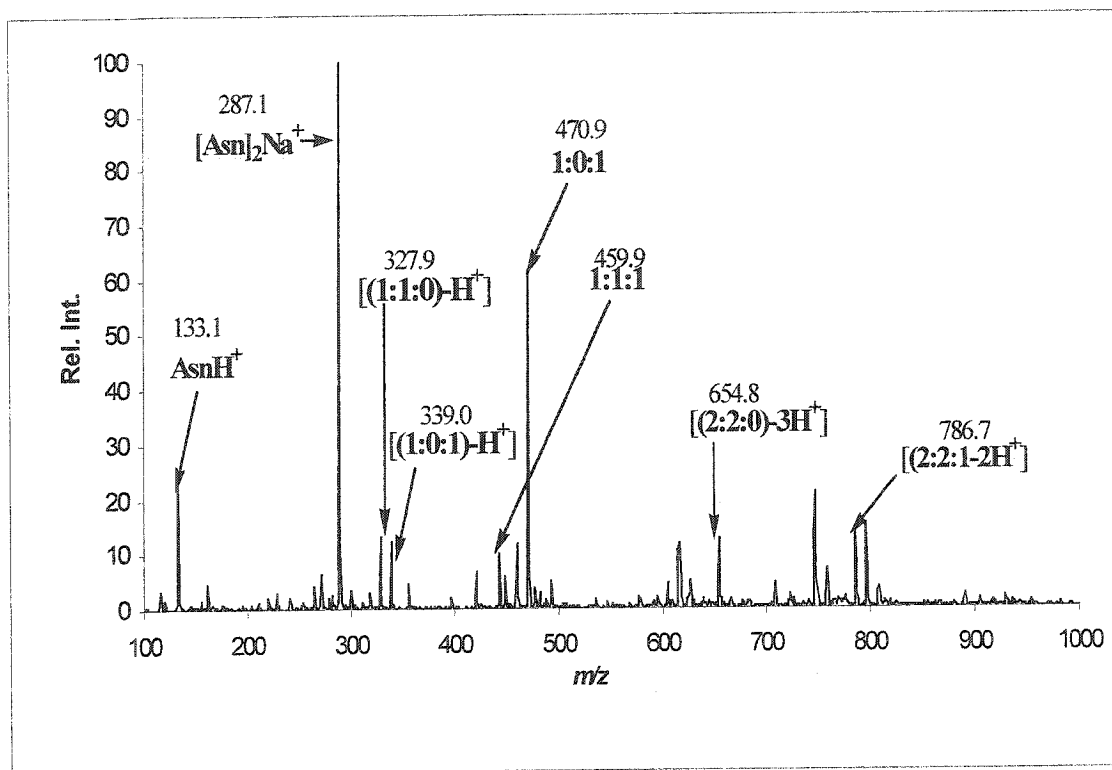


**Figure 7.4:** ESI-MS of a solution containing bismuth nitrate, L-cysteine, and L-asparagine in 50% ethanol. Peak assignments of bismuth containing monocations are given as Bi:Cys:Am ratios present in the corresponding complexes.

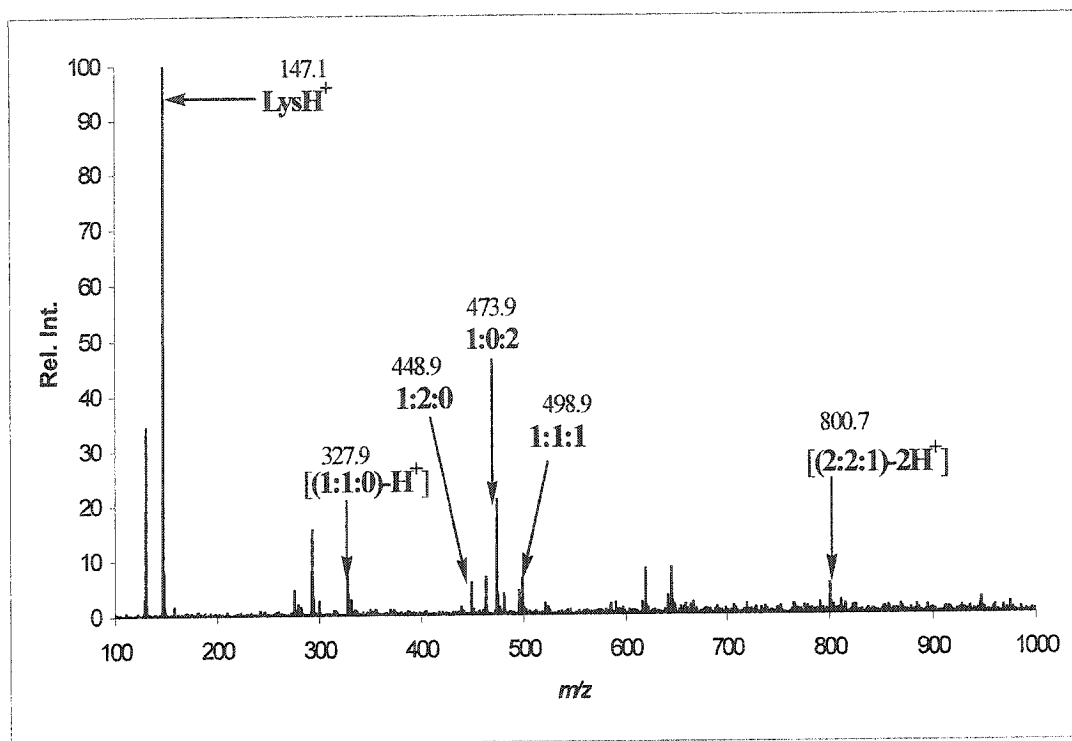


**Figure 7.5:** ESI-MS of a solution containing bismuth nitrate, L-cysteine, and L-lysine in 50% ethanol. Peak assignments of bismuth containing monocations are given as Bi:Cys:Am ratios present in the corresponding complexes.

### 7.3.2 Identification of Bismuth Complexes Involving Glutathione by ESI-MS

ESI-MS of reaction mixtures containing either  $\text{BiCl}_3$ ,  $\text{Bi}(\text{NO}_3)_3$  or BSS with glutathione in 50 % ethanol are independent of reaction stoichiometry (1:1, 1:2, 1:3; Bi:Ligand). Prominent peaks are observed at  $m/z$  513.9 and 820.9 corresponding to monocations of  $[(1:1)\text{-H}^+]$  and 1:2 Bi:glutathione ratios, respectively. In addition, a peak at  $m/z$  384.9 is assigned to a dipeptide complex ( $[(1:1')\text{-H}^+]$ ) of bismuth, in which the glutamic acid residue has been lost from the  $[(1:1)\text{-H}^+]$  complex. This observation is consistent with the data collected from the ESI-MS experiments on bismuth-amino acid mixtures where bismuth was shown not to interact with the amino acids containing the carboxylic acid side chains (Asp and Glu). Therefore, it is postulated that the glutamic acid residue of glutathione does not interact with bismuth in any significant manner and that the anchoring of this ligand on bismuth most likely occurs through the thiolate functionality of the cysteine residue as speculated previously.<sup>103</sup> A representative mass spectrum of a reaction mixture containing  $\text{Bi}(\text{NO}_3)_3$  and glutathione is provided in Figure 7.6 along with proposed structures of the assignments.

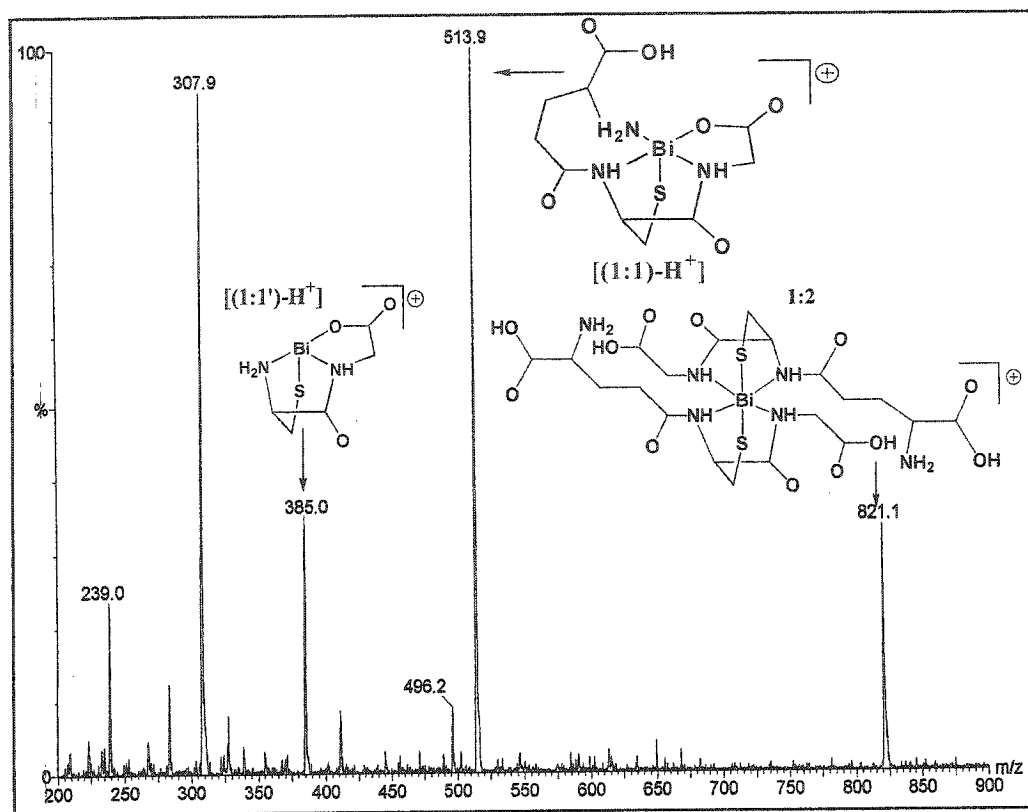


**Figure 7.6:** ESI-MS of a solution containing bismuth nitrate and glutathione in 50% ethanol. Peak assignments of bismuth containing monocations are given as Bi:glutathione ratios.

It is interesting to note that when ESI-MS was performed on reaction mixtures involving bismuth nitrate with cystine or oxidized glutathione (the disulfide bound dimers of cysteine and glutathione) there were no peaks observed consistent with those bismuth-cysteine or bismuth-glutathione cations discussed previously. Hence, it is tentatively concluded that bismuth does not affect these dimers in such a way as to break the disulfide bonds to form complexes with free cysteine or glutathione.

### 7.3.3 *Synthesis and Structure of the First Bismuth-Amino Acid Conjugate Base*

#### *Complex*

ESI-MS of reaction mixtures containing bismuth nitrate pentahydrate, L-cysteine and 1,10-phenanthroline in 50 % ethanol show peaks that correspond to the bismuth-cysteinate complex ions listed in Table 7.1, as well as protonated phenanthroline. Crystalline material isolated by slow evaporation of solvent from the reaction mixture has been characterised as the nitrate salt of a dicationic complex of bismuth with a cysteinate ligand and a 1,10-phenanthroline ligand, consistent with the previous realisation of the apparent stabilizing influence of this chelate ligand.<sup>67</sup> Figure 7.7 shows a crystallographic view of the formula unit of  $\text{Bi}(\text{Cys})(\text{Phen})(\text{NO}_3)_2\text{H}_2\text{O}$  (**7.2**). The octa-coordinate environment of bismuth is imposed by *O,S*-chelation from the cysteinate ligand, *N,N*-chelation from the phenanthroline ligand, *O,O*-chelation from a nitrate anion, one oxygen center of the second nitrate anion and a water molecule. The solid state structure definitively confirms the interaction of bismuth with the thiolate and carboxylate functionalities of the cysteinate anion and charge balance for a bismuth(III) center requires that the pendant nitrogen center of the cysteinate ligand represents an

ammonium moiety. The structure is in contrast to the thiolate-anchored amine complexes 3.1aCl<sub>2</sub>, 3.2aCl, 3.3a<sup>52</sup> and 7.1,<sup>114</sup> that exhibit Bi-N distances of less than 3 Å. The phenanthroline-bismuth interaction is consistent with related complexes.<sup>67</sup>

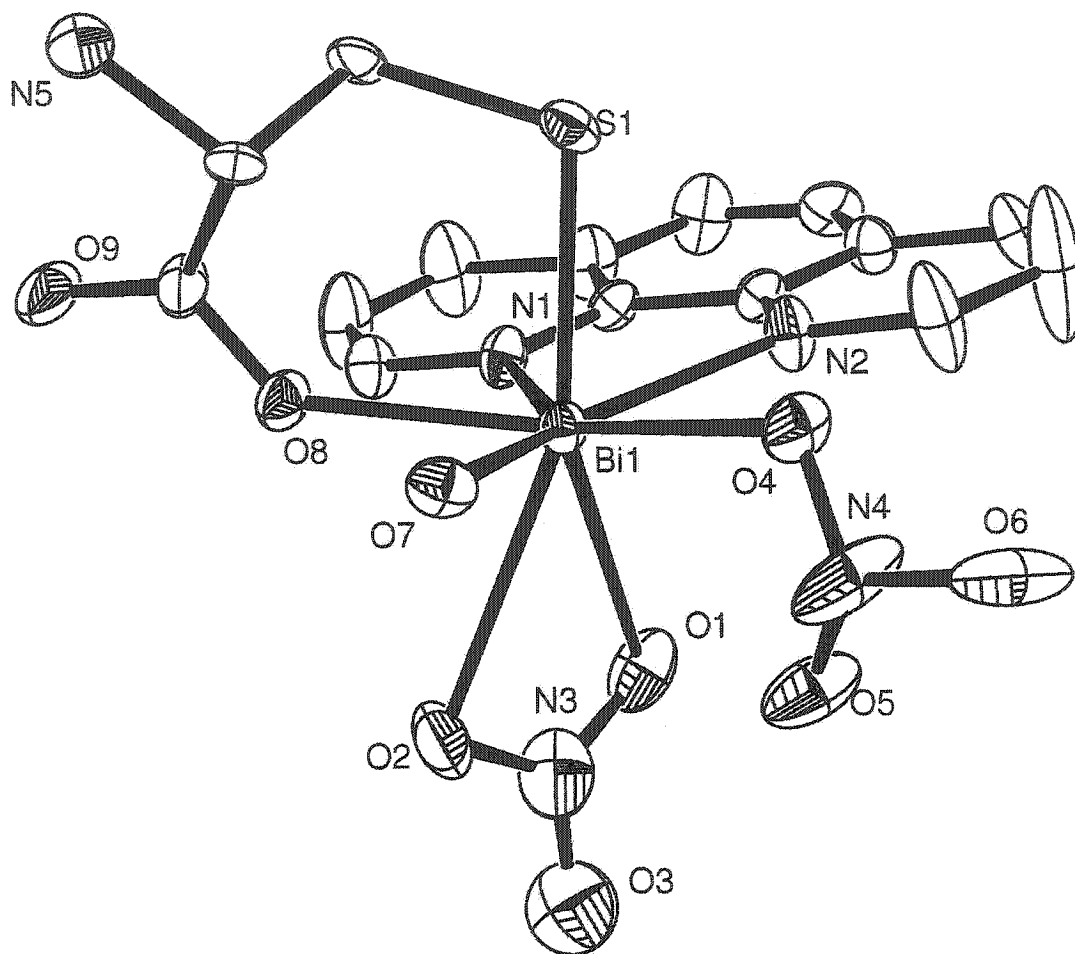


**Figure 7.7:** Crystallographic view of  $\text{Bi}(\text{Cys})(\text{Phen})(\text{NO}_3)_2\text{H}_2\text{O}$  (**7.2**). Atoms O3 and O6 as well as all atoms in the cysteinate ring except for S1 and O8 have been split over two positions (each with an occupancy of a half); only one position has been shown for each. Hydrogen atoms are also omitted for clarity. Selected internuclear distances (Å): Bi1-S1 2.529(4), Bi1-N1 2.48(1), Bi1-N2 2.50(1), Bi1-O1 2.92(1), Bi1-O2 2.91(1), Bi1-O4 2.60(1), Bi1-O5 3.12(1), Bi1-O7 2.65(1), Bi1-O8 2.34(1).



Compound **7.1**, a bismuth complex involving a derivative of L-cysteine, adopts a bicyclic or cage structure that includes a relatively short Bi-N interaction [2.345(6) Å] as part of a five-membered *N,S*-chelate ring,<sup>114</sup> also typical of amino-thiolate complexes **3.1a**, **3.2a** and **3.3a**.<sup>52</sup> Although the contrasting structure of Bi(Cys)(Phen)(NO<sub>3</sub>)<sub>2</sub>H<sub>2</sub>O (**7.2**) involves a distinctly *O,S*- bidentate ring only, this six-membered chelate moiety is structurally similar to that in **7.1**. Moreover, the Bi-O and Bi-S distances are consistent with those in the range of bismuth complexes involving bifunctional thiolate ligands. Indeed, it can be envisaged that the preference for the bismuth thiolate interaction anchors the bifunctional ligand and facilitates the interaction of the weaker donor [C(O)OH in Bi(Cys)(Phen)(NO<sub>3</sub>)<sub>2</sub>H<sub>2</sub>O] with bismuth. The shortest Bi-O distance in **7.2** [2.34(1) Å] is consistent with those in bismuth complexes containing lactate,<sup>78</sup> malate and tartrate<sup>79</sup> [Bi-O 2.21-2.57 Å]. Similar features are reported with other thiolate bifunctional ligands involving functional groups prevalent in biosystems (i.e. amino-,<sup>52</sup> hydroxy-,<sup>50</sup> and ester-<sup>5</sup> groups). Although a broad range of Bi-O distances is observed in Bi(Cys)(Phen)(NO<sub>3</sub>)<sub>2</sub>H<sub>2</sub>O, the energetic value of a Bi-O distance greater than 3 Å is questionable, so that the designation of a coordination number for bismuth is subjective.

In considering the interaction of bismuth with the conjugate base(s) of an amino acid, it is useful to compare the relative pK<sub>a</sub> values for the key functional groups [C(O)OH, 0-5; NH<sub>3</sub><sup>+</sup>, 5-10; SH, 7-10; OH, 10-17; NH<sub>2</sub>, 36]. While the difference in pK<sub>a</sub> values between ammonium and thiol groups is not large, additional thermodynamic preference for Bi-S bond formation strongly favours the deprotonation of a thiol in the presence of bismuth for thiolate-containing amino acids. The polyprotic nature of amino acids, illustrated for cysteine in Figure 7.8, allows access to (i) dianionic, (ii)

monoanionic, (iii) neutral, and (vi) cationic ligands with various potential modes of coordination towards metal centers. Further tautomeric diversity is imposed by protic equilibria illustrated for each scenario. Compound 7.1, containing a dimethyl derivative of cysteine,<sup>114</sup> is a complex of the dianion (i), which offers the highest Lewis basicity of the species in Figure 7.8.  $\text{Bi}(\text{Cys})(\text{Phen})(\text{NO}_3)_2\text{H}_2\text{O}$  (7.2) is a complex of the (ammonium) monoanion (ii), which is more viable in acidic media and therefore provides a closer model of the potential interaction of bismuth with cysteine in the gastric environment. In this context, the solid state structure of 7.2 and the supportive mass spectrometric data offer the first definitive identification of a bismuth complex containing a biomolecule. It is apparent that the non-biocompatible 1,10-phenanthroline facilitates the isolation of  $\text{Bi}(\text{Cys})(\text{Phen})(\text{NO}_3)_2\text{H}_2\text{O}$  in the solid state. Nevertheless, the consistent mass spectrometric data obtained for a variety of amino acids and cysteine/amino acid combinations provides further evidence for the viability of bismuth-amino acid complexes.

Based on previous observations for isolated complexes involving thiolate<sup>50;52;54</sup> and carboxylate ligands,<sup>78;79</sup> Bi:Am ratios of 1:1 and 1:2 can be envisaged as derivatives of 3.1 and 3.2, while the dibismuth cations (2:2 and 2:3) are likely bridged by one of either the two or three bifunctional ligands analogous to those observed for ester-thiolate complexes of bismuth.<sup>50</sup>

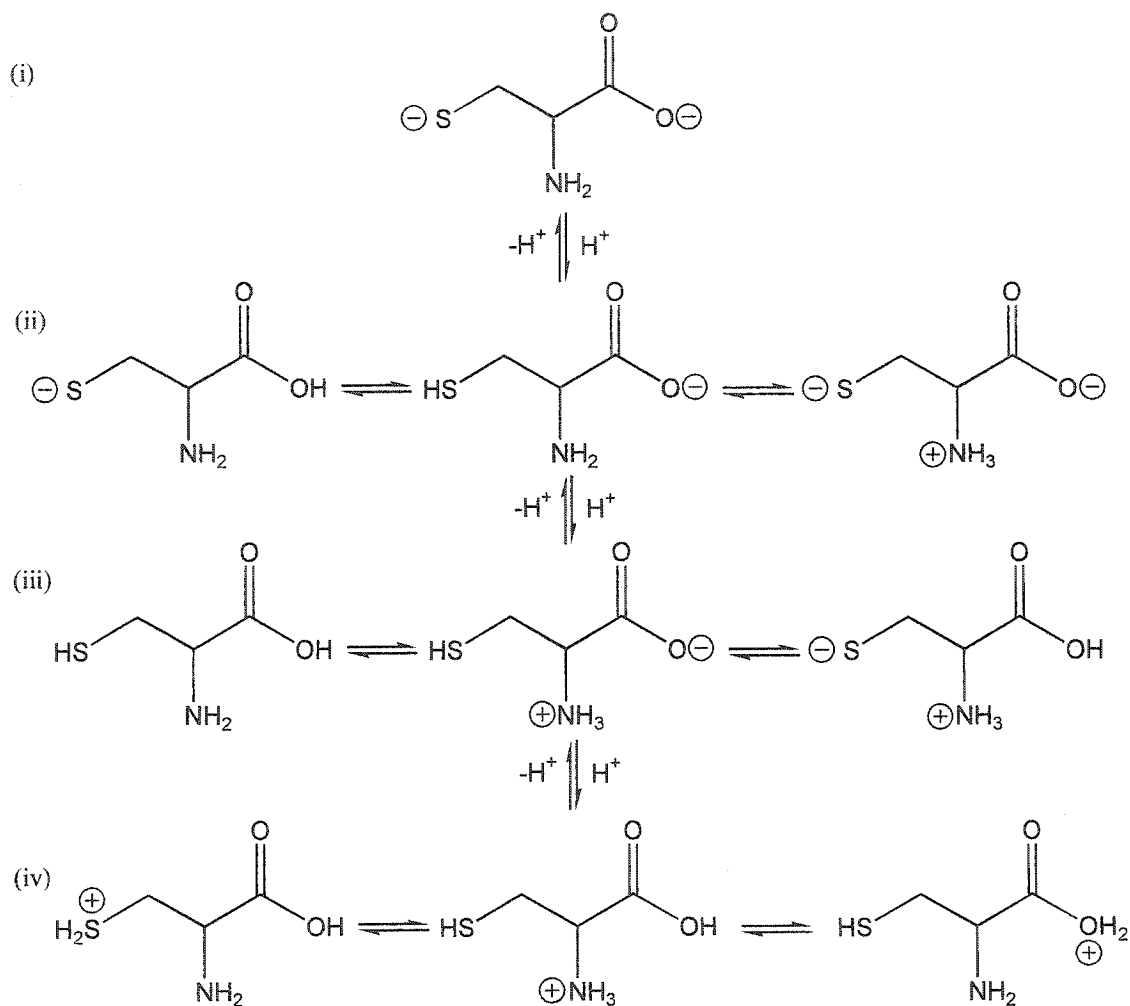


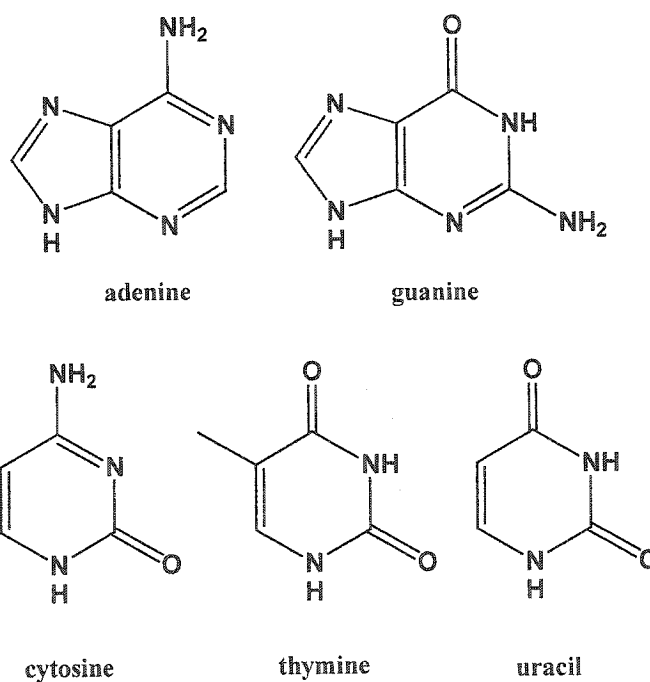
**Figure 7.8:** Proposed polyprotic equilibria of L-cysteine leading to a variety of coordination modes towards metals.

#### 7.4 Conclusions and Future Directions

The interaction of bismuth nitrate with the naturally occurring amino acids has been assessed using ESI-MS, and seven amino acids are observed to form complexes exhibiting four distinct Bi:Am ratios, [(1:1)-H<sup>+</sup>], 1:2, [(2:2)-3H<sup>+</sup>], and [(2:3)-2H<sup>+</sup>]. As is expected based on the thiophilicity exhibited by bismuth, the most kinetically stable complexes in the gas phase are observed for cysteine, homocysteine and methionine, providing support for the speculation that thiolation of bismuth is the primary biochemical fate for bismuth pharmaceuticals. Indeed, it has been shown that the solubility of BSS is enhanced by the addition of cysteine, homocysteine and glutathione. This is in accordance with previous observations where the solubility of bismuth compounds is increased by various other biological molecules (ascorbic acid,<sup>115-117</sup> uracil, thiouracil,<sup>118</sup> citric acid) as well as by citrus juice and wines.<sup>119</sup> Moreover, cysteine facilitates interactions of bismuth with other amino acids such that peaks corresponding to “mixed” amino acid-bismuth monocations are observed. This observation lends important insight into what amino acid residues bismuth may interact with when engaging peptides and proteins to form the speculated cytoprotective coating.<sup>4</sup>

The solid state structure of a cysteine complex has been confirmed by X-ray crystallography and represents the first solid state structure of bismuth involving an amino acid. This structure is consistent with the mass spectrometric data and, more importantly, offers valuable insight into the coordination mode for cysteine in the acidic gastric environment. With the success of using 1,10-phenanthroline as a trapping agent to isolate crystalline material, this procedure should be further explored such that coordination trends among the amino acids with bismuth can be determined.

The investigation of the bismuth-glutathione system by ESI-MS further substantiates the results from the bismuth-amino acid mixtures. Unfortunately, attempts to isolate solid products from these systems were unsuccessful, even with the introduction of a stabilising ligand such as 1,10-phenanthroline or 2,2'-bipyridine and variation of the concentration of reagents. However, it may prove worthwhile to explore the effect of smaller stabilising ligands, (i.e. pyridine) or even the effect of biologically relevant bases (adenine, guanine, cytosine, thymine, and uracil) as well as further varying reaction conditions (pH, temperature).



In addition to continuing the evaluation of the chemistry of bismuth with amino acids and glutathione, the investigation of the interaction of bismuth with other biomolecules is of paramount importance especially in the quest for possible

pharmaceutical agents. Most obvious is the study of bismuth-polypeptide and protein systems by mass spectrometry, especially those proteins for which some analytical data have already been collected (i.e. transferrin,<sup>104,105</sup> albumin,<sup>106</sup> metallothionein<sup>111</sup> and renal metal binding proteins<sup>113</sup>). Not so obvious is the investigation of bismuth complexes involving carbohydrates, such as saccharides, and the DNA/RNA bases. Preliminary ESI-MS studies have already demonstrated interactions of bismuth with simple carbohydrates such as ribose and glucose to form kinetically stable monocations assigned to 1:2 (Bi:Ligand<sup>-</sup>; Ligand<sup>-</sup> is a monoanionic conjugate base of the ligand) complexes.

## **Chapter 8: Identification of Lead-Amino Acid Adducts by Electrospray Ionisation Mass Spectrometry and Crystallographic Characterisation of the First Lead-Amino Acid Complex**

### **8.1 Introduction**

The toxicological properties of lead compounds are associated with proteins and are manifested in anemia, neuropathy and hypertension.<sup>120-122</sup> Inhibition of heme synthesis is established as a principal biochemical action<sup>123</sup> and a key lead-enzyme interaction has been modeled.<sup>124</sup> Although Pb(IV) and Pb(II) labels have been used in crystallographic studies of some proteins,<sup>120</sup> lead complexes of proteins relevant to lead toxicity have yet to be definitively characterised. Moreover, complexes of lead involving amino acids are incompletely characterised.<sup>120,125</sup>

The opportunity to sample solutions by ESI-MS and the distinctive isotopic array [<sup>204</sup>Pb (1.48 %), <sup>206</sup>Pb (23.6 %), <sup>207</sup>Pb (22.6 %), <sup>208</sup>Pb (52.3 %)] naturally exhibited by lead,<sup>120,126-128</sup> have enabled the unequivocal identification of lead complexes with the naturally occurring amino acids.<sup>129</sup> Additionally, the assignment of one example has been supported by the crystallographic characterisation of a lead-valine complex representing the first complex of lead(II) involving an amino acid.

## 8.2 Results and Discussion

Reaction mixtures containing lead(II) nitrate and a stoichiometric equivalent of an amino acid in 50 % ethanol were examined by ESI-MS. Mass spectrometric data are summarised in Table 8.1 where prominent  $m/z$  peaks (highest peak amongst the cluster of isotopic peaks) are listed together with their relative intensity and monocationic assignment (given as a Pb:Am ratio; Am = amino acid or conjugate base of the amino acid). All of the assignments have been confirmed by MS/MS experiments.

Unlike for bismuth(III), which only formed complexes in the gas phase with seven amino acids, lead(II) forms complexes with each of the naturally occurring amino acids, as well as homocysteine. Most of the reaction mixtures exhibit monocations of the **1:1**, **[(1:2)+H<sup>+</sup>]**, **[(2:2)-H<sup>+</sup>]** and **2:3** Pb:Am ratios (where Am is a monoanionic conjugate base of the amino acid) and the amino acids with hydrophobic side chains (glycine, alanine, valine, leucine, isoleucine, and phenylalanine) were shown to form highly abundant **2:3** complexes. L-threonine, L-methionine and L-aspartic acid also adopt a **[(3:2)-2H<sup>+</sup>]** Pb:Am ratio. As well, threonine and aspartic acid form a cation of the **[(3:3)-2H<sup>+</sup>]** Pb:Am ratio and a representative spectrum is given in Figure 8.1 for the reaction mixture of Pb(NO<sub>3</sub>)<sub>2</sub> and L-threonine illustrating the cluster of peaks assigned to the **[(3:3)-2H<sup>+</sup>]** Pb:Am ratio. Monocations of lead with alanine, valine, histidine, glutamic acid, arginine or proline are observed to contain nitrate groups and/or water molecules. Interestingly, the lead-arginine system is unique in that no multi-lead complexes were observed, only complexes of **1:1 - 1:6** Pb:Am ratios. This may be indicative of only the guanidine group in the side chain of arginine interacting with the lead centre.



Although  $\text{Pb}^{2+}$  has been shown to inhibit coordination of cysteine residues in certain enzymes to zinc(II)<sup>5</sup> and adopt thiolate complexation,<sup>130</sup> ESI-MS of reaction mixtures containing lead nitrate, cysteine and an amino acid, did not demonstrate lead-cysteine cations or mixed amino acid complexes of lead, suggesting that lead(II) does not have a preference for cysteine over other amino acids, as observed for bismuth.<sup>130</sup>

**Table 8.1:** ESI-MS data for reaction mixtures containing lead nitrate and an amino acid in 50 % ethanol/water for spectra that show prominent cation peaks ( $m/z$ , highest peak amongst the cluster of isotope peaks) containing lead. All assignments have been confirmed by MS/MS.

	$m/z$	Pb:Am	%		$m/z$	Pb:Am	%		$m/z$	Pb:Am	%
Gly	282.1	1:1	100	Tyr	388.1	1:1	100	Asn	339.0	1:1	100
	636.9	2:3	35	His	362.1	1:1	100		470.9	[(1:2)+H <sup>+</sup> ] C <sub>8</sub> H <sub>12</sub> N <sub>4</sub> O <sub>3</sub> Pb <sub>2</sub> <sup>+</sup>	12
Ala	296.1	1:1	90		723.0	[(2:2)-H <sup>+</sup> ] 2:2:NO <sub>3</sub>	25		658.9	[(2:2)-H <sup>+</sup> ]	10
	358.9	[(1:1:NO <sub>3</sub> )+H <sup>+</sup> ]	15		785.9	2:3	20		676.9	2:3	20
	385.0	[(1:2)+H <sup>+</sup> ]	25		875.8	1:1	10		806.9	1:1	50
	606.8	[(2:2:H <sub>2</sub> O)-H <sup>+</sup> ]	20	Ser	312.1	1:1	95	Gln	353.1	1:1	80
Val	677.9	2:3	100	Thr	326.0	1:1	100		667.0	C <sub>10</sub> H <sub>13</sub> N <sub>4</sub> O <sub>3</sub> Pb <sub>2</sub> <sup>+</sup>	50
	296.0	C <sub>3</sub> H <sub>8</sub> NO <sub>2</sub> Pb <sup>+</sup>	15		648.9	[(2:2)-H <sup>+</sup> ]	40		684.8	C <sub>10</sub> H <sub>15</sub> N <sub>4</sub> O <sub>3</sub> Pb <sub>2</sub> <sup>+</sup>	75
	324.0	1:1	100		854.9	[(3:2)-2H <sup>+</sup> ]	39		703.0	[(2:2)-H <sup>+</sup> ]	100
	386.9	[(1:1:NO <sub>3</sub> )+H <sup>+</sup> ]	50		973.8	[(3:3)-2H <sup>+</sup> ]	30		848.9	2:3	74
	441.0	[(1:2)+H <sup>+</sup> ]	45	Met	356.1	1:1	100	Lys	335.3	C <sub>3</sub> H <sub>7</sub> N <sub>2</sub> O <sub>2</sub> Pb <sup>+</sup>	50
Leu	662.7	[(2:2:H <sub>2</sub> O)-H <sup>+</sup> ]	25		504.9	1:2	7		353.1	1:1	40
	707.9	[(2:2:NO <sub>3</sub> )-2H <sup>+</sup> ]	20		691.9	C <sub>10</sub> H <sub>18</sub> N <sub>2</sub> O <sub>3</sub> S <sub>3</sub> Pb <sub>2</sub> <sup>+</sup>	10		460.8	C <sub>12</sub> H <sub>23</sub> N <sub>4</sub> O <sub>2</sub> Pb <sup>+</sup>	100
	761.9	2:3	75		709.1	[(2:2)-H <sup>+</sup> ]	5		850.0	2:3	80
	338.0	1:1	10		857.9	2:3	50	Arg	381.0	1:1	50
	469.0	[(1:2)+H <sup>+</sup> ]	35	Cys	328.1	1:1	100		443.9	[(1:1:NO <sub>3</sub> )+H <sup>+</sup> ] [(1:2)+H <sup>+</sup> ]	15
Ile	673.1	[(2:2)-H <sup>+</sup> ]	15		448.9	[(1:2)+H <sup>+</sup> ]	55		555.1	[(1:2)+H <sup>+</sup> ]	100
	804.0	2:3	100		654.9	[(2:2)-H <sup>+</sup> ]	50		617.7	1:2:NO <sub>3</sub> +2H <sup>+</sup>	10
	338.0	1:1	10	Hcys	324.1	C <sub>4</sub> H <sub>6</sub> NOSPB <sup>+</sup>	35		728.9	[(1:3)+2H <sup>+</sup> ]	40
	469.0	[(1:2)+H <sup>+</sup> ]	35		342.1	1:1	100		791.9	1:3:NO <sub>3</sub> +3H <sup>+</sup>	25
	673.1	[(2:2)-H <sup>+</sup> ]	15		474.8	[(1:2)+H <sup>+</sup> ]	15		902.9	[(1:4)+3H <sup>+</sup> ]	20
Phe	804.0	2:3	100		680.9	[(2:2)-H <sup>+</sup> ]	55		966.1	[(1:4:NO <sub>3</sub> )+4H <sup>+</sup> ]	27
	372.1	1:1	85	Asp	340.1	1:1	100		1139.9	[(1:5:NO <sub>3</sub> )+5H <sup>+</sup> ]	16
	534.9	[(1:2)+H <sup>+</sup> ]	25		561.7	C <sub>4</sub> H <sub>6</sub> NO <sub>3</sub> Pb <sub>2</sub> <sup>+</sup>	15		1314.4	[(1:6:NO <sub>3</sub> )+6H <sup>+</sup> ]	14
	722.9	C <sub>18</sub> H <sub>17</sub> N <sub>2</sub> O <sub>3</sub> Pb <sub>2</sub> <sup>+</sup>	20		677.0	[(2:2)-H <sup>+</sup> ]	55	Pro	322.0	1:1	35
Trp	740.8	[(2:2)-H <sup>+</sup> ]	15		882.9	[(3:2)-2H <sup>+</sup> ]	10		385.0	[(1:1:NO <sub>3</sub> )+H <sup>+</sup> ]	55
	905.9	2:3	100		1015.9	[(3:3)-2H <sup>+</sup> ]	30		437.1	[(1:2)+H <sup>+</sup> ]	99
	411.1	1:1	100	Glu	354.0	1:1	100		758.0	2:3	100
	614.9	[(1:2)+H <sup>+</sup> ]	30		558.1	[(2:1)-2H <sup>+</sup> ]	10				
	801.1	C <sub>22</sub> H <sub>19</sub> N <sub>4</sub> O <sub>3</sub> Pb <sub>2</sub> <sup>+</sup>	3		576.0	[(2:1:H <sub>2</sub> O)-2H <sup>+</sup> ]	35				
	818.9	[(2:2)-H <sup>+</sup> ]	5		705.0	[(2:2)-H <sup>+</sup> ]	30				
	1023.1	2:3	35								

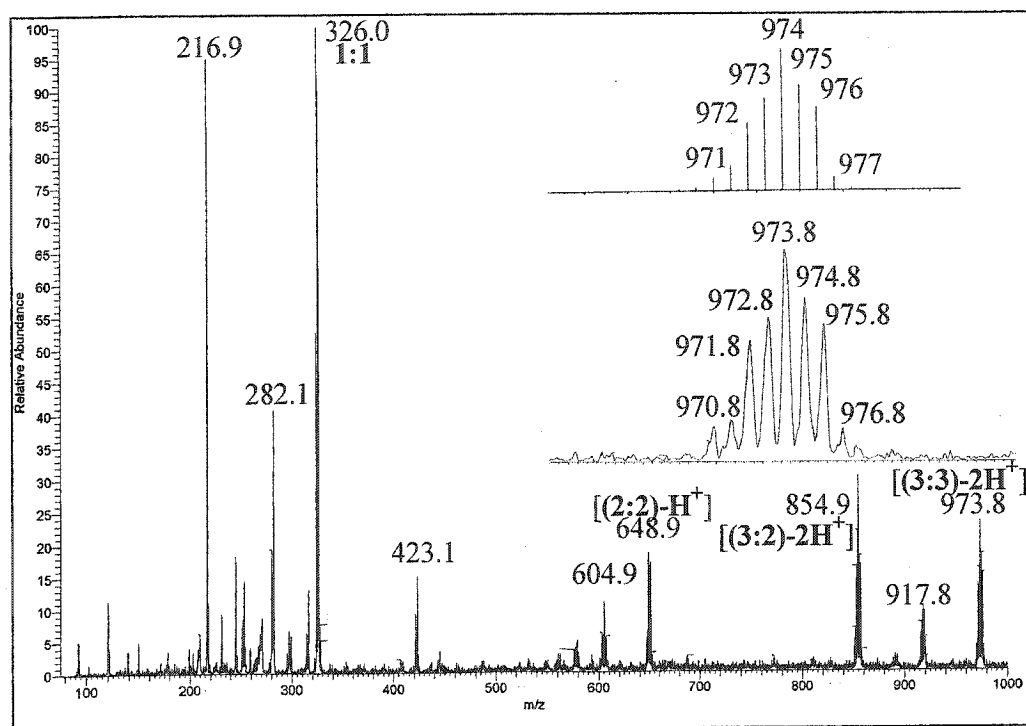


**Figure 8.1:** ESI-MS of a solution containing lead nitrate and L-threonine in 50 % ethanol. Peak assignments of lead containing monocations are listed in Table 8.1. The isotopic peaks and calculated (above) isotopic peaks for a complex consistent with a 3:3 Pb:Am ratio is shown.

Speciation of lead in biological and environmental solutions is likely complicated and limited structural data is available. The use of ESI-MS provides insight into the coordination chemistry of metals and in some instances  $m/z$  peaks can be directly correlated to samples isolated and structurally characterised.<sup>54</sup> In this context, crystalline material suitable for X-ray crystallography that has been confirmed as the valine complex  $\text{Pb}(\text{Val})_2(\text{H}_2\text{O})_2(\text{NO}_3)_2$  (**8.1**) shown in Figure 8.2(i), represents the first crystallographically characterised lead complex involving an amino acid. In this structure an eight-coordinate holodirected<sup>42</sup> lead environment is observed, imposed by oxygen centres through chelation from one valine ligand, a second monodentate valine ligand, two water molecules, interaction from one oxygen centre (O10) in a nitrate group and chelation (O8 and O9) from a symmetry related nitrate group of the next complex resulting in a polymeric solid state structure (Figure 8.2(ii)). The solid state structure contains a second nitrate group that does not interact with the lead centre. The charge balance for lead(II) requires that the pendant nitrogen centres of the valine ligands represent ammonium functionalities, such that the complex is best considered as two neutral valine ligands coordinated to  $\text{Pb}(\text{NO}_3)_2$ .

In the mass spectrum of the lead-valine reaction mixture, dications are not apparent possibly indicating that  $\text{Pb}(\text{Val})_2^{2+}$  is not kinetically stable in the gas phase. However, there are prominent peaks present, as listed in Table 8.1, corresponding to a monocation of 1:2 Pb:Val ratio as well as those containing a nitrate group or water molecule ( $[(1:1:\text{NO}_3)+\text{H}^+]$ ,  $[(2:2:\text{NO}_3)+2\text{H}^+]$ ,  $[(2:2:\text{NO}_3)-2\text{H}^+]$ ).

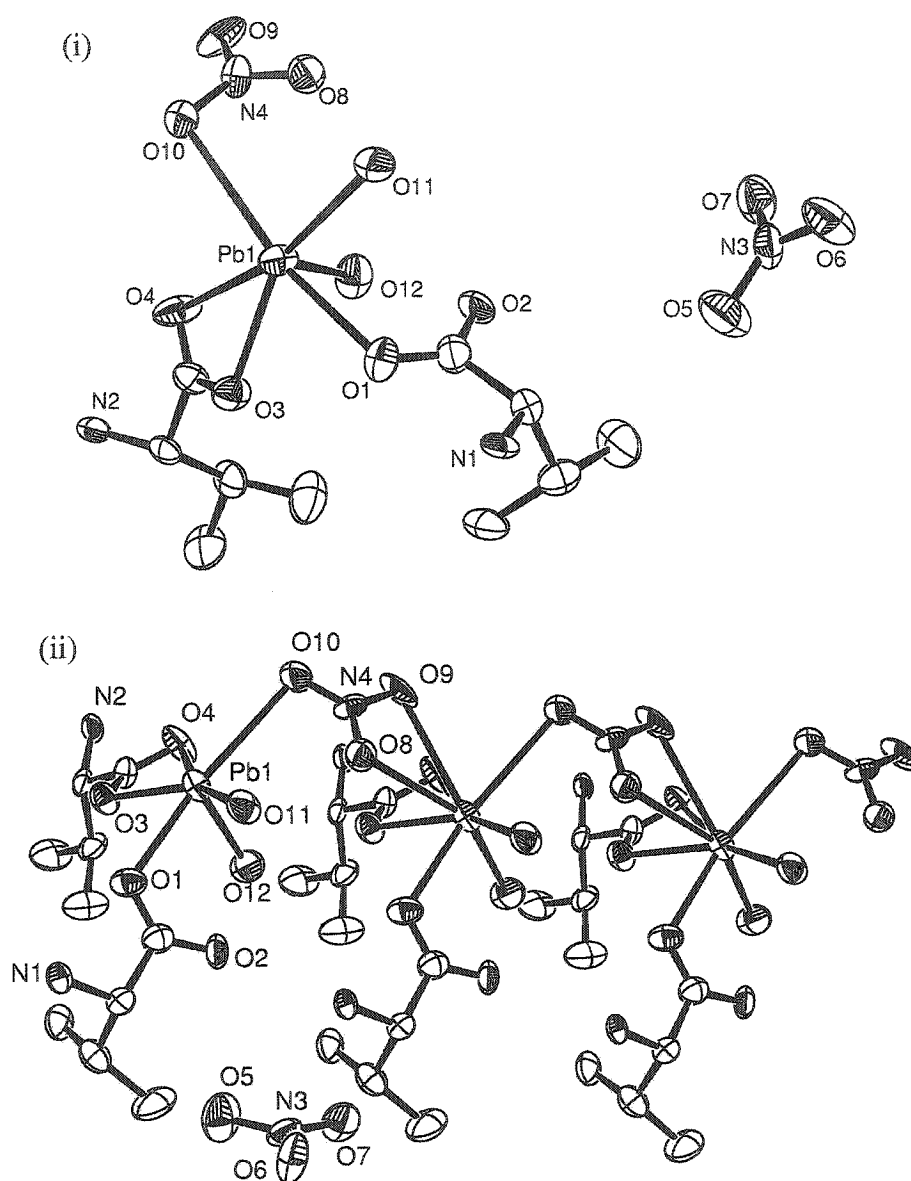


**Figure 8.2:** (i) Crystallographic view of the empirical formula unit of  $\text{Pb}(\text{Val})_2(\text{H}_2\text{O})_2(\text{NO}_3)_2$  (**8.1**). (ii) Crystallographic view of the polymeric arrangement of **8.1**. Hydrogen atoms have been omitted for clarity. Selected internuclear distances (Å): Pb1-O3 2.36(1), Pb1-O1 2.44(1), Pb1-O12 2.50(1), Pb1-O8a 2.78(1), Pb1-O9a 2.85(2), Pb1-O4 2.87(1), Pb1-O11 2.89(1), Pb1-O10 2.95(1).

### 8.3 Conclusions and Future Directions

ESI-MS has been demonstrated as a data-rich approach for the identification of complexes formed by lead(II) with twenty-one of the common amino acids. As well, insight has been gained into the kinetic stability of such complexes, especially those complexes of lead with cysteine and homocysteine. These observations greatly contrast those from similar experiments performed with mixtures containing  $\text{Bi}^{3+}$ , as discussed in the preceding chapter, which showed great affinity towards those amino acids containing sulfur and much less reactivity with the other amino acids.

An efficient investigation of lead(II) and chemistry with other biologically relevant molecules (peptides, proteins, carbohydrates, DNA/RNA bases) can now be undertaken as the value of ESI-MS for gaining a broad appreciation of the coordination chemistry of heavy metals by virtue of the distinctive  $m/z$  values has been demonstrated.

## Chapter 9: Application of Electrospray Ionisation Mass Spectrometry to Identify Heavy Metal Complexes Involving Amino Acids

### 9.1 Introduction

Reactions of mercury(II) with sulfur-containing amino acids have been thoroughly studied,<sup>131-144</sup> and the solid state structures of two antimony(III) fluoride complexes involving glycine,<sup>145</sup> a thallium(I)-cysteinate complex<sup>146</sup> and a tryptophan complex of mercury(II)<sup>147</sup> have been reported. However, these complexes represent unique examples for a particular amino acid. In addition, compounds of this type have proven difficult to structurally characterise for arsenic and cadmium, resulting in structural assignments and formulations that are speculative.<sup>100;148</sup>

ESI-MS is a powerful tool for the identification of interactions between biomolecules and heavy metals by virtue of their distinctive  $m/z$  values. This chapter presents preliminary ESI-MS data for reaction mixtures containing arsenic, antimony, thallium, mercury or cadmium with each of the naturally occurring amino acids.

### 9.2 Results and Discussion

Reaction mixtures containing an amino acid and a heavy metal reagent ( $\text{As}_2\text{O}_3$ ,  $\text{SbCl}_3$ ,  $\text{TlNO}_3$ ,  $\text{Hg}(\text{NO}_3)_2 \cdot \text{H}_2\text{O}$ ,  $\text{Hg}_2(\text{NO}_3)_2 \cdot 2\text{H}_2\text{O}$ , or  $\text{Cd}(\text{NO}_3)_2 \cdot 4\text{H}_2\text{O}$ ) in 50 % ethanol were analysed by positive ion ESI-MS. Table 9.1 lists the assignments of monocationic complexes observed between each of the metal ions with the amino acids as determined by ESI-MS and confirmed by MS/MS. The assignments are provided as HM:Am ratios (HM = heavy metal; Am = amino acid, a monoanionic or a dianionic conjugate base of

the amino acid). Thallium(I), mercury(II), and cadmium(II) were found to form kinetically stable complexes with each of the essential amino acids, as well as with homocysteine analogous to Pb(II). Interestingly, thallium(I) forms complexes of **1:1** ratio (Tl:Am) for all of the amino acids except glycine, tyrosine, and aspartic acid and **2:1** ratios (Tl:Am) were observed with all except tyrosine, cysteine, homocysteine and arginine. Many of the amino acids are also found to form multi-thallium complexes of **3:2** or **3:1** ratios. As with the lead(II), only complexes of the type **1:1**, **1:2**, **1:3**, **1:4**, and **1:5** Tl:Am form between  $Tl^+$  and arginine.

From the reaction mixtures containing  $Hg^{2+}$ , most of the amino acids are observed to form complexes of **1:1**, **1:2**, **2:2**, **2:3** Hg:Am ratios. Asparagine also forms a cation of **1:3** and glycine, alanine, leucine, isoleucine, serine, threonine, and asparagine form **3:3** monocations with mercury(II). Glycine, alanine, valine, leucine, isoleucine also form complexes with  $Hg^{2+}$  containing ethanol molecules. A representative mass spectrum is provided in Figure 9.1 for the reaction mixture containing mercury(II) nitrate and L-cysteine.

Cadmium(II) forms a number of complexes containing nitrate groups with all of the amino acids. Most of the reaction mixtures exhibit monocations of the **1:1**, **1:2**, **2:2**, **2:3** and **3:3** Cd:Am ratios. Homocysteine was the only amino acid observed to form a **3:2** ratio with  $Cd^{2+}$ .



**Table 9.1:** Monocation assignments from ESI-MS data of reaction mixtures containing a heavy metal reagent and an amino acid in 50 % ethanol. Assignments are given as HM:Am (HM = heavy metal; Am = amino acid).

	Gly	Ala	Val	Leu	Ile	Phe	Trp	Tyr	His	Ser	Thr	Met	Cys	Hcys	Asp	Glu	Asn	Gln	Lys	Arg	Pro
As <sup>3+</sup>										1:1	1:2		1:1 1:2 1:3 <sup>a</sup>				1:1 1:2	1:1 1:2			
Sb <sup>3+</sup>									1:2				1:1 1:2 2:3			1:2		1:2			
Tl <sup>+</sup>	2:1 3:2	1:1 2:1	1:1 2:1 3:2	1:1 2:1	1:1 2:1 3:2	1:1 2:1	1:1 2:1	3:2	1:1 2:1 3:2	1:1 2:1	1:1 2:1	1:1 2:1	1:1 2:3	1:1	2:1 3:1	1:1 3:1	2:1 2:2	1:1 2:1 2:2	1:1 2:1 3:2	1:1 2:1 1:3 1:4 1:5	1:1 2:1 3:2
Hg <sup>2+</sup>	1:1 <sup>b</sup> 3:3	1:1 <sup>b</sup> 1:2 2:2 2:3 3:3	1:1 <sup>b</sup> 1:1 <sup>b</sup> 1:2 3:3	1:1 1:1 <sup>b</sup> 1:2 3:3	1:1 1:1 <sup>b</sup> 1:2 3:3	1:1 <sup>c</sup> 1:2 1:2 <sup>c</sup> 2:2 2:3	1:1 1:2 2:2 3:3	1:2 2:2 2:3 3:2 3:3	1:2 2:3 3:2 3:3	1:2 2:2 2:3 3:2 3:3	1:2 2:2 2:3 3:2 3:3	1:1 1:2 2:2 2:3 3:3	1:2 2:3	1:2	2:2 <sup>b</sup>	2:2	1:1 1:2 1:3 2:2 2:3 3:3	2:2 2:3	1:1 1:2 2:2 2:3 3:3	1:1 1:2 2:2 2:3 3:4	1:1 1:2 2:2 2:3
Hg <sup>+</sup>	1:1 1:1 <sup>b</sup>		1:1 <sup>b</sup> 2:1 <sup>b</sup>	1:2 2:3 2:4 2:4 <sup>d</sup> 3:4 4:4	1:2 2:3 2:4 3:4 4:4	1:1 1:2 1:2	2:1 2:2 <sup>d</sup> 3:3 <sup>d</sup>	1:1 <sup>b</sup> 1:2 1:2	1:2 2:2 2:3	1:1 <sup>b</sup> 2:2 2:3	1:1 <sup>b</sup> 2:3	1:2 2:2 2:3	1:2				1:2 2:3		1:1 1:2 2:2 2:3 3:3	1:2 2:2 2:3 3:4	1:1 <sup>b</sup> 2:3
Cd <sup>2+</sup>	1:1 <sup>d</sup> 3:3 <sup>d</sup> 3:5 <sup>d</sup>	1:1 <sup>d</sup> 1:2 1:2 <sup>d</sup> 2:2 2:3 3:3 3:4 <sup>d</sup>	1:1 <sup>d</sup> 1:2 1:2 <sup>d</sup> 2:2 2:3 3:3 3:4 <sup>d</sup>	1:1 <sup>d</sup> 2:3 4:6 <sup>d</sup> 4:6 <sup>d</sup>	1:1 <sup>d</sup> 2:3 4:6 <sup>d</sup> 4:6 <sup>d</sup>	1:1 <sup>d</sup> 1:2 <sup>d</sup> 2:3 3:3	1:1 <sup>d</sup> 1:2 2:2 <sup>d</sup> 2:3	1:1 <sup>d</sup> 1:2 2:2 <sup>d</sup> 2:3	1:1 <sup>d</sup> 1:1 <sup>d</sup> 2:2 <sup>d</sup> 3:3 <sup>d</sup>	1:1 <sup>d</sup> 1:1 <sup>d</sup> 2:2 <sup>d</sup> 3:3 <sup>d</sup>	1:1 <sup>d</sup> 1:1 <sup>d</sup> 2:2 <sup>d</sup> 3:3 <sup>d</sup>	1:1 <sup>d</sup> 1:2 2:2 <sup>d</sup> 2:3	1:1 <sup>d</sup> 1:2 2:2 <sup>d</sup> 2:3	1:1 <sup>d</sup> 1:2 2:2 <sup>d</sup> 2:3	1:1 <sup>c</sup> 1:1 <sup>d</sup> 2:2 <sup>d</sup>	1:1 <sup>d</sup>	1:1 <sup>d</sup> 2:2 <sup>d</sup> 2:3	1:1 <sup>d</sup> 2:2 <sup>d</sup> 2:3	1:1 <sup>d</sup> 2:2 <sup>d</sup> 2:3	1:1 <sup>d</sup> 1:2 2:2 <sup>d</sup> 2:3	1:1 <sup>d</sup> 1:2 2:2 <sup>d</sup> 2:3

<sup>a</sup> Contains Na<sup>+</sup> (i.e. 1:3Na) <sup>b</sup> Contains EtOH (i.e. 1:1:EtOH) <sup>c</sup> Contains H<sub>2</sub>O (i.e. 1:1:H<sub>2</sub>O) <sup>d</sup> Contains NO<sub>3</sub> (i.e. 1:1:NO<sub>3</sub>)

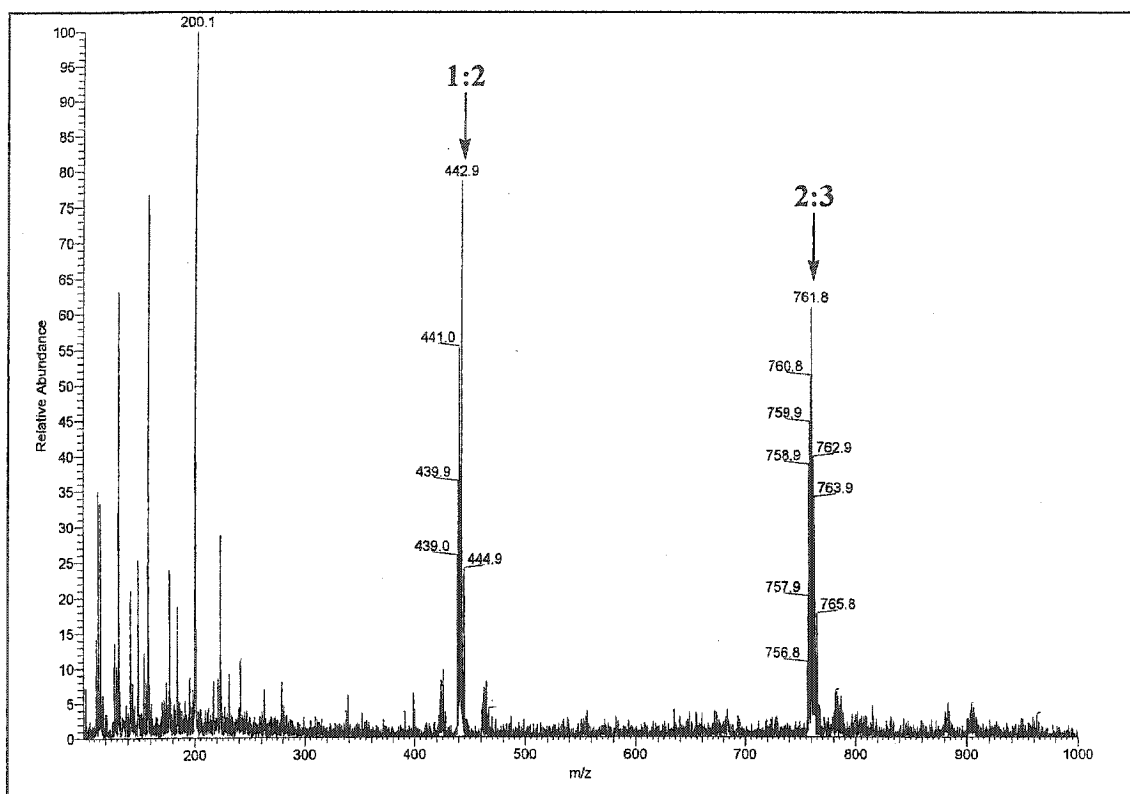


**Figure 9.1:** An ESI-MS of the reaction mixture containing  $\text{Hg}(\text{NO}_3)_2 \cdot \text{H}_2\text{O}$  and L-cysteine in 50 % ethanol. The assigned peaks given as Hg:Am ratios have been confirmed by MS/MS.

Mercury(I), arsenic(III) and antimony(III) were found to only form complexes detectable by ESI-MS with sixteen, five and four amino acids, respectively. Complexes involving alanine, homocysteine, aspartic acid, glutamic acid and glutamine were not observed from reaction mixtures containing  $\text{Hg}_2(\text{NO}_3)_2 \cdot 2\text{H}_2\text{O}$  and these amino acids. Arsenic(III) forms complexes of the type **1:1** and **1:2** As:Am with serine, threonine, cysteine, asparagine and glutamine. L-cysteine also forms a sodiated **1:3** complex with  $\text{As}^{3+}$ . Antimony(III) forms **1:2** Sb:Am ratios with histidine, cysteine, glutamic acid, and glutamine. Complexes of **1:1** and **2:3** ratios are also observed from antimony/cysteine reaction mixtures. It is interesting to note that with the exception of the **1:2** monocation observed for glutamic acid with  $\text{Sb}^{3+}$ , arsenic and antimony form kinetically stable complexes with amino acids that are among the seven observed to interact with bismuth(III). Although bismuth also forms monocations involving homocysteine, neither arsenic nor antimony were observed to form complexes with this amino acid.

### 9.3 Conclusions and Future Directions

Reaction mixtures containing certain heavy metals and amino acids have been assessed using ESI-MS. The heavy metals arsenic, antimony, bismuth, lead, thallium, mercury and cadmium behave differently and the coordination environment of these metals with the amino acids is not universal, with each metal giving distinct trends of HM:Am ratios. As such, this work demonstrates the suitability of the ESI-MS method for assessing the coordination chemistry of metals in general and offers the possibility for development of toxicity screenings using ESI-MS.

Investigations of mixed amino acid systems with these metals should now be undertaken, especially in the cases of  $\text{Hg}^+$ ,  $\text{As}^{3+}$  and  $\text{Sb}^{3+}$ , to determine whether interactions of certain amino acids could lend kinetic stability to metal-amino acid complexes, as observed from ESI-MS of bismuth(III) nitrate/cysteine/amino acid reaction mixtures. In addition, a thorough study can now be undertaken to evaluate the chemistry of heavy metals with other biomolecules such as peptides (e.g. glutathione) and proteins. A combinatorial type approach can be used to generate peptides of various lengths and combinations of amino acid residues that can be assessed with each heavy metal.

The chemistry of the metals with carbohydrates and nucleotides can also now be considered. It has been shown that arsenic induces damage directly on DNA strands causing gaps, strand breaks and aberrations in the biological information located in the chromosomes and chromatids.<sup>149-152</sup> Isolation of an adenosine-5'-arsenate suggests that arsenic could perhaps displace phosphate in the DNA backbone.<sup>153;154</sup> However, attempts to model accurately the behaviour of arsenic with DNA have been difficult and, as such, ESI-MS may prove to be particularly useful in this investigation.

## Chapter 10: Experimental

### 10.1 General Procedures

Melting points were recorded on an Electrothermal melting point apparatus. IR spectra were recorded as Nujol mulls on CsI plates using a Nicolet 510P spectrometer. Raman spectra were obtained for powdered and crystalline samples on a Bruker RFS 100 spectrometer. Vibrational spectra are presented as wavenumber ( $\text{cm}^{-1}$ ) maxima with ranked intensities for absorptions given in parentheses and the most intense peak is given a ranking of 1. Canadian Microanalytical Service Ltd., Delta, British Columbia, performed all chemical analyses. ESI-MS were obtained using a VG Micromass Quattro quadrupole mass spectrometer (1), Sciex Qtrap triple quadrupole/ion trap mass spectrometer (2) and/or a Finnigan LCQ Duo ion trap mass spectrometer (3). Samples were injected directly into the electrospray source at a flow rate of 1.2 ml/hr with a source temperature of 385 K (1, 2) or 473 K (3) and a cone voltage (1) or declustering potential (2) of 50 V. MS/MS spectra were obtained using argon (1), nitrogen (2) or helium (3) as the collision gas and the collision energy was optimised for each sample. Solid state structures were obtained by X-ray crystallographic studies performed by Drs. T.S. Cameron and K.N. Robertson. X-ray crystallographic data were obtained on a Rigaku AFC5R diffractometer.

### 10.2 Synthetic Procedures

All compounds were used as received from Aldrich, except for potassium hydroxide, which was used as received from BDH. All reactions involving thiols were

performed under an atmosphere of  $N_2$  to prevent oxidation of thiols to disulfides. All reactions were performed at room temperature. All compounds are air and moisture stable.

#### *Preparation of **3.1cCl<sub>2</sub>***

Addition of MTG (5.45 mmol) to a slurry of  $BiCl_3$  (5.56 mmol) in absolute ethanol immediately produced a pale yellow solution that was stirred overnight and suction filtered. On standing for one week, the filtrate gave yellow crystalline plates of **3.1cCl<sub>2</sub>**. Yield: 1.36 mmol, 25%; dp: 180°C; Anal. Calcd. (Found): C 12.04 (12.28); H 1.77 (1.80) %; FT-IR: 278(4), 372(9), 865(8), 1012(4), 1110(11), 1152(6), 1199(4), 1266(10), 1314(2), 1369(3), 1383(5,sh), 1441(7), 1462(1,sh), 1662(6); FT-Raman: 58(14), 92(10), 98(8), 129(7), 176(6), 211(5), 241(1), 265(4), 317(2), 373(12), 564(25), 867(19), 890(24), 1113(23), 1156(22), 1200(13), 1442(18), 1665(20), 2867(17), 2895(16), 2910(3), 2932(11), 2944(21), 2976(15), 2982(9). A mass spectrometric sample was prepared by the same method with the filtrate collected used for ESI-MS on instrument (1). Crystal data are provided in Table 10.1.

#### *Preparation of Mass Spectrometric Samples Containing $BiCl_3$ and MTG*

(1) Addition of  $BiCl_3$  (5.3 mmol) to MTG (10 mmol) in 95% ethanol or methanol (150 mL) gave a yellow reaction mixture that was stirred overnight, suction filtered to remove any precipitate. The filtrate collected was used for ESI-MS on instrument (1). **3.2cCl** is prepared by a similar method.<sup>54</sup>

(2) Addition of  $\text{BiCl}_3$  (5.2mmol) to MTG (15.7mmol) and KOH (16mmol) in 95% ethanol (150mL) gave a dark yellow reaction mixture that was stirred overnight, suction filtered to remove any precipitate. The filtrate collected was used for ESI-MS on instrument (1). **3.3c** is prepared by a similar method.<sup>54</sup>

#### *Preparation of 3.4*

A solution of MTS (21.4 mmol) and KOH (22.3 mmol) in ethanol (50 mL) was added dropwise to a stirred slurry of  $\text{BiCl}_3$  (7.29 mmol) in ethanol (50 mL) under nitrogen. The product was removed by suction filtration and recrystallized from DMF (yellow needles). Yield: 4.7 mmol, 64%; mp 141 °C; Anal. Calc. (Found): C, 40.57 (40.48); H, 2.98 (3.21); FT-IR: 1716 (9), 1699 (6), 1675 (3), 1582 (18), 1456 (11), 1437 (8), 1423 (16), 1310 (12), 1291 (7), 1274 (5), 1248 (1), 1194 (20), 1134 (15), 1129 (17), 1112 (13), 1054 (2), 1037 (19), 749 (10), 743 (4), 303 (14). Mass spectrometric samples were prepared by the same method with the filtrates collected used for ESI-MS on instrument (1). Crystal data are provided in Table 10.1.

#### *Preparation of Mass Spectrometric Samples Containing $\text{BiCl}_3$ and Msuc or Tsal*

Msuc or Tsal (0.99 – 1.11 mmol) was added to a slurry of  $\text{BiCl}_3$  (1.02 – 1.15 mmol) in 50 % ethanol (30 mL) to produce a yellow mixture (Msuc or Tsal). The resulting reaction mixture was stirred overnight at RT and then suction filtered to remove any precipitate. The filtrate collected was used for ESI-MS on instrument (3).

*Preparation of Mass Spectrometric Samples Containing  $\text{Bi}(\text{NO}_3)_3$  and Mal or Suc*

Mal or Suc (0.95 – 1.01 mmol) was added to a slurry of  $\text{BiCl}_3$  (0.98 – 1.07 mmol) in 50 % ethanol (30 mL) to produce a white reaction mixture (Mal or Suc). The resulting reaction mixture was stirred overnight at RT and then suction filtered to remove any precipitate. The filtrate collected was used for ESI-MS on instrument (3).

*Preparation of **5.5***

MTS (5.12 mmol) and KOH (5.15 mmol) in ethanol (50 mL) were added in a dropwise fashion to a stirred slurry of **5.1** or **5.2**<sup>85</sup> (5.08 mmol) in ethanol (50 mL). The resulting yellow reaction mixture was allowed to stir overnight at room temperature. The precipitate was removed by suction filtration. The filtrate was reduced in volume on a rotary evaporator and was left to evaporate over a period of 4 days to give yellow needles of **5.5**. Yield: 3.00 mmol, 59%; mp: 139 °C; Anal. Calcd. (Found): C 27.27 (27.39); H 2.86 (3.06) %; FT-IR: 273(1), 866(2), 875(3), 1716(4), 1423(5), 1136(6), 1274(7), 1437(8), 532(9), 749(10), 307(11), 970(11), 1041(12), 1123(13), 1309(14). Crystal data are presented in Table 10.1. Compounds **5.3a**, **5.3b** and **5.4a** were prepared by a similar method.<sup>84</sup>

*Preparation of **5.6a***

Compound **5.6a** was prepared by addition of a solution of KOH (3.57 mmol) and 2-mercaptoethanol (Metl) (3.54 mmol) in ethanol (50 mL) to a slurry of bismuth chloride (3.48 mmol) in ethanol (50 mL). The resulting yellow reaction mixture was stirred for three hours at which point an ethanolic solution (50 mL) containing KOH and 2-



aminoethanethiol (Aet) hydrochloride was added dropwise. This reaction mixture was allowed to stir overnight at room temperature. The reaction mixture was suction filtered to remove any precipitate. The filtrate was reduced in volume by rotary evaporation and was left to evaporate over a period of 4 days to give green-gold plates of **5.6a**. Yield: 1.74 mmol, 50%; mp: 168 - 173 °C; Anal. Calcd. (Found): C 13.30 (13.51); H 2.79 (2.89) %; FT-IR: 1035(1), 334(2), 1275(3), 1005(4), 510(5), 1366(6), 317(7), 964(8), 381(9), 833(10), 1052(11), 1418(12), 1205(13), 288(14), 925(15), 1084(16), 271(17), 1160(18), 663(19), 721(20). Crystal data are presented in Table 10.1.

*Preparation of Mass Spectrometric Samples Involving BiCl<sub>3</sub> and ACA*

ACA ( 3.83 mmol) was added to a slurry of BiCl<sub>3</sub> (1.24 g, 3.92 mmol) in methanol (100 mL) to produce a yellow solution. The solution was stirred for six hours at RT and diluted by a factor of 10 with methanol. The filtrate collected was used for ESI-MS on instrument (1).

*Preparation of Bi(NO<sub>3</sub>)<sub>3</sub>/Amino acid Samples for Mass Spectrometry*

Mixtures of Bi(NO<sub>3</sub>)<sub>3</sub>·5H<sub>2</sub>O (8.86 – 5.90 mmol) and one or two amino acids (8.86 – 5.90 mmol) in equimolar stoichiometry were stirred overnight in 10 mL ethanol and 10 mL water. The reaction mixture was then suction filtered to remove any precipitate and injected as described above. The filtrates collected were used for ESI-MS on instruments (2) and (3).

### *Preparation of 7.2*

A mixture of  $\text{Bi}(\text{NO}_3)_3 \cdot 5\text{H}_2\text{O}$  (0.57 mmol), L-cysteine (0.61 mmol) and 1,10-phenanthroline (0.68 mmol) was stirred overnight in 15 mL water and 30 mL ethanol. The reaction mixture was then suction filtered and the filtrate was allowed to evaporate slowly over seven days to give yellow crystals; yield: 0.18 mmol, 31%; mp/dp: 171-179°C; Anal. Calcd. (Found): C 27.66 (27.80), H 2.48 (2.48), N 10.79 (10.75)%; FT-IR ( $\text{cm}^{-1}$ ): 2924(1), 2854(2), 1624(11, sh), 1518(7, sh), 1458(3), 1377(4), 1290(5), 1099(10), 1017(9), 846(8), 773(12), 721(6), 641(13), 523(14), 419(15); FT-Raman ( $\text{cm}^{-1}$ ): 3088(7), 3060(21), 2982(24), 2954(14), 2920(22), 1623(20), 1604(18), 1591(8), 1518(12), 1448(2), 1412(1), 1344(17), 1304(3), 1206(19), 1101(16), 1055(10), 1040(5), 1018(11), 865(23), 724(9), 555(15), 421(4), 323(6), 296(13). Attempts to isolate other complexes involving conjugate bases of amino acids with bismuth were unsuccessful. Crystal data are provided in Table 10.1.

### *Preparation of $\text{Pb}(\text{NO}_3)_2$ /Amino acid Samples for Mass Spectrometry*

A mixture of  $\text{Pb}(\text{NO}_3)_2$  (1.05-1.11 mmol) and the amino acid (1.05-1.19 mmol) was stirred overnight in 10 mL distilled water and 10 mL ethanol at RT and then was suction filtered to remove any precipitate. The filtrates collected were used for ESI-MS on instrument (3).

### *Preparation of 8.1*

$\text{Pb}(\text{NO}_3)_2$  (1.07 mmol) and L-valine (1.10 mmol) was stirred in 10 mL ethanol and 10 mL of water overnight at room temperature to form a clear solution. The solution

was suction filtered and the filtrate was left to evaporate for 1 week at which point white needles of  $\text{Pb}(\text{Val})_2(\text{H}_2\text{O})_2(\text{NO}_3)_2$  were isolated Yield: 0.59 mmol (55 %), mp: 105 °C. FT-IR ( $\text{cm}^{-1}$ : 1515(1), 1568(2), 1613(3), 1632(4) 1768(5), 1022(6), 804(7), 752(8), 586(9). 558(10). Attempts to isolate other complexes involving conjugate bases of amino acids with lead were unsuccessful. Crystal data are provided in Table 10.1.

*Preparation of Heavy Metal/Amino acid Samples for Mass Spectrometry*

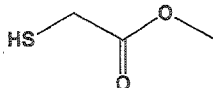
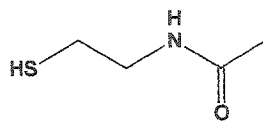
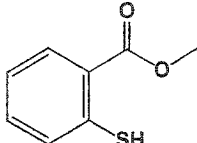
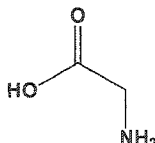
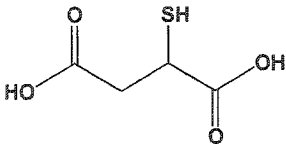
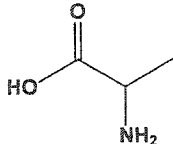
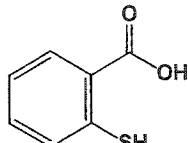
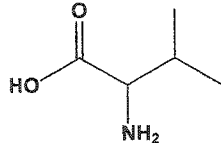
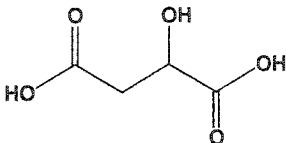
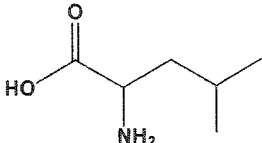
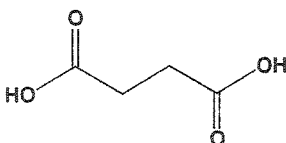
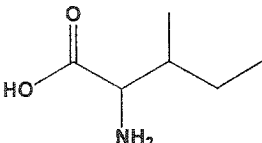
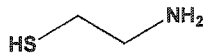
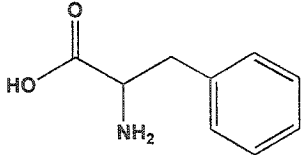
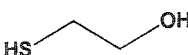
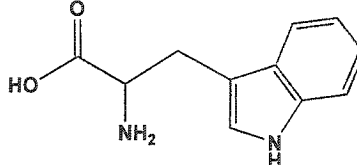
A mixture of a heavy metal reagent ( $\text{As}_2\text{O}_3$ ,  $\text{SbCl}_3$ ,  $\text{TlNO}_3$ ,  $\text{Hg}(\text{NO}_3)_2 \cdot \text{H}_2\text{O}$ ,  $\text{Hg}_2(\text{NO}_3)_2 \cdot 2\text{H}_2\text{O}$ , or  $\text{Cd}(\text{NO}_3)_2 \cdot 4\text{H}_2\text{O}$ ) (0.32 mmol – 0.55 mmol) and the amino acid (0.31 mmol – 0.59 mmol) was stirred overnight at RT in 10 mL distilled water and 10 mL ethanol. The reaction mixture was then suction filtered to remove any precipitate. The filtrates collected were used for ESI-MS on instrument (3).

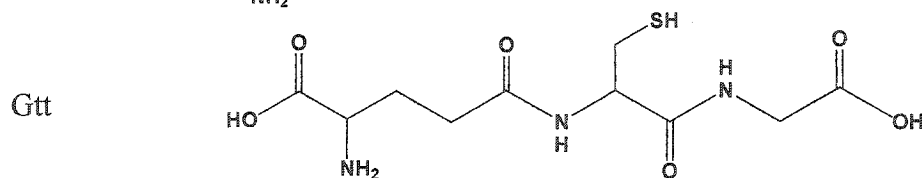
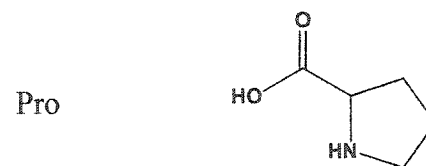
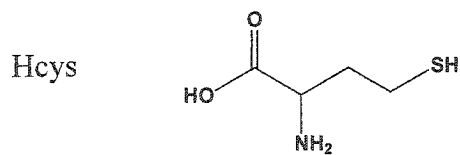
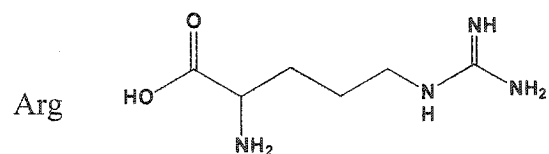
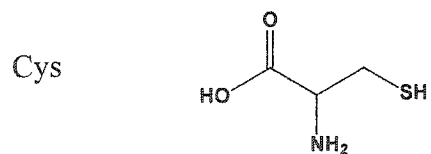
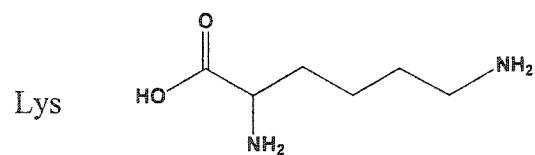
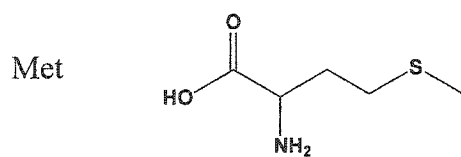
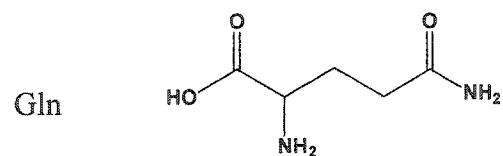
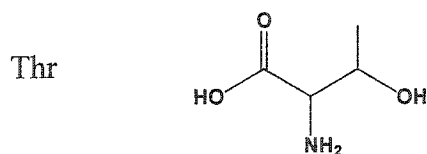
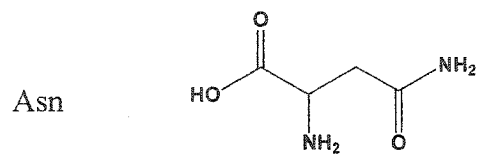
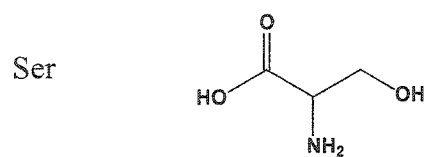
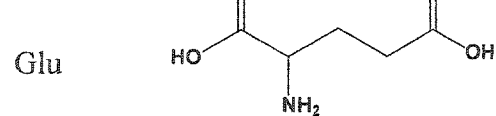
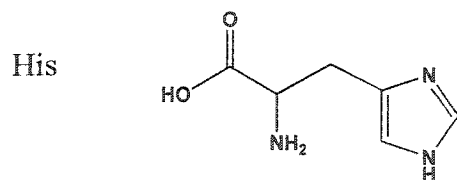
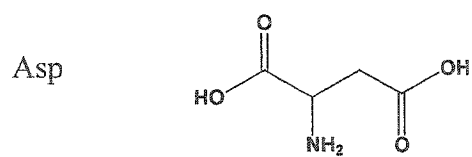
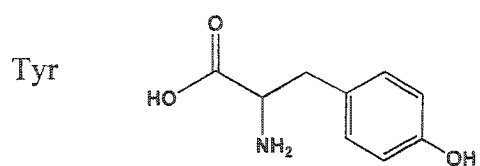
**Table 10.1:** Crystal data for **3.1cCl<sub>2</sub>**, **3.4**, **5.5**, **5.6a**, **7.2**, and **8.1**.

	<b>3.1cCl<sub>2</sub></b>	<b>3.4</b>	<b>5.5</b>	<b>5.6a</b>	<b>7.2</b>	<b>8.1</b>
Formula	C <sub>4</sub> H <sub>7</sub> BiCl <sub>2</sub> O <sub>2</sub> S	C <sub>24</sub> H <sub>21</sub> BiO <sub>6</sub> S <sub>3</sub>	C <sub>12</sub> H <sub>15</sub> BiO <sub>2</sub> S <sub>4</sub>	C <sub>4</sub> H <sub>10</sub> BiNOS <sub>2</sub>	C <sub>13</sub> H <sub>16</sub> BiN <sub>5</sub> O <sub>9</sub> S	C <sub>10</sub> H <sub>26</sub> N <sub>4</sub> O <sub>12</sub> Pb
Fw	399.04	710.59	528.47	361.23	399.04	601.53
space group	<i>P</i> 2 <sub>1</sub> / <i>a</i>	<i>P</i> -1	<i>P</i> 2 <sub>1</sub>	<i>P</i> 2 <sub>1</sub> / <i>c</i>	<i>P</i> -1	<i>P</i> 2 <sub>1</sub> 2 <sub>1</sub> 2 <sub>1</sub>
<i>a</i> (Å)	8.055(3)	12.683(5)	8.147(2)	8.233(3)	9.219 (2)	13.609(6)
<i>b</i> (Å)	10.284(4)	14.118(4)	8.736(2)	6.492(4)	13.422(4)	26.75(1)
<i>c</i> (Å)	11.099(4)	8.123(2)	11.941(2)	16.738(3)	8.755(2)	5.416(5)
$\alpha$ (deg)	90	105.19(2)	90	90	93.39(3)	90
$\beta$ (deg)	100.69(4)	105.29(2)	103.54(2)	111.96(2)	110.01(2)	90
$\gamma$ (deg)	90	104.22(3)	90	90	101.34(2)	90
<i>V</i> (Å <sup>3</sup> )	903.5(6)	1274.2(9)	826.3(3)	829.6(5)	988.6(5)	1971(2)
<i>Z</i>	4	2	2	4	2	4
<i>T</i> (°C)	-130±1	23 ±1	23 ±1	23 ±1	-130±1	-130±1
<i>D<sub>c</sub></i> (Mg m <sup>-1</sup> )	2.993	1.852	2.124	2.892	2.188	2.027
<i>R<sup>a</sup></i>	0.029 ( <i>I</i> >2σ)	0.068	0.044 (obs 2σ data)	0.0570 (obs 3σ data)	0.0635 ( <i>F</i> <sup>2</sup> > 2σ)	0.0427 ( <i>F</i> <sup>2</sup> > 2σ)
<i>R<sub>w</sub><sup>b</sup></i>		0.074		0.073 (obs 3σ data)	0.1651 (all data)	0.1092 (all data)
<i>WR<sub>2</sub><sup>c</sup></i>	0.079 (all data)		0.124 (all data)			

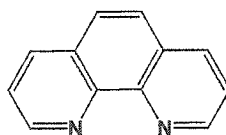
$$^a R = \sum ||F_o| - |F_c|| / \sum |F_o|, \quad ^b R_w = [(\sum w(|F_o| - |F_c|)^2 / \sum |F_o|^2)]^{1/2}, \quad ^c WR^2 = \{\sum [w(F_o^2 - F_c^2)^2] / \sum (F_o^2)^2\}^{1/2}$$

## Appendix: List and Structures of Ligands

MTG		ACA	
MTS		Gly	
Msuc		Ala	
Tsal		Val	
Mal		Leu	
Suc		Ile	
Aet		Phe	
Metl		Trp	



phen



## References

- (1) Russell, J. B. *General Chemistry*; 1992; p 249.
- (2) Thompson, K. H.; Orvig, C. *Science* **2003**, *300*, 936-939.
- (3) Briand, G. G.; Burford, N. *Chem. Rev.* **1999**, *99*, 2601-2657.
- (4) Hall, D. W. R. *Scand. J. Gastroenterol.* **1989**, *24* (suppl 157), 3-6.
- (5) Payne, J. C.; ter Horst, M. A.; Arnold Godwin, H. *J. Am. Chem. Soc.* **1999**, *121*, 6850-6855.
- (6) National Research Council, *Arsenic in Drinking Water*; National Academy Press: Washington D.C., 1999.
- (7) Oremland, R. S.; Stolz, J. F. *Nature* **2003**, *300*, 939-944.
- (8) Aschner, M.; Walker, S. J. *Molecular Psychiatry* **2002**, *7*, S40-S41.
- (9) Emsley, J. *The Elements*; 2nd ed., Clarendon Press: Oxford, 1990.
- (10) Arena, J. M. *Poisoning: Toxicology, Symptoms, Treatments*; Thomas: Springfield, Ill., U.S.A., 1986.
- (11) Sadler, P. J.; Guo, Z. *Pure & Appl. Chem.* **1998**, *70*, 863-871.
- (12) Sadler, P. J.; Li, H.; Sun, H. *Coord. Chem. Rev.* **1999**, *185-186*, 689-709.
- (13) Sun, H.; Li, H.; Sadler, P. J. *Chem. Ber./Recueil* **1997**, *130*, 669-681.
- (14) Baxter, G. F. *Pharm. J.* **1989**, *243*, 805-810.
- (15) Baxter, G. F. *Chem. Br.* **1992**, 445-448.
- (16) Kopf-Maier, P.; Klapotke, T. *Inorg. Chim. Acta* **1988**, *152*, 49-52.
- (17) Kopf-Maier, P. *Eur. J. Clin. Pharmacol.* **1994**, *47*, 1-16.
- (18) Gorbach, S. L. *Gastroenterology* **1990**, *99*, 863-875.
- (19) Marshall, B. J. *Am. J. Gastroenterol.* **1991**, *86*, 16-25.
- (20) Lambert, J. R. *Scand. J. Gastroenterol.* **1991**, *26*, 13-21.
- (21) Boersch, G. *Med. Monatsschr. Pharm.* **1988**, *11*, 301-307.

- (22) Gavey, C. J.; Szeto, M.-L.; Nwokolo, C. U.; Sercombe, J.; Pounder, R. E. *Aliment. Pharmacol. Ther.* **1989**, *3*, 21-28.
- (23) Asato, E.; Driessen, W. L.; de Graaff, R. A. G.; Hulsbergen, F. B.; Reedijk, J. *Inorg. Chem.* **1991**, *30*, 4210-4218.
- (24) Asato, E.; Hol, C. M.; Hulsbergen, F. B.; Klooster, N. T. M.; Reedijk, J. *Inorg. Chim. Acta* **1993**, *214*, 159-167.
- (25) Asato, E.; Katsura, K.; Mikuriya, M.; Turpeinen, U.; Mutikainen, I.; Reedijk, J. *Inorg. Chem.* **1995**, *34*, 2447-2454.
- (26) Herrmann, W. A.; Herdtweck, E.; Pajdla, L. *Inorg. Chem.* **1991**, *30*, 2579-2581.
- (27) Herrmann, W. A.; Herdtweck, E.; Pajdla, L. *Z. Krist.* **1992**, *198*, 257-264.
- (28) Parkinson, J. A.; Sun, H.; Sadler, P. J. *Chem. Commun.* **1998**, 881-882.
- (29) Veldhuyzen van Zanten, S. J. O.; Sherman, P. M. *Can. Med. Assoc. J.* **1994**, *150*, 177-185.
- (30) Veldhuyzen van Zanten, S. J. O.; Sherman, P. M. *Can. Med. Assoc. J.* **1994**, *150*, 189-198.
- (31) Graham, D. Y. *Gastroenterology* **1989**, *96*, 615-625.
- (32) Thompson, J. J. *Rays of Positive Electricity and their Application to Chemical Analysis*; Longmans, Green & Co.: London, 1913.
- (33) Johnson, B. F. G.; McIndoe, J. S. *Coord. Chem. Rev.* **2000**, *200-202*, 901-932.
- (34) Chen, P. *Angew. Chem., Int. Ed. Engl.* **2003**, *42*, 2832-2847.
- (35) Hofstadler, S. A.; Bakhtiar, R. D.; Smith, R. D. *J. Chem. Educ.* **1996**, *73*, A82.
- (36) Fenn, J. B.; Mann, M.; Meng, C. K.; Wong, S. F.; Whitehouse, C. M. *Mass Spectrosc. Rev.* **1990**, *9*, 37-70.
- (37) Fenn, J. B.; Mann, M.; Meng, C. K.; Wong, S. F.; Whitehouse, C. M. *Science* **1989**, *246*, 64-71.
- (38) Gaskell, S. J. *J. Mass. Spectrom.* **1997**, *32*, 677-688.
- (39) Reed, A. E.; Schleyer, P. V. R. *J. Am. Chem. Soc.* **1990**, *112*, 1434-1435.
- (40) Farrugia, L. J.; Lawlor, F. J.; Norman, N. C. *Dalton Trans.* **1995**, 1163-1171.



- (41) Levason, W.; Reid, G. *Dalton Trans.* **2001**, 2953-2960.
- (42) Reger, D. L.; Wright, T. D.; Little, C. A.; Lamda, J. J. S.; Smith, M. D. *Inorg. Chem.* **2001**, *40*, 3810-3814.
- (43) Farrugia, L. J.; Lawlor, F. J.; Norman, N. C. *Polyhedron* **1995**, *14*, 311-314.
- (44) Carmalt, C. J.; Cowley, A. H.; Decken, A.; Norman, N. C. *J. Organomet. Chem.* **1995**, *496*, 59-67.
- (45) Carmalt, C. J.; Clegg, W.; Elsegood, M. R. J.; Errington, R. J.; Havelock, J.; Lightfoot, P.; Norman, N. C.; Scott, A. J. *Inorg. Chem.* **1996**, *35*, 3709-3712.
- (46) Norman, N. C.; Pickett, N. L. *Coord. Chem. Rev.* **1995**, *145*, 27-54.
- (47) Briand, G. G.; Burford, N. *Adv. Inorg. Chem.* **2000**, *50*, 285-357.
- (48) Pearson, R. G. *J. Am. Chem. Soc.* **1963**, *85*, 3533-3539.
- (49) Shriver, D. F.; Atkins, P. W.; Langford, C. H. *Inorganic Chemistry*; W.H. Freeman Company: USA, 1990.
- (50) Agocs, L.; Briand, G. G.; Burford, N.; Cameron, T. S.; Kwiatkowski, W.; Robertson, K. N. *Inorg. Chem.* **1997**, *36*, 2855-2860.
- (51) Asato, E.; Kamamuta, K.; Akamine, Y.; Fukami, T.; Nukada, R.; Mikuriya, M.; Deguchi, S.; Yokota, Y. *Bull. Chem. Soc. Jpn.* **1997**, *70*, 639-648.
- (52) Briand, G. G.; Burford, N.; Cameron, T. S.; Kwiatkowski, W. *J. Am. Chem. Soc.* **1998**, *120*, 11374-11379.
- (53) Briand, G. G.; Burford, N.; Cameron, T. *Chem. Commun.* **2000**, 13-14.
- (54) Briand, G. G.; Burford, N.; Eelman, M. D.; Cameron, T. S.; Robertson, K. N. *Inorg. Chem.* **2003**, *42*, 3136-3141.
- (55) Burford, N.; Eelman, M. D.; Cameron, T. S. *Chem. Commun.* **2002**, 1402-1403.
- (56) Asato, E.; Katsura, K.; Mikuriya, M.; Fujii, T.; Reedijk, J. *Inorg. Chem.* **1993**, *32*, 5322-5329.
- (57) Barrie, P. J.; Djuran, M. I.; Mazid, M. A.; McPartlin, M.; Sadler, P. J.; Scowen, I. J.; Sun, H. *Dalton Trans.* **1996**, 2417-2422.
- (58) Li, W.; Jin, L.; Zhu, N.; Hou, X.; Deng, F.; Sun, H. *J. Am. Chem. Soc.* **2003**, *125*, 12408-12409.

- (59) Loudon, G. M. *Organic Chemistry*; 3rd ed. Benjamin/Cummings Publishing Company, Inc.: New York, 1995.
- (60) Carmalt, C. J.; Farrugia, L. J.; Norman, N. C. *Z. Anorg. Allg. Chem.* **1995**, 621, 47-56.
- (61) Burgess, J.; Fawcett, J.; Parsons, S. A.; Russell, D. R. *Acta Cryst.* **1994**, C50, 1911-1913.
- (62) Diemer, R.; Keppler, B. K.; Dittes, U.; Nuber, B.; Seifried, V.; Opferkuch, W. *Chem. Ber.* **1995**, 128, 335-342.
- (63) Parola, S.; Papiernik, R.; Hubert-Pfalzgraf, L. G.; Jagner, S.; Håkansson, M. *Dalton Trans.* **1997**, 4631-4635.
- (64) Fukin, G. K.; Pisarevskii, A. P.; Yanovskii, A. I.; Struchkov, Yu. T. *Russ. J. Inorg. Chem. (Transl. of Zh. Neorg. Khim.)* **1993**, 38, 1205.
- (65) Reglinski, J. *Chemistry of Arsenic, Antimony, and Bismuth*; Norman, N. C., Ed., Blackie Academic & Professional: London, 1998; pp 403-440.
- (66) Asato, E.; Katsura, K.; Arakaki, M.; Mikuriya, M.; Kotera, T. *Chem. Lett.* **1994**, 2123-2126.
- (67) Thurston, J. H.; Marlier, E. M.; Whitmire, K. H. *Chem. Commun.* **2002**, 2834-2835.
- (68) Fabrègue *J. Pharm. Chim.* **1922**, 25, 341-344.
- (69) Moles, E.; Portillo, R. *Anales. Soc. Espan. Fis. Quím.* **1922**, 20, 571-576.
- (70) Turkevich, N. M. **SU Pat. 126,483**, 1960. (*Chem. Abs.* **1960**, 54, 1781(d-e)).
- (71) Kirkhgof, G. A.; Spektor, M. O. *Khim. Farm. Prom* **1933**, 122-123.
- (72) Picon, M. *J. Pharm. Chim.* **1926**, 4, 529-533.
- (73) Turkevich, N. M. *Med. Prom. S. S. S. R.* **1961**, 15, 24-25.
- (74) Turkevich, M. M. *Farmatsevt. Zh. (Kiev)* **1963**, 18, 30-31.
- (75) Von Oettingen, W. F.; Ishikawa, Y. *J. Am. Pharm. Assoc.* **1928**, 17, 124-128.
- (76) Turkevich, N. M. *Zhur. Obschei Khim.* **1952**, 22, 1930-1933.
- (77) Kirkhgof, G. A. **Russ.** **31,013**, 1933. (*Chem. Abs.* **1932**, 26, 3877).

- (78) Kiprof, P.; Scherer, W.; Pajdla, L.; Herdtweck, E.; Herrmann, W. A. *Chem. Ber.* **1992**, *125*, 43-46.
- (79) Herrmann, W. A.; Herdtweck, E.; Scherer, W.; Kiprof, P.; Pajdla, L. *Chem. Ber.* **1993**, *126*, 51-56.
- (80) Sagatys, D. S.; O'Reilly, E. J.; Patel, S.; Bott, R. C.; Lynch, D. E.; Smith, G.; Kennard, C. H. L. *Aust. J. Chem.* **1992**, *45*, 1027-1034.
- (81) Streitwolf, K., Fehrle, A., Herrmann, W. A., and Fritzshche, P. **US Pat. 1,864,679**, 1932. (*Chem. Abs.* **1932**, *26*, 4417).
- (82) Lauter, W. M.; Jurist, A. E.; Christiansen, W. G. *J. Am. Pharm. Assoc.* **1933**, *22*, 531-534.
- (83) Christiansen, W. G. and Lauter, W. M. **US Pat. 1,859,288**, 1932. (*Chem. Abs.* **1932**, *26*, 3877).
- (84) Agocs, L.; Briand, G. G.; Burford, N.; Eelman, M. D.; Aumeerally, N.; MacKay, D.; Robertson, K. N.; Cameron, T. S. *Can. J. Chem.* **2003**, *81*, 632-637.
- (85) Agocs, L.; Burford, N.; Cameron, T. S.; Curtis, J. M.; Richardson, J. F.; Robertson, K. N.; Yhard, G. B. *J. Am. Chem. Soc.* **1996**, *118*, 3255-3232.
- (86) Powell, P. *J. Chem. Soc. (A)* **1968**, 2587-2588.
- (87) Andrews, P. C.; Deacon, G. B.; Jackson, W. R.; Maguire, N. M.; Scott, B. W.; White, A. H. *Dalton Trans.* **2002**, 4643-4648.
- (88) Janvier, P.; Drumel, S.; Piffrad, Y.; Bujoli, B. *C. R. Acad. Sci., Paris, Serie II.* **1995**, *320*, 29-35.
- (89) Mascherpa, P.; Callegari, L. *Arch. Sci. Biol.* **1933**, *18*, 452-462.
- (90) Mascherpa, P.; Callegari, L. *Arch. Ital. Biol.* **1934**, *91*, 115-122.
- (91) Burford, N.; Eelman, M. D.; Mahony, D.; Morash, M. *Chem. Commun.* **2003**, 146-147.
- (92) McAuliffe, C. A.; Quagliano, J. V.; Vallarino, L. M. *Inorg. Chem.* **1966**, *5*, 1996-2003.
- (93) Alonzo, G.; Bertazzi, N.; Consiglio, M. *Inorg. Chim. Acta* **1984**, *85*, L35-L37.
- (94) Napoli, A. *Ann. Chim.* **1982**, *72*, 575-583.

- (95) Herrmann, W. A. D.; Herdtweck, E.; Pajdla, L. *Chem. Ber.* **1993**, *126*, 895-898.
- (96) Ercoli, N. AU Pat. **440,336**, 1973. (*Chem. Abs.* **1974**, *80*, 112638x).
- (97) Friedheim, E. A. H. NL Pat. **6,412,438**, 1965. (*Chem. Abs.* **1966**, *64*, 534(d-e)).
- (98) Rumyantseva, L. S.; Tedorovich, I. L. *Dokl. Akad. Nauk Uzb. SSR.* **1971**, *28*, 43-44.
- (99) Sharma, U.; Sharma, S. K.; Rani, U. *Thermochim. Acta.* **1989**, *147*, 401-403.
- (100) Kulkarni, V. G.; Bhansali, P. K.; Nemade, B. I. *Trans. SAEST.* **1984**, *19*, 299-303.
- (101) Ruskin, S. L. US Pat. **2,250,553**, 1941. (*Chem. Abs.* **1941**, *35*, 7117(3)).
- (102) Sadler, P. J.; Sun, H.; Li, H. *Chem. Eur. J.* **1996**, *2*, 701-708.
- (103) Sun, H.; Li, H.; Sadler, P. J. *J. Inorg. Biochem.* **1995**, *59*, 190-195.
- (104) Li, H.; Sadler, P. J.; Sun, H. *Eur. J. Biochem.* **1996**, *242*, 387-393.
- (105) Li, H.; Sadler, P. J.; Sun, H. *J. Biol. Chem.* **1996**, *271*, 9483-9489.
- (106) Rao, N.; Feldman, S. *Pharm. Res.* **1990**, *7*, 188-191.
- (107) Jesserer, H.; Lieben, F. *Biochem. Z.* **1938**, *297*, 369-378.
- (108) Mascherpa, P.; Callegari, L. *Arch. Ital. Biol.* **1934**, *91*, 107-115.
- (109) Mascherpa, P.; Callegari, L. *Arch. Sci. Biol.* **1933**, *18*, 438-451.
- (110) Zlatarov, As.; Pencheva, V. *Ann. Univ. Sofia II, Faculte Phys.-Math.* **1934**, *30*, 203-216.
- (111) Nielson, K. B.; Atkin, C. L.; Winge, D. R. *J. Biol. Chem.* **1985**, *260*, 5342-5350.
- (112) Piotrowski, J. K.; Szymanska, J. A.; Mogilnicka, E. M.; Zelazowski, A. J. *Experientia Supplement* **1979**, *34*, 363-371.
- (113) Szymanska, J. A.; Stillman, M. J. *Biochem. Biophys. Res. Commun.* **1982**, *108*, 919-925.
- (114) Herrmann, W. A.; Herdtweck, E.; Pajdla, L. *Chem. Ber.* **1993**, *126*, 895-898.
- (115) Pellerin, F.; Goulle, J. P.; Dumitrescu, D. *Ann. Pharm. Fr.* **1977**, *35*, 281-286.

- (116) Musil, J.; Dolezal, J.; Vorlicek, J. *J. Electroanal. Chem. Interfacial Electrochem.* **1970**, *24*, 447-457.
- (117) Elenkova, N.; Palashev, C.; Ilcheva, L. *Talanta* **1971**, *18*, 355-359.
- (118) Singh, B.; Khan, S. A.; Bhanu, U. *Indian. J. Chem., Sect.A.* **1987**, *26A*, 1066-1068.
- (119) Pellerin, F.; Goulle, J. P.; Dumitrescu, D. *Bull. Acad. Natl. Med., Paris.* **1976**, *160*, 268-273.
- (120) Claudio, E. S.; Arnold Godwin, H.; Magyar, J. S. Fundamental Coordination Chemistry, Environmental Chemistry, and Biochemistry of Lead (II); In *Progress in Inorganic Chemistry*; Karlin, K. D., ed. John Wiley & Sons, Inc.: Hoboken, N.J., 2003; pp 1-145.
- (121) Sun, X.; Tian, X.; Tomsig, J. L.; Suszkiw, J. B. *Toxicology and Applied Pharmacology* **1999**, *156*, 40-45.
- (122) Chisholm, J. J. *Scientific American* **1971**, *224*, 15-23.
- (123) Warren, M. J.; Cooper, J. B.; Wood, S. P.; Shoolingan-Jordan, P. M. *Trends Biochem. Sci.* **1998**, *23*, 217-221.
- (124) Bridgewater, B. M.; Parkin, G. *J. Am. Chem. Soc.* **2000**, *122*, 7140-7141.
- (125) Sigel, H.; Fischer, B. E.; Farkas, E. *Inorg. Chem.* **1983**, *22*, 925-934.
- (126) National Research Council *Measuring lead exposure in infants, children, and other sensitive populations*; Washington, D. C., 1993.
- (127) Salpin, J.-Y.; Tortajada, J. *J. Phys. Chem. A* **2003**, *107*, 2943-2953.
- (128) Salpin, J.-Y.; Tortajada, J. *J. Mass Spectrom.* **2002**, *37*, 379-388.
- (129) Burford, N.; Eelman, M. D.; LeBlanc, W. G.; Cameron, T. S.; Robertson, K. N. *Chem. Commun.* **2003**, In press.
- (130) Abu-Dari, K.; Ekkehardt Hahn, F.; Raymond, K. N. *J. Am. Chem. Soc.* **1990**, *112*, 1519-1524.
- (131) Wong, Y. S.; Chieh, P. C.; Carty, A. J. *Can. J. Chem.* **1973**, *51*, 2597-2599.
- (132) Wong, Y. S.; Taylor, N. J.; Chieh, P. C.; Carty, A. J. *Chem. Commun.* **1974**, 625-626.
- (133) Wong, Y. S.; Carty, A. J.; Chieh, P. C. *Dalton Trans.* **1977**, 1157-1160.

- (134) Wong, Y. S.; Carty, A. J.; Chieh, P. C. *Dalton Trans.* **1977**, 1801-1808.
- (135) Wong, Y. S.; Chieh, P. C.; Carty, A. J. *Chem. Commun.* **1973**, 741-742.
- (136) Taylor, N. J.; Wong, Y. S.; Chieh, P. C.; Carty, A. J. *Dalton Trans.* **1975**, 438-442.
- (137) Fairhurst, M. T.; Rabenstein, D. L. *Inorg. Chem.* **1975**, *14*, 1413-1415.
- (138) Rabenstein, D. L.; Fairhurst, M. T. *J. Am. Chem. Soc.* **1975**, *97*, 2086-2092.
- (139) Rabenstein, D. L.; Reid, R. S. *Inorg. Chem.* **1984**, *23*, 1246-1250.
- (140) Reid, R. S.; Rabenstein, D. L. *Can. J. Chem.* **1981**, *59*, 1505-1514.
- (141) Alex, S.; Savoie, R. *J. Raman, Spectrosc.* **1987**, *18*, 17-21.
- (142) Simpson, P. G.; Hopkins, T. E.; Haque, R. *J. Phys. Chem.* **1973**, *77*, 2282-2285.
- (143) Hojo, Y.; Sugiura, Y.; Tanaka, H. *J. Inorg. Nucl. Chem.* **1976**, *38*, 641-644.
- (144) Arnold, A. P.; Carty, A. J. *Can. J. Chem.* **1983**, *61*, 1428-1434.
- (145) Davidovich, R. L.; Logvinova, V. B.; Zemnukhova, L. A.; Udovenko, A. A.; Kondratyuk, I. P. *Koord. Khim.* **1991**, *17*, 1342-1348.
- (146) Freeman, H. C.; Moore, C. J. *Acta. Cryst.* **1977**, *B33*, 2690-2692.
- (147) Corbeil, M. C.; Beauchamp, A. L. *Can. J. Chem.* **1988**, *66*, 2458-2464.
- (148) Moiseenko, V. N.; Kolesnik, I. P.; Shchetinkin, V. S.; Vinichenko, I. G.; Chernushenko, E. A.; Zegzhda, G. D. *Opt. Spektrosk.* **1996**, *81*, 430-433.
- (149) Wienke, J. K.; Yager, J. W. *Environ. Mol. Mutagen.* **1992**, *19*, 195-200.
- (150) Tezuka, M.; Hanioka, K. I.; Yamanaka, K.; Okada, S. *Biochem. Biophys. Res. Comm.* **1993**, *191*, 1178-1183.
- (151) Christie, N. T.; Costa, M. *Biol. Trace Elem. Res.* **1983**, *5*, 55-71.
- (152) Nordenson, I.; Sweins, A.; Beckman, L. *Scan. J. Work. Environ. Health* **1981**, *7*, 277-281.
- (153) Lagunas, R.; Pestana, D.; Diez Masa, J. C. *Biochemistry* **1984**, *23*, 955-960.
- (154) Jacobson Kram, D.; Montalbano, D. *Environ. Mut.* **1985**, *7*, 787-804.